



Spain | 2013

Julien Bourgeois

Simulation of the effect of auxiliary ties used in the construction of  
Mallorca Cathedral



ADVANCED MASTERS IN STRUCTURAL ANALYSIS  
OF MONUMENTS AND HISTORICAL CONSTRUCTIONS

## Master's Thesis

Julien Bourgeois

Simulation of the effect of  
auxiliary ties used in the  
construction of Mallorca  
Cathedral



UNIVERSITAT POLITÈCNICA  
DE CATALUNYA



UNIVERSITÀ DEGLI STUDI DI PADOVA



Education and Culture

## Erasmus Mundus



ADVANCED MASTERS IN STRUCTURAL ANALYSIS  
OF MONUMENTS AND HISTORICAL CONSTRUCTIONS



# Master's Thesis

**Julien Bourgeois**

## Simulation of the effect of auxiliary ties used in the construction of Mallorca Cathedral

This Masters Course has been funded with support from the European Commission. This publication reflects the views only of the author, and the Commission cannot be held responsible for any use which may be made of the information contained therein.



## DECLARATION

Name: Bourgeois

Email: julienbourgeois5@gmail.com

Title of the Msc Dissertation: Simulation of the effect of auxiliary ties used in the construction of Mallorca Cathedral

Supervisor(s): Professor Luca Pelà

Year: 2013

I hereby declare that all information in this document has been obtained and presented in accordance with academic rules and ethical conduct. I also declare that, as required by these rules and conduct, I have fully cited and referenced all material and results that are not original to this work.

I hereby declare that the MSc Consortium responsible for the Advanced Masters in Structural Analysis of Monuments and Historical Constructions is allowed to store and make available electronically the present MSc Dissertation.

University: Universitat Politècnica de Catalunya

Date: July 18, 2013

Signature:





This page is left blank on purpose.

## ACKNOWLEDGEMENTS

First of all, I would like to express my gratitude to my supervisor, Professor Luca Pelà, for his strong implication concerning the present thesis. His cheerfulness, motivation and patience have been key elements for the success of this work. I would also like to thank Professor Pere Roca for his full implication in the MSc SAHC Masters Course and his will to share his knowledge as well as his passion for historical constructions. I am also thankful to the PhD candidates Yohei Endo for letting me run some analyses on his computer and Mira Vasic who gave me useful information on the ties of Milano Cathedral.

I would like to thank all the people I met this year in Padova and Barcelona, and especially my SAHC colleagues without whom this experience wouldn't have been unforgettable. A special thank goes to my SAHC flatmates Chavon Grande, Juan Arias, and Savvas Saloustros for their friendship and support in Barcelona.

Last but not least, I would like to thank my family and close friends in France for their unfailing support, their precious help and their reliable advice. Merci à vous!

This page is left blank on purpose.

## ABSTRACT

The thesis is oriented on the study of Mallorca Cathedral taking into account its construction process and, particularly, the influence of iron ties used as auxiliary devices during the construction. Some previous studies (Roca et al., 2013, 2012) have presented some possible hypotheses about the construction process of this gothic cathedral. This study complements the previous results by considering the possibility of the adoption of auxiliary ties, since some evidences of their application can be recognized in the structure nowadays. Before focusing on Mallorca Cathedral, a first part is devoted to the effective use of iron elements during medieval times with a special interest on temporary and long-lasting ties in gothic architecture. The main goal of this research is to show the widespread adoption of iron in gothic constructions.

Then, a thorough investigation of the bays of Mallorca Cathedral has been carried out in order to estimate the location of the temporary ties. It is assumed that such ties were adopted to stabilize the lateral vaults before the construction of the central ones, and were cut afterwards.

After this preliminary work, three different ties configurations are considered (upper tie, lower tie and two ties) together with a reference configuration without any tie. The ties were added to an existing model of a typical bay of the cathedral. The four models developed are used to study the role of the ties during the construction and the effects resulting from being later cut. The study also includes the analysis of the long-term deformation of the structure taking into account the effects resulting from the removal of the ties, as well as parametric analyses: one focused on the influence of the section of the ties and another one on the influence of the tensile strength of the masonry.

This page is left blank on purpose.

## RESUM

### **Simulació de l'efecte dels tirants auxiliars utilitzats en la construcció de la Seu de Mallorca.**

La tesina s'orienta a l'estudi de la Seu de Mallorca tot considerant el seu procés constructiu i, sobretot, la influència dels tirants de ferro utilitzats com a dispositius auxiliars durant la construcció. Abans de centrar-se en la Seu de Mallorca, la primera part està dedicada a la utilització efectiva d'elements de ferro durant l'Edat Mitjana, amb especial interès en tirants temporals o definitius en l'arquitectura gòtica. El principal objectiu d'aquesta investigació és mostrar l'adopció generalitzada de ferro en les construccions gòtiques.

S'ha dut a terme una investigació detallada de les crugies de la Catedral de Mallorca per tal d'estimar la ubicació dels tirants temporals. Se suposa que aquests tirants es van disposar per estabilitzar les voltes laterals abans de la construcció de les centrals, i es van tallar després.

Després d'aquest treball preliminar, es consideren tres configuracions diferents de tirants (tirant superior, tirant inferior i dos tirants) juntament amb una configuració de referència sense cap tirant. Els tirants s'han afegit a un model existent d'una crugia típica de la catedral. Els quatre models desenvolupats s'utilitzen per estudiar el paper dels tirants durant la construcció i els efectes resultants en ser posteriorment tallats. L'estudi també inclou l'anàlisi de la deformació a llarg termini de l'estructura tenint en compte els efectes resultants de l'eliminació dels tirants, així com dues anàlisis paramètriques: una primera anàlisi centrada en la influència de la secció dels tirants i una segona sobre la influència de la resistència a la tracció de la maçoneria.

This page is left blank on purpose.

## RÉSUMÉ

### **Simulation des conséquences de l'utilisation de tirants temporaires au cours de la construction de la cathédrale de Majorque.**

La présente thèse est orientée sur l'étude de la cathédrale de Majorque, en prenant en compte ses différentes phases de construction avec un intérêt particulier sur l'influence de l'utilisation de tirants en fer comme dispositifs auxiliaires durant la construction. Des études précédentes (Roca et al., 2013, 2012) avaient avancé de possibles hypothèses quant au procédé de construction de cette cathédrale gothique. Cette étude complète les résultats existants en considérant la possible utilisation de tirants auxiliaires durant les phases de construction, hypothèse basée sur la présence de vestiges de tirants toujours observables dans la structure. Avant de s'intéresser spécifiquement à la cathédrale, une étude préliminaire dédiée à l'utilisation effective d'éléments en fer au Moyen-âge est effectuée, notamment sur l'intégration de tirants temporaires et permanents dans l'architecture gothique. Cette section a pour but de prouver que le fer fut un des matériaux les plus utilisés dans l'architecture gothique, que ce soit d'un point de vue structurel ou non.

Une recherche approfondie in-situ des baies de la cathédrale de Majorque a ensuite été réalisée dans le but de conclure sur la possible existence de vestiges de tirants et d'estimer la position de ces derniers. Il a été en effet supposé que de tels tirants furent adoptés pour stabiliser les voûtes latérales avant la construction des voûtes centrales, puis retirer après que la construction eut été achevée.

A la suite de ces recherches, trois différentes configurations de tirants ont été considérées : tirant en position haute, tirant en position basse, tirants en positions haute et basse. Une configuration sans aucun tirant servant de « configuration témoin » a également été considérée. Quatre modèles aux éléments finis d'une baie typique de la cathédrale, correspondant aux quatre configurations listées ci-dessus, ont été implémentés à partir d'un modèle déjà existant dans le but d'étudier le rôle structurel des tirants durant la construction, ainsi que les conséquences de leur rapide retrait. Cette étude inclut également l'analyse de la déformation de la structure sur le long terme lorsque que le fluage de la maçonnerie est considéré ainsi que deux études paramétriques : l'influence de la surface de la section transversale des tirants et l'influence de la résistance à la traction de la maçonnerie.



This page is left blank on purpose.

## TABLE OF CONTENTS

|  |           |
|--|-----------|
| <b>1. INTRODUCTION .....</b>   | <b>1</b>  |
| 1.1. GENERAL .....   | 1         |
| 1.2. OBJECTIVES.....   | 1         |
| 1.3. ORGANIZATION .....  | 2         |
| <b>2. THE USE OF IRON IN GOTHIC CONSTRUCTIONS .....</b>  | <b>5</b>  |
| 2.1. PAST CONTROVERSY .....  | 5         |
| 2.2. OVERVIEW OF THE DIFFERENT IRON ELEMENTS PRESENT IN GOTHIC ARCHITECTURE .....                                | 7         |
| 2.2.1. <i>Structural elements</i> .....  | 8         |
| Bars in glass stained windows .....  | 8         |
| Clamps .....   | 9         |
| Studs .....  | 10        |
| Dowels .....   | 11        |
| Hooks .....  | 12        |
| Chaining system.....   | 13        |
| 2.2.2. <i>Non-structural elements</i> .....  | 14        |
| 2.3. IRON TIES .....   | 16        |
| 2.3.1. <i>Definition</i> .....   | 16        |
| 2.3.2. <i>Temporary ties</i> .....   | 17        |
| Role.....  | 17        |
| Examples.....  | 19        |
| 2.3.3. <i>Long-lasting ties</i> .....  | 23        |
| Role.....  | 23        |
| Examples.....  | 24        |
| 2.3.4. <i>Past interventions: strengthening</i> .....  | 27        |
| 2.3.5. <i>Iron properties and ties dimensions</i> .....  | 28        |
| Iron production during medieval times .....  | 28        |
| Ties properties .....  | 33        |
| 2.4. WOODEN TIES .....   | 34        |
| <b>3. MALLORCA CATHEDRAL: PAST STUDIES.....</b>  | <b>37</b> |
| 3.1. HISTORICAL DATA.....  | 38        |
| 3.2. DIMENSIONS AND INTERESTING FEATURES.....  | 40        |
| 3.3. EXISTING DAMAGES AND STRUCTURAL ALTERATIONS .....   | 42        |
| 3.4. CONSTRUCTION PROCESS OF THE 4 <sup>TH</sup> BAY OF THE CATHEDRAL.....                                       | 44        |
| 3.5. PREVIOUS WORKS .....  | 46        |
| 3.5.1. <i>Thrust lines and photo-elasticity studies</i> .....  | 46        |
| 3.5.2. <i>FEM analysis</i> .....   | 48        |
| Roca (2001).....   | 48        |
| Salas (2002) .....   | 49        |
| Clemente (2006, 2002) .....  | 50        |
| Roca et al. (2013, 2012) .....   | 53        |
| <b>4. ON-SITE EVIDENCES OF THE USE OF AUXILIARY TIES IN THE CONSTRUCTION PROCESS OF MALLORCA CATHEDRAL .....</b> | <b>61</b> |
| 4.1. INVESTIGATION .....   | 61        |
| 4.1.1. <i>On-site investigation</i> .....  | 61        |
| 4.1.2. <i>Previous photogrammetric study</i> .....   | 67        |
| 4.2. DIMENSIONS AND POSITIONS.....   | 67        |
| 4.2.1. <i>Ties locations</i> .....   | 67        |
| 4.2.2. <i>Ties dimensions</i> .....  | 73        |
| <b>5. STRUCTURAL ANALYSIS .....</b>  | <b>75</b> |

|        |  |            |
|--------|--|------------|
| 5.1.   | MODEL DESCRIPTION .....  | 76         |
| 5.1.1. | <i>Integration of the ties</i> .....   | 76         |
|        | Location of the ties .....   | 77         |
|        | Anchorage system .....   | 77         |
| 5.1.2. | <i>Materials parameters</i> .....  | 79         |
| 5.1.3. | <i>Additional weights</i> .....  | 80         |
| 5.1.4. | <i>Boundary conditions</i> .....   | 80         |
| 5.2.   | MODELING STRATEGY .....  | 80         |
| 5.2.1. | <i>Different configurations</i> .....  | 80         |
| 5.2.2. | <i>Formulation</i> .....   | 81         |
| 5.2.3. | <i>Sequential analysis</i> .....   | 81         |
| 5.2.4. | <i>Parallel studies</i> .....  | 82         |
| 5.3.   | STUDY OF THE USE OF AUXILIARY TIES DURING THE CONSTRUCTION OF THE BAY .....  | 82         |
| 5.3.1. | <i>General assumptions and outcomes</i> .....  | 82         |
| 5.3.2. | <i>Construction process and ties removal</i> .....   | 83         |
|        | Displacements and correction .....   | 84         |
|        | Mechanical behavior of the ties .....  | 87         |
|        | Tensile damage .....   | 90         |
| 5.3.3. | <i>Fourth step: long-term creep behavior of the masonry after the ties removal</i> .....   | 93         |
|        | Preliminary considerations .....   | 93         |
|        | Results .....  | 94         |
|        | Observations .....   | 95         |
|        | Further works .....  | 96         |
| 5.4.   | PARAMETRIC STUDY: INFLUENCE OF THE TIE CROSS-SECTION .....   | 96         |
| 5.5.   | PARAMETRIC STUDY: INFLUENCE OF THE TENSILE STRENGTH OF THE MASONRY IN THE LOWER TIE CONFIGURATION .....  | 98         |
| 6.     | <b>CONCLUSIONS</b> .....   | <b>101</b> |
| 6.1.   | SUMMARY .....  | 101        |
| 6.2.   | MAIN CONTRIBUTIONS .....   | 102        |
| 6.3.   | SUGGESTIONS FOR FUTURE WORK .....  | 102        |
| 7.     | <b>REFERENCES</b> .....  | <b>105</b> |
|        | PAPERS, BOOKS AND PUBLICATIONS .....   | 105        |
|        | NORMS AND CODES .....  | 107        |
|        | WEBSITES .....   | 108        |
|        | <b>ANNEX A: VISCOELASTICITY AND DAMAGE MODEL</b> .....   | <b>109</b> |
|        | VISCOELASTICITY MODEL .....  | 109        |
|        | TENSION –COMPRESSION DAMAGE MODEL .....  | 111        |
|        | <b>ANNEX B: HORIZONTAL DISPLACEMENTS AT STAGES 1, 2 AND 3 FOR THE FOUR DIFFERENT TIES CONFIGURATIONS UNDER THE ASSUMPTION OF SMALL STRAINS/LARGE DISPLACEMENTS (RESULTS ARE GIVEN IN METERS). TIES AREA: 25 CM<sup>2</sup></b> ..... | <b>115</b> |
|        | <b>ANNEX C: TENSILE DAMAGE AT STAGES 1, 2 AND 3 FOR THE FOUR DIFFERENT TIES CONFIGURATIONS UNDER THE ASSUMPTION OF SMALL STRAINS/LARGE DISPLACEMENTS. TIES AREA: 25 CM<sup>2</sup></b> .....   | <b>116</b> |
|        | <b>ANNEX D: HORIZONTAL DISPLACEMENTS AT STAGES 1, 2 AND 3 FOR THE FOUR DIFFERENT TIES CONFIGURATIONS UNDER THE ASSUMPTION OF SMALL STRAINS/LARGE DISPLACEMENTS (RESULTS ARE GIVEN IN METERS). TIES AREA: 50 CM<sup>2</sup></b> ..... | <b>119</b> |
|        | <b>ANNEX E: TENSILE DAMAGE AT STAGES 1, 2 AND 3 FOR THE FOUR DIFFERENT TIES CONFIGURATIONS UNDER THE ASSUMPTION OF SMALL STRAINS/LARGE DISPLACEMENTS. TIES AREA: 50 CM<sup>2</sup></b> .....   | <b>120</b> |

## LIST OF FIGURES

|  |    |
|--|----|
| Figure 1 – Part of the different types of expenses for a smith from the accounts of the fabrics of the cathedrals of Rouen and Troyes (L'Héritier, 2007).  | 7  |
| Figure 2 – Saint-Julien Cathedral, Le Mans.  | 9  |
| Figure 3 – Church of Notre-Dame des Victoires, Bruxelles: Example of bars reinforcing a stained glass window.  | 9  |
| Figure 4 – Cathedral Notre-Dame of Chartres: example of a clamp.   | 9  |
| Figure 5 – Cathedral Santa Maria of Palma.   | 9  |
| Figure 6 – Chartres Cathedral: Clamps within the masonry of one of the spires.   | 10 |
| Figure 7 – Cathedral Notre Dame of Laon: Stud in a vertical element.   | 11 |
| Figure 8 – Schematic view of stud and rings.   | 11 |
| Figure 9 – Cathedral Notre-Dame of Noyon: existing proof of the use of studs within the vaulting system.   | 11 |
| Figure 10 – Cathedral Notre-Dame of Rouen: Dowel used for the construction of the wooden framework.  | 12 |
| Figure 11 – Cathedra Notre-Dame of Chartres: hook.   | 13 |
| Figure 12 – Church Santa Maria del Mar, Barcelona.   | 13 |
| Figure 13 – Church Saint-Ouen of Rouen: Example of a chaining system.  | 14 |
| Figure 14 – Detail of a possible connection between two metallic elements constituting a chaining system. (Viollet-le-Duc, 1854-1868)  | 14 |
| Figure 15 – Church Saint-Ouen of Rouen : Examples of chaining in the second floor of the crossing tower. (L'Héritier, 2007; Moufle D., 2000)   | 14 |
| Figure 16 – (Up, left) Church Santa Maria del Mar: rings used possibly to hold a torch.  | 15 |
| Figure 17 – (Up, right) Church Santa Maria del Mar: hook.  | 15 |
| Figure 18 – (Down) Church Santa Maria del Mar: rings used possibly to hold a banner.   | 15 |
| Figure 19 – Connection of a typical iron hook with the rest of the structure. (Viollet-le-Duc, 1854-1868)  | 17 |
| Figure 20 – Schematic view of the connection of a typical iron hook with the rest of the structure. (Viollet-le-Duc, 1854-1868)  | 17 |
| Figure 21 – Milano Cathedral: typical anchorage system of the lateral naves. (Vasic, 2013)   | 17 |
| Figure 22 – Milano Cathedral: typical anchorage system of the main nave (Vasic, 2013)  | 17 |
| Figure 23 – Spatial localization of some French monuments where different types of ties were used.   | 19 |
| Figure 24 – Cathedral Notre-Dame of Reims: Possible locations of temporary ties used during the construction process of one the bays highlighted with arrows. Original drawing of Villard de Honnecourt. | 20 |
| Figure 25 – Reims Cathedral: construction process advancement. (Interpretation of a sketch of Villard de Honnecourt by Choisy, 1899).  | 20 |
| Figure 26 – (Up) Presence of hooks at the upper part of the columns which have been used to support temporary ties in the ambulatory of the choir.   | 21 |
| Figure 27 – (Down) South Aisle: possible temporary ties which have been cut after the completion of the construction.  | 21 |
| Figure 28 – Drawing of the principal nave where the hooks are shown.   | 22 |
| Figure 29 – Principal nave with the tie-system used.   | 22 |
| Figure 30 – Westminster Cathedral, Chapter House: remaining hooks.   | 23 |
| Figure 31 – Sant-Ouen Church: architecture devices to bear the vault thrust. a) With flying arches and buttresses; b) With ties. (from Guadet, 1909)   | 24 |
| Figure 32 – Cathedral Santa Maria de Palma: thrust line analysis. (Rubio, 1912).   | 24 |
| Figure 33 – Basilica San Petronio, Bologna: a) outside; b) inside. Example of combined effect of buttresses and iron ties.   | 25 |
| Figure 34 – Cathedral Santa Maria del Fiore, Firenze: a) outside; b) inside. The long-lasting ties are highlighted in orange.  | 25 |
| Figure 35 – Cathedral Saint-Gervais-et-Saint-Protais of Soissons, France.  | 25 |
| Figure 36 – Rouen Cathedral: iron ties of the arcs, found at the entrance of the Tour du Beurre. (L'Héritier, 2007)  | 26 |
| Figure 37 – Rouen Cathedral : reinforcement of the small columns of the choir. (L'Héritier, 2007)  | 26 |
| Figure 38 – Beauvais Cathedral : External iron ties.   | 27 |
| Figure 39 – Wind forces acting on the external slender buttresses.   | 27 |

|   |    |
|---|----|
| Figure 40 – Plan view of the Cathedral Saint-Gervais-et-Saint-Protais of Soissons. The added strengthening system is shown in red. ....   | 27 |
| Figure 41. Direct Process: the transformation of ore into metal. ....   | 29 |
| Figure 42 – Cathedral Notre-Dame of Rouen: heterogeneity of a typical iron tie observed with a microscope. ....   | 30 |
| Figure 43 – Vincennes Castle: Tensile tests on typical ties. The direct process has been used to design those ties. (Juhin, 2005). ....   | 30 |
| Figure 44 – Hydraulic hammer principle from Rouillard, 2003 and example of a hydraulic hammer still in use in the smith of J. Brösl at Merdzev in Slovakia. ....  | 31 |
| Figure 45 – Indirect process: production of cast iron within a blast furnace with the help of hydraulic blowers. Painting of Henri Bles, “Paysage avec forges”, 16 <sup>th</sup> century. ....  | 32 |
| Figure 46 – Indirect process: refining of the cast iron in order to obtain iron. Painting of Henri Bles. ....   | 32 |
| Figure 47 – Graph that is used to differentiate iron produced with the direct process from the one produced with indirect process thanks to their different chemical composition. (Dillmann, 2006a) ....  | 32 |
| Figure 48 – Partition of the elements and of the phases in function of the reduction process. (Dillmann et al., 2002). ....   | 33 |
| Figure 49 – A) Cut wooden tie; B) Remaining wooden tie. Drawing by Viollet-le-Duc. ....   | 35 |
| Figure 50 – Church Saint-Philibert of Tournus: Example of remaining wooden ties in the narthex. ....  | 35 |
| Figure 51. Picture of Mallorca Cathedral from est view. ....  | 37 |
| Figure 52 – Mallorca Cathedral: plan at roof level (a), transverse section (b), longitudinal section (c) and façade (d). ....   | 38 |
| Figure 53 – Construction stages of Mallorca Cathedral. (González et al, 2008) ....  | 40 |
| Figure 54 – Arrangement of the stone blocks of the octogonal piers. (From Gonzáles, 2008). ....   | 41 |
| Figure 55 – Presence of dead weights placed over the transverse arches and central vault keystones. (Roca, 2001). ....  | 42 |
| Figure 56 – Double battery of flying arches. (Roca, 2001) ....  | 42 |
| Figure 57 – Deformed shapes of the different bays of the cathedral. The fourth bay is highlighted in red. (Gonzáles, 2008). ....  | 43 |
| Figure 58. Horizontal displacements given in cm of the different bays of Mallorca Cathedral. The displacements obtained for the fourth bay are highlighted in red. (Roca, 2013) ....  | 43 |
| Figure 59 – Construction process of the fourth bay from historical data. (Gonzáles, 2008) ....  | 46 |
| Figure 60 – Photo-elastic analysis (Mark, 1982). ....   | 47 |
| Figure 61 – Thrust line analysis by means of the static graphic method (Rubío and Bellver, 1912). ....  | 47 |
| Figure 62 – Thrust line analysis by means of computational programming (Maynou, 2001). ....   | 47 |
| Figure 63 – Distribution of the principal construction stresses for a typical bay of Mallorca Cathedral for two different analyses: same stiffness for the material of buttresses and piers (a) and a significant higher stiffness for the piers compared to the one of the buttresses. ( Roca, 2001). .... | 49 |
| Figure 64 – Collapse mechanism for a gravity load factor of 1.7 given with GMF (Salas, 2002). ....  | 50 |
| Figure 65 – Stresses and deformed shape of the GMF model corresponding to a gravity load factor of 1.7 in the case for which the upper battery of flying arches has been neglected (Salas, 2002). ....  | 50 |
| Figure 66 – Stress distribution obtained for the GMF model where extra weights are not considered. The gravity load factor in that case is equal to 0.9 (Salas, 2002). ....   | 50 |
| Figure 67 – deformed shape obtained for the same model of Figure 66. (Salas, 2002). ....  | 50 |
| Figure 68 – 3D and 2D geometrical models of a typical bay. (Clemente, 2002). ....   | 51 |
| Figure 69 – Collapse mechanism of the structure and distribution of tensile damage under gravity load considering a smeared crack model and a small strains/small displacements formulation for the 2D and the 3D models (Clemente, 2006). ....   | 52 |
| Figure 70 – Influence of the masonry tensile strength on the collapse gravity load multiplier for 2D smeared crack model and 2D localized damage model. (Clemente, 2006). ....  | 52 |
| Figure 71 – Comparison of the tensile damage state for (a) an instantaneous analysis (deformation factor of 300) and (b) a sequential analysis involving two stages (deformation factor of 50). (Clemente, 2007) ....   | 53 |
| Figure 72 – Implemented correction of the location of the upper part of the structure after the completion of the first stage. ....   | 55 |

|  |    |
|--|----|
| Figure 73 – Simulation of the construction process of the 4 <sup>th</sup> bay of Mallorca Cathedral. Deformed shape with horizontal displacements contours are presented on the left whereas tensile damage contours are presented on the right (Roca et al, 2013) .   | 57 |
| Figure 74 – Construction process simulation with geometric non-linearity: (a) deformed shape (x50) with horizontal displacement contour (left) and tensile damage (right) for a participation ratio of 0.875, (b) deformed shape (x10) with horizontal displacement contour (left) and tensile damage (right) for a participation ratio of 0.975 (Roca et al, 2013). | 58 |
| Figure 75 – Evolution of the horizontal displacement at the top of the pier in function of pseudo-time for different participation ratios and for linear (a) and non-linear (b) geometry assumptions. (Roca et al., 2013)  | 58 |
| Figure 76. Long term creep behavior: horizontal displacements at the top of the pier vs. time obtained for three different participation ratio values a) obtained for the whole analysis; b) around the neighborhood of the monitoring period. (Roca et al., 2012)   | 59 |
| Figure 77 – Previously taken picture where the two remaining ties in the northern lateral nave are visible (highlighted in orange).  | 62 |
| Figure 78 – Northern nave, bay 7-8, exterior. A special interest must be taken on the almost perfect rectangular shape of the lower remain and the damage found in the surroundings of the upper one.  | 63 |
| Figure 79 – Northern nave, bay 6-7, exterior. Remaining upper iron tie, and lower tie remain with a rectangular shape.   | 63 |
| Figure 80 – Northern nave, bay 4-5, exterior. Presence of damage in the surroundings of the ties anchorages.   | 63 |
| Figure 81 – Southern nave, bay 4-5, exterior. Remaining iron hook attached to the vault.   | 63 |
| Figure 82 – Example of iron hook that linked the auxiliary iron tie with the masonry work.   | 64 |
| Figure 83 – Example of sawn ties located near the springing of one of lateral vaults: exterior.  | 64 |
| Figure 84 – Example of sawn ties located near the springing of one of lateral vaults: interior.  | 64 |
| Figure 85 - mapping of the ties remains locations: interior.   | 65 |
| Figure 86 – mapping of the ties remains locations: exterior.   | 66 |
| Figure 87 – Existing AutoCAD elevation of the south nave based on the photogrammetric study of Mallorca Cathedral. Possible remains of ties anchorages are highlighted in red on the lower pictures.   | 67 |
| Figure 88 – Plan view of Mallorca Cathedral with the bays designation.   | 68 |
| Figure 89 – Cut A-A: South lateral nave, exterior elevation  | 69 |
| Figure 90 – Cut B-B: South lateral nave, interior elevation  | 70 |
| Figure 91 – Cut C-C: North lateral nave, interior elevation  | 71 |
| Figure 92 – Cut D-D: North lateral nave, exterior elevation  | 72 |
| Figure 93 – Overview of the model with the two auxiliary ties.   | 75 |
| Figure 94 – Corresponding FEM mesh: 3D tetrahedral elements for the masonry, 2D truss elements for the ties.   | 75 |
| Figure 95 – Definition of the different sets of the present model and their localization.  | 76 |
| Figure 96 – Location of the ties anchorages: (a) outside the masonry; (b) inside the masonry (they are represented in dark green and blue).  | 78 |
| Figure 97 – Schematic view of the anchorage system of an iron hook within the masonry (from Viollet-le-Duc, 1854-1868).  | 79 |
| Figure 98 – Localization of the tensile damage after the second stage of construction for 2 different positions of the anchorage: (a) outside the masonry; (b) inside the masonry. Only the lower tie is activated.  | 79 |
| Figure 99 – Nodes considered to calculate the averaged correction of the upper part (black line below the arrows).   | 82 |
| Figure 100 – Exponential softening law in tension and compression considering finite fracture energies in tension and compression.   | 83 |
| Figure 101 - Evolution of the absolute horizontal displacement of the nodes on the orange line in function of the length of the upper part of the construction after the completion of the first stage (m).  | 84 |
| Figure 102 – Evolution of the horizontal displacement (absolute value) at node 5383 after each step four the four different configurations.  | 87 |
| Figure 103 – Ratio $\frac{\text{horizontal displ. with no tie} - \text{horizontal displ.}}{\text{horizontal displ. with no tie}}$ expressing the restrain effectiveness of each ties configuration. The values are given in %.   | 87 |
| Figure 104 – Overall tensile force taken by the ties in each configuration and after each phase of construction.   | 90 |

|  |     |
|--|-----|
| Figure 105 – Comparison of the tensile damage contour and the deformed shape at the end of the first stage for two different configurations. The principal differences are shown by an arrow. ....   | 91  |
| Figure 106 – Comparison of the tensile damage contour at the end of the third stage for two different configurations. The principal differences are shown by an arrow. ....  | 92  |
| Figure 107 – Calibration of the retardation time for the lower tie configuration. ....   | 94  |
| Figure 108 – FE simulation of long-term creep deformation: comparison of the increase of the horizontal displacement at the top of the pier for the lower tie configuration and for the one with no tie. a) Overall results; b) zoom of the curves between 0 and 600 years; c) zoom of the curves on the neighborhood of the monitoring period. .... | 95  |
| Figure 109 – Viscoelasticity model: (a) Maxwell chain schematization, (b) strain, (c) stress and (d) stiffness time dependent laws. (Roca et al., 2013).....   | 111 |
| Figure 110 – Composite damage surface adopted for the masonry (Roca et al., 2013). ....  | 113 |

## LIST OF TABLES

|  |     |
|--|-----|
| Table 1 – Approximate masses of iron used in the cathedrals of Rouen and Troyes with the assumption of a cost of iron proportional to its mass. ....   | 7   |
| Table 2 – Mechanical properties of wrought iron given in the literature. ....  | 34  |
| Table 3 – Main chronological events of Mallorca Cathedral. ....  | 40  |
| Table 4 – Mechanical properties of the materials used by Clemente, 2002. ....  | 51  |
| Table 5 – Material parameters implemented in the model. ....   | 55  |
| Table 6 – Heights of the remains of the upper ties from the capital for the 4 <sup>th</sup> bay. The results are given in meters and have been measured from the top of the capital of the columns which will be the reference for the study developed later. .... | 73  |
| Table 7 – Heights of the remains of the lower ties from the capital for the 4 <sup>th</sup> bay. The results are given in meters and have been measured from the top of the capital of the columns. ....   | 73  |
| Table 8 – Ties area assumed from the results of the photogrammetric study (unit: cm <sup>2</sup> ). ....   | 73  |
| Table 9 – Width of the remaining ties measured on the pictures and the corresponding area is a square section is assumed (unit: cm and cm <sup>2</sup> ). ....   | 74  |
| Table 10 – Assumed heights from photogrammetric, photographic and laser data and the final heights chosen in the model. All the values are given in meters. ....   | 77  |
| Table 11 – Materials properties used in the model. ....  | 80  |
| Table 12 – Horizontal and vertical corrections applied on the nodes of the upper-part after the first stage of the sequential analysis with respect to the reference axis of GID. ....   | 85  |
| Table 13 – Horizontal and vertical displacements found at the top of the pier after each stage for different ties configurations (the results are given in meters). ....   | 85  |
| Table 14 – Horizontal and vertical displacements found at the connection between the upper tie and the pier after each stage for different ties configurations (the results are given in meters). ....   | 85  |
| Table 15 – Horizontal and vertical displacements found at the connection between the lower tie and the pier after each stage for different ties configurations (the results are given in meters). ....   | 86  |
| Table 16 – Mechanical behavior of the ties, considering a small strains/large displacements configuration. ....  | 89  |
| Table 17 – Outcomes of the models calibration together with the data collected on-site. ....   | 95  |
| Table 18 – Horizontal and vertical corrections applied on the nodes of the upper-part after the first stage of the sequential analysis considering a tie cross-section of 50 cm <sup>2</sup> . ....  | 97  |
| Table 19 – Horizontal and vertical displacements found at the top of the pier after each stage for different ties configurations considering a tie cross-section of 50 cm <sup>2</sup> (the results are given in meters). ....                                     | 97  |
| Table 20 – Comparison of the mechanical behavior of the ties considering a tie cross section of 25 cm <sup>2</sup> and a tie cross-section of 50 cm <sup>2</sup> . ....  | 98  |
| Table 21 – Horizontal and vertical displacements at node 5383 obtained either until the end of the third stage, or either until divergence of the solution. Configuration with no tie. ....  | 99  |
| Table 22 – Horizontal and vertical displacements at node 5383 obtained either until the end of the third stage, or either until divergence of the solution. Configuration with lower tie. ....   | 99  |
| Table 23 – Comparison of the tensile damage contour for either the laster converging step or the end of the third stage for 2 configurations. ....   | 100 |



This page is left blank on purpose.

## **1. INTRODUCTION**

### **1.1. General**

Preserving historical constructions in Today's society is of primary importance from a cultural point of view as well as an economic one. This preservation should be carried out in such a way that the restoration of the monuments is both efficient and respectful which can only be achieved with sufficient knowledge of that monument, and especially in structures. Recently the development of complex reliable numeral tools such as the Finite Elements Method has allowed to have a better structural understanding of constructions in general (Roca et al., 2010). Nevertheless its specific use in historical construction is still a challenge in numerous cases when for example the long-term creep behavior of the masonry or the construction process have significant repercussions on Today's state of the structure. The latter is especially true for monuments built during the gothic era for which the stable equilibrium state of the structure has been only reached after the completion of the overall construction: before that, the master builders had to find temporary ways to maintain the stability of the parts of the building. Temporary devices such as wooden and iron ties were commonly used in Europe to withstand the unbalanced thrust of the arches and vaults of the lateral naves on the piers before the completion of the main nave.

The case of Mallorca Cathedral, one of the most impressive gothic monuments of the Mediterranean area, is a perfect example of the combined consequences of both the construction process and the long-term creep behavior of the masonry. Numerous structural studies of the cathedral have already been carried out during the last two centuries and recently more and more realistic models of the cathedral have been implemented considering the Finite Elements Method. Nevertheless, even if the construction process has been consider in the most recent models, it was assumed that no auxiliary structural devices were used: it was in effect assumed that the initial tensile strength of the masonry was able to carry the horizontal thrust of the lateral naves but at the cost of significant deformations and displacements of the unfinished structure (Clemente, 2006; Roca et al., 2013, 2012). After some on-site investigations, several elements that remind remains of ties have been located for each bay of the cathedral together with two remaining ties. From these visual observations, the use of temporary iron ties during the construction process couldn't be disregarded. The main purpose of the present work is to consider the use of temporary ties during the construction process of one of the typical bays of the cathedral and thus implement them within the already existing Finite Elements model.

### **1.2. Objectives**

The main objectives of the present work are the following ones:

- To carry out a historical research on the use of iron as a structural element in gothic architecture with a focus on iron ties;

- To give useful information on the structure of Mallorca Cathedral and to summarize the previous studies of a typical bay of the monument;
- To carry out a thorough on-site investigation of the cathedral, including a mapping of the ties remains;
- To estimate the locations of the ties as well as their dimensions and mechanical properties;
- To Study the FEM modeling technique and constitutive equations to be used for the model;
- To upgrade the already existing model by considering the use of temporary ties during the construction process;
- To perform an analysis of the long-term deformation of the bay by means of a time-dependent analysis;
- To carry out two parametric studies concerning the influence of the ties cross-section and the influence of the masonry tensile strength on the global behavior of the bay;
- To give conclusions on the influence of the construction process and the role of the ties.

### 1.3. Organization

In order to reach the objectives listed above, the present thesis is divided into six different sections which are:

#### **Chapter 1 – Introduction**

**Chapter 2 – The use of iron in gothic constructions.** It is of primary importance to understand the key role that played iron in gothic architecture even if that recognition has only been considered recently. After having given an overview of the different structural iron elements present in gothic architecture with a special focus on temporary and long-lasting iron ties has been done. The case of wooden ties is also briefly discussed in this part.

**Chapter 3 – Mallorca Cathedral: past studies.** This part gathers useful data on Mallorca Cathedral, such as its history, its dimensions and features and the existing damage and structural alterations. A special interest has been taken on the construction process of the 4<sup>th</sup> bay of the cathedral. In this part is also presented a brief of several previous works based on numerical models as well as their main conclusions.

**Chapter 4 – On-site evidences of the use of auxiliary ties in the construction process of Mallorca Cathedral.** A thorough on-site investigation of the presence of ties remains has been carried out. This part presents the information collected during this investigation.

**Chapter 5 – Structural analysis.** From the visual inspection performed, a numeral Finite Elements model taking into account the use of temporary iron ties during the construction process of the 4<sup>th</sup> bay

of the cathedral has been developed. After a description of the model and the modelling strategy considered, the results obtained for each ties configuration and after each stage of the model are presented. This part also includes two parametrical studies based respectively on the influence of the ties cross-section and the influence of the tensile strength of the masonry.

**Chapter 6 – Conclusions.** Finally this last part gives the mains conclusions of the present study, together with some recommendations for possible further works.

This page is left blank on purpose.

## 2. THE USE OF IRON IN GOTHIC CONSTRUCTIONS

Even if plenty of authors, architects and engineers of the 18<sup>th</sup>, 19<sup>th</sup> and 20<sup>th</sup> centuries have decried iron as one of the principal structural elements in the construction of gothic monuments, recent and thorough researches (L'Héritier, 2007, L'Héritier et al. 2007, 2005; Taupin, 1996) have shown it has been currently used for the construction of these monuments since the very beginning of the gothic era. Iron has been used both as a temporary and a long-lasting device, and for structural and non-structural means. In effect, thanks to its mechanical properties, it was the key element for gothic architects and builders to realize their dream of space, lightness and height.

The first part of this chapter will treat about the past controversy concerning the use of iron in gothic monuments. The second part will focus on the purpose of metallic elements in the construction of gothic constructions. Key dates will also be given in order to replace the use of iron in a chronological scale. Afterwards an overview of the different iron elements, structural and non-structural, with a focus on ties will be given. Finally a succinct description of wooden ties will be done.

### 2.1. Past controversy

Before starting properly the study of the use of iron ties in the construction of gothic monuments, it is of primary importance to understand that its acceptance as one of the principal elements of such constructions is relatively new. In the past three centuries and even before, numerous architects and historians underestimated the importance of the use of iron in construction when they didn't completely decry it. Plenty of critics have been done on its non-durability due to rust problems and consequently the bursting of the stone due to the considerable extension of corroded iron, its subjective non-aesthetic, and above all its poor value as a construction material compared to the nobility of stone and its rupture with traditional ways of construction. Iron was also considered by some specialists as an 'easy' way to build, a trick that should not have been used for the construction of the great gothic monuments. In his 'Traité Complet pour Bâtir' written in 1568, the well-known architect Philibert Delorme considered that the mason masters of the gothic era used in ways that were abusive iron in order to save lithic material:

"If one would have stopped them to use iron in the construction, they would have been forced to build the walls thicker and with a greater force than they are". (Delorme P., 1568)

In his book 'Elements and Theory of Architecture', published in 1909, Julien Guadet, a French architect who fiercely defended the use of iron ties, summarized the critics done on the use of ties as follows:

"What didn't one say about iron ties? A whole intransigent school hadn't enough curses for this practice that allowed to use others means that the ones considered as only admissible. One said that the vault, a masonry work, must not in any case take everything else than masonry: that it is not

overcome a difficulty to suppress it with the use of a trick, to suppress the vault thrust is the very negation of the vaults architecture.” (Guadet, J., 1909)

Later, in 1841, a paper was written and included in the important French ‘Revue Générale de l’Architecture et des Travaux Publics’ (General Review of Architecture and Public Works) about the use of iron in gothic monuments. The main goal of this article was to gather examples on the disorders due to the use of iron. The author of this article, M. Gau, wrote those lines:

“The use of iron as a means of consolidation, is not only unnecessary but also that its use is in numerous cases, on the contrary, damageable for the construction. [...] We hope that the persons of the Commission will let them persuade to abandon a theory that would lead, with great expense, to the acceleration of the destruction of the monuments.” (Gau M., 1841)

Nevertheless he didn’t completely deny the use of iron in gothic constructions even if he only considered its use as punctual:

“The use of iron was scarcely encountered in the constructions of gothic monuments of early periods. But with the evolution of gothic style and the alleviation of the shapes, one sometimes has been reduced to use iron in order to increase the bearing capacity of some parts or in the hope of preventing the effects of soil settlements and other causes of tilting.” (Gau M., 1841)

To justify his convictions, he attached to his article letters of two architects: M. Zwirner architect in charge of the restoration of Cologne Cathedral and M. Landon, Architect of the town of Beauvais who wrote:

“In general, the use of iron in gothic monuments can be summarized to few things”.

The careful studies of gothic architecture led by Viollet-le-Duc in his ‘Dictionnaire Raisoné de l’Architecture Française du XIème au XVIème siècle’ changed significantly the way of considering iron in the gothic constructions. Iron is no more seen as a dangerous material but, on the contrary, as a useful one that serves completely the goals of this type of constructions. With the support of well-documented plans and drawings he showed the importance of iron elements as structural and non-structural devices. Nevertheless, even if he understood this importance, he considered the gothic architecture as lithic essentially: the stone was the principal structural element and iron was only a secondary device. Even if Julien Guadet, as it was already mentioned above, defended the use of iron ties in gothic construction, it is only at the beginning of the 90s that the recent researches on Beauvais Cathedral carried out by M. Jean-Louis Taupin, Architect of the monuments of France, have proved the importance of the presence of iron elements in gothic construction and their essential structural roles (Taupin, 1996). From his thorough work started a new era of researches focused on that field. One can mention the researches of Maxime L’Héritier (L’Héritier, 2007, L’Héritier et al 2007, 2005) who estimated the tremendous quantity of structural and non-structural iron elements present in several French gothic buildings: it can be considered that many tens of tons of iron in a huge church were used and many tons were used for smaller churches. These estimations have been carried out

from inspection but also from historical data such as the account of the construction site. Half of the iron was used for the construction of the stained glasses. It is also considered that the cost of the iron used in the construction was 2% to 4% of the total price. Even if it was generally used, iron was not cheap and that is why iron elements that no longer served were reused.

Figure 1 gives a comparison of the cost of the different iron elements of two typical gothic cathedrals, based on the work of L'Héritier, 2007. By assuming that the cost of each element is proportional to its mass, it is possible to estimate the quantity of structural iron used for the construction of these two monuments (Table 1).

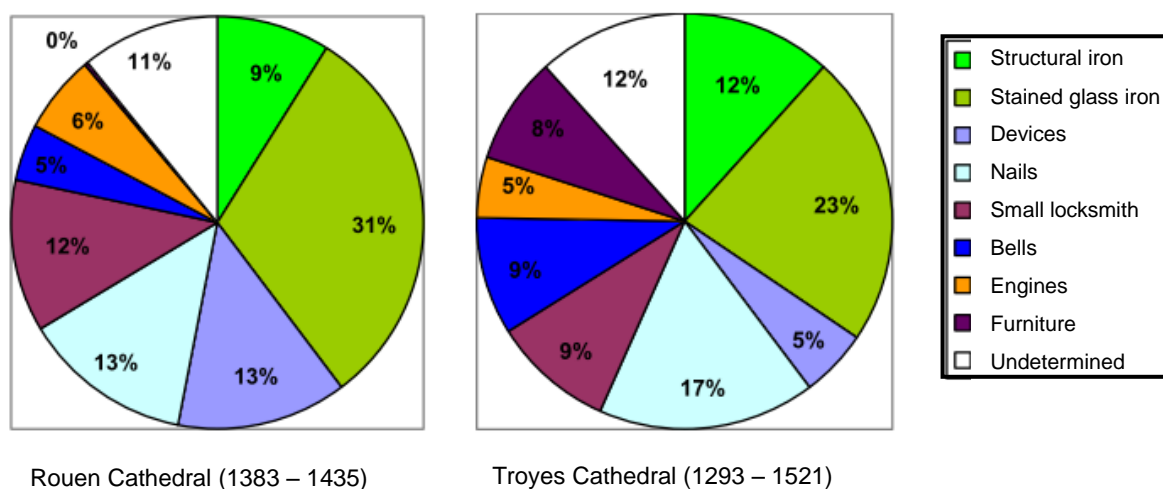


**Figure 1** – Part of the different types of expenses for a smith from the accounts of the fabrics of the cathedrals of Rouen and Troyes (L'Héritier, 2007).

|  | Cathedral of Rouen | Cathedral of Troyes |
|--|--------------------|---------------------|
| Approximative total mass of iron used based on the expenses                        | 48.4 tons          | 108.7 tons          |
| Approximative mass of iron used only for structural purposes based on the expenses | 4.4 tons           | 13 tons             |

**Table 1** – Approximate masses of iron used in the cathedrals of Rouen and Troyes with the assumption of a cost of iron proportional to its mass.

## 2.2. Overview of the different iron elements present in Gothic Architecture

Iron is one of the main structural elements in gothic architecture. It is possible to find iron elements almost in every single part of gothic monuments, from the stained glass windows to the pinnacles. Its structural roles are obvious; nevertheless it can be useful to remind them in the following. First of all, iron and more generally metallic elements are easier to shape than stone elements, therefore where small pieces with a specific design are needed, it is natural to use those metallic elements. Secondly and most importantly, masonry has a very low tensile strength which is not the case for iron. Thus



structural iron elements such as iron ties, bars in stained windows, were used to release the tensile stresses from the masonry. In a more complex way, patterns of iron elements were also used to confine a whole part of a monument such as the towers located at the transepts cross-section or even the whole nave or transept of a church (L'Héritier, 2007). James H. Acland in his book 'Medieval Structure: the gothic vault' published in 1972 gives useful examples of the use of iron in the construction of gothic monuments:

"Improvement of the smelting and forging of iron made wrought iron a useful metal tool to resist hidden strains. As the piers and buttresses were raised, window bars of wrought iron to hold the glass were grouted across the window openings. In some particularly delicate structures, iron reinforcement was used in the fabric: a chain was embedded in the walls of the Saint Chapel and the vaulting ribs were stiffened with iron bars. Iron cramps and dowels were commonly used to clamp together the delicate fabric of spires. Iron was boiled in linseed oil, tallow, resins, and fats to retard its rusting. By the fifteenth century it was quite customary to use tension bars of wrought iron to take the thrust of vaults and arch rings." (Acland, 1972)

From this quotation, it is also interesting to consider the means used to try to stop the corrosion.

In the following, a succinct description of structural and non structural will be carried out. Then will be developed an entire part on the iron ties with a focus on their main roles, their dimensions, their specificities. Several examples of the use of temporary and long-lasting iron ties will be also given to prove that their use was not scarce but on the contrary widespread in Europe during the gothic period.

### **2.2.1. Structural elements**

Structural iron elements can be divided roughly into seven different categories: bars in stained windows, clamps, studs, dowels, hooks, chaining system and finally ties. In this part, a focus will be done on the first six categories.

#### *Bars in glass stained windows*

One of the main goals of gothic architecture was to reach tremendous height with a maximum surface of openings. This led to the design of wider and wider stained glass windows. This larger plane surfaces are exposed to strong wind pressure which would have been high enough to destroy the brittle and non-resistant stained glass windows. For example, it has been proved that for Beauvais Cathedral, for which the wider stained glass window reaches an area of 110 m<sup>2</sup>, a frontal wind of 100 km/h leads to a thrust of 12.7 tons (Timbert and Dillmann, 2010). To bear those tremendous forces and to maintain in place the windows, iron bars were used. These elements are able to carry the tensile stresses produced by the wind. They also bear the weight of the stained glass which, for a large surface of openings, is not able to carry its self-weight. Those bars can be individual elements

with only one span or can go through the masonry in between the openings, leading to a chaining system (See also Chaining system).

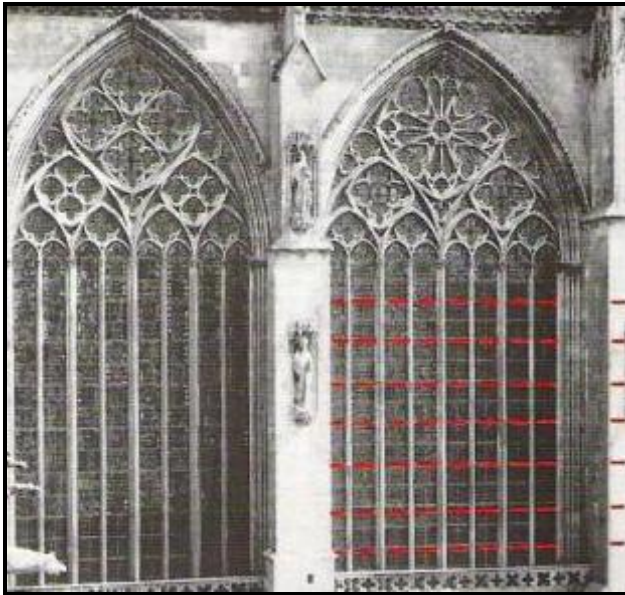


**Figure 2** – Saint-Julien Cathedral, Le Mans.

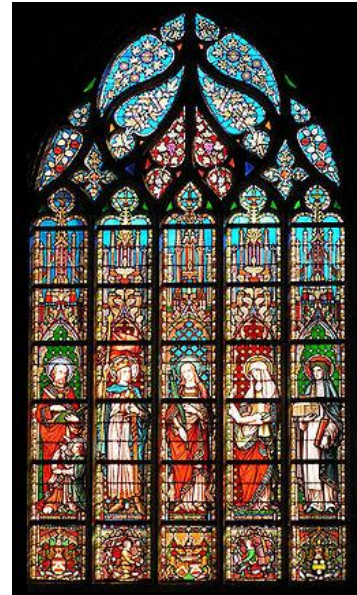


**Figure 3** – Church of Notre-Dame des Victoires, Bruxelles: Example of bars reinforcing a stained glass window.

### *Clamps*

Clamps are metal pieces of relatively small dimensions that were used to link together two stones elements. There are often present in the pillars of churches and cathedrals in order to consolidate them. It is also possible to find them in the slender spires. In that case, their main goal was to help the masonry withstand the wind forces.



**Figure 4** – Cathedral Notre-Dame of Chartres: example of a clamp.

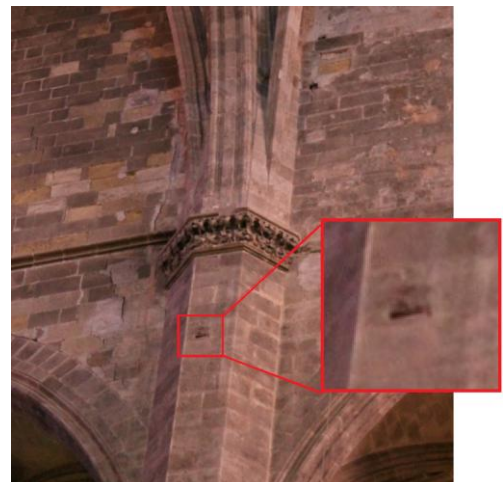


**Figure 5** – Cathedral Santa Maria of Palma.



**Figure 6** – Chartres Cathedral: Clamps within the masonry of one of the spires.

### *Studs*

A stud is a discrete vertical iron piece that serves to link together monolithic blocks of stone. This element allows the connection between two stone elements without compromising their natural settlement. There were used also to fix the pinnacles with the rest of the monuments. They were also used, even if it is not known for the moment if it was a standardized technique or not, to reinforce the keystone of the vault and even the whole vaulting system (Timbert and Dillmann, 2010). Even if discussing about this topic is out of this work, it is interesting to note that the presence of such an element at this location can change the understanding of the way vault carries loads.

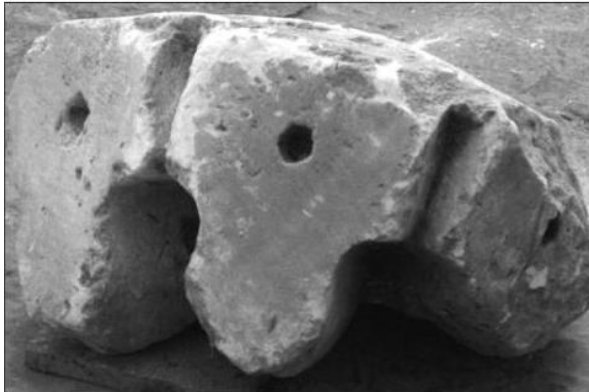
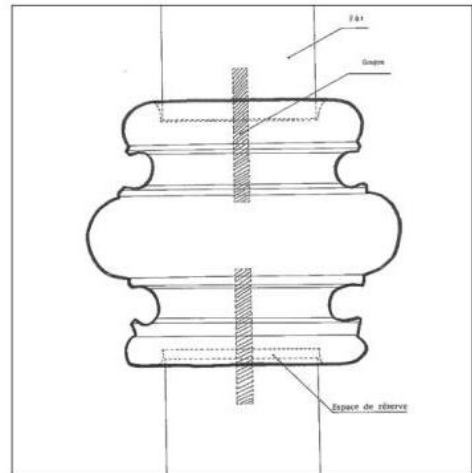
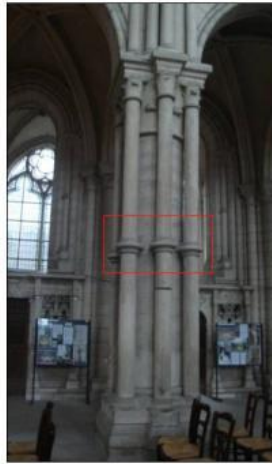


**Figure 7** – Cathedral Notre Dame of Laon: Stud in a vertical element.

**Figure 8** – Schematic view of stud and rings.

**Figure 9** – Cathedral Notre-Dame of Noyon: existing proof of the use of studs within the vaulting system.

### *Dowels*

Unlike the previous elements that were used principally for stones, a dowel is a piece of metal used to reinforce timber frameworks in gothic architecture since the 13<sup>th</sup> century. Their use became frequent during the 14<sup>th</sup> century which is contradiction with what Viollet-le-Duc wrote in his 'Dictionnaire Raisonné':

"For the framework, iron was used only very late and it was not used during all the gothic period."  
(Viollet-le-Duc, 1854-1868)



**Figure 10** – Cathedral Notre-Dame of Rouen: Dowel used for the construction of the wooden framework.

### *Hooks*

Hooks are also another very important device in the gothic architecture: they were used to support iron ties working in tension. As it will be explain in details later, the hooks allow a certain flexibility of design: ties can be removed after the construction phases for example or maintain in place. Nevertheless one has to be careful about the goal of these hooks. In effect as it was observed by Fitchen in his book 'Construction of Gothic Cathedrals – A Study of Medieval Vault Erection' that:

“Not all the iron hooks that remain in medieval churches were necessarily placed there for attachment of tie-rods or tie-beams.” (Fitchen, 1981)

Indeed hooks were also used as temporary devices in order to hoist the materials during the construction as in Chartres Cathedral. They were also employed as non-structural elements at which hangings were attached.





**Figure 11** – Cathedra Notre-Dame of Chartres: hook.



**Figure 12** – Church Santa Maria del Mar, Barcelona.

### *Chaining system*

Even if a chaining system is not a proper element but more an assembly of several ones, its structural role is of outmost importance. The best definition of chaining has been given by Viollet-le-Duc: it concerns the ties beams in wood, the patterns of iron clamps designed as a link of a chain, and continuous iron bars supporting the stained glass windows and inside the thickness of the walls. Its main goal is to prevent the masonry structure from spreading out, tilting and dislocating. (Viollet-le-Duc, 1854-1868) Iron chaining appeared at the end of the 12<sup>th</sup> century and progressively replaced wooden chaining systems thanks to its longer lifetime. Nevertheless wooden chaining system was still in use until the middle of the 13<sup>th</sup> century, essentially in militaries and civil constructions. Maxime L'Héritier in his thesis gives useful examples of the use of chaining systems in gothic architecture such as for the façade of Strasbourg Cathedral which “from the base up to the height of spire base, is chained carefully at every level, by the means of long flat iron bars, designed within [the masonry]” (L'Héritier, 2007). He also describes another goal of the chaining system that wasn't described by Viollet-le-Duc: it was also employed as a temporary device during the construction process in order to withstand the thrust of the collateral arches on the interior pillars. They were removed afterwards when the structure was completed. This kind of chaining was usually in wood because it was easier to remove than iron.



**Figure 13** – Church Saint-Ouen of Rouen: Example of a chaining system.

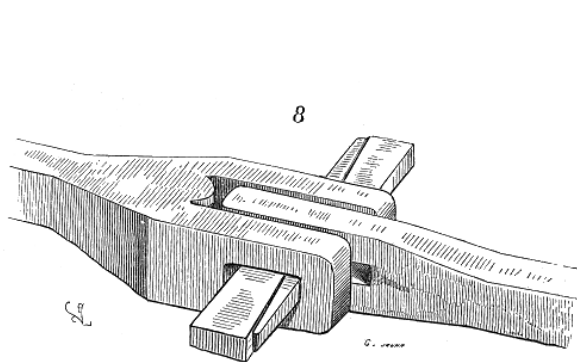


**Figure 14** – Detail of a possible connection between two metallic elements constituting a chaining system. (Viollet-le-Duc, 1854-1868)

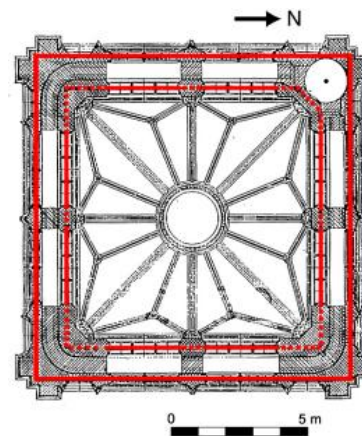


**Figure 15** – Church Saint-Ouen of Rouen : Examples of chaining in the second floor of the crossing tower. (L'Héritier, 2007; Moufle D., 2000)

### 2.2.2. Non-structural elements

Nevertheless not all the iron elements present in a gothic monuments have a structural role and thus one must be careful during an inspection not to confound them with a structural one, which is a mistake easy to make because of the relative darkness of the place and the difficulty to reach the element. Below are given some examples of non-structural elements found in Santa Maria del Mar in Barcelona.

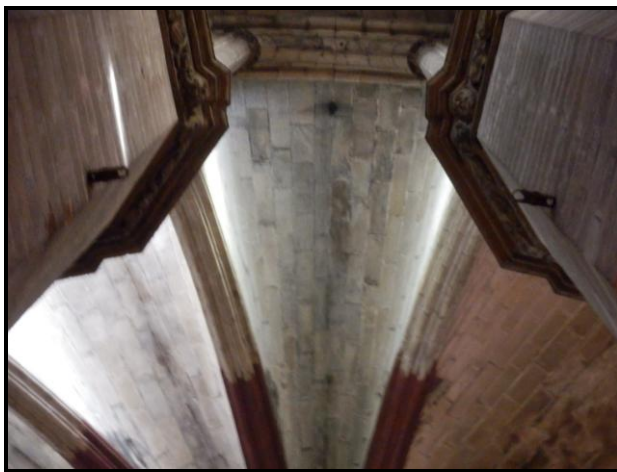
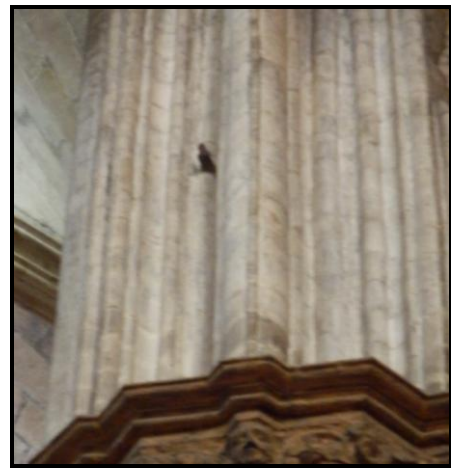


**Figure 16** – (Up, left) Church Santa Maria del Mar: rings used possibly to hold a torch.

**Figure 17** – (Up, right) Church Santa Maria del Mar: hook.

**Figure 18** – (Down) Church Santa Maria del Mar: rings used possibly to hold a banner.



## 2.3. Iron ties

Now that an overview of the principal existing iron elements employed in the construction of gothic architecture has been done, the following will focus exclusively on iron ties. This part, as well as developing the features of this type of elements, will give numerous examples of the use of ties in gothic constructions. It is of outmost importance to provide these detailed examples in order to fully understand not only their structural role but also their widespread utilization in Europe.

### 2.3.1. Definition

Once again the definition of the purpose of iron ties will be based on Viollet-le-Duc's work. He defined them as follow:

"[A tie] is a piece of metal or wood that maintains the spacing of the truss beams of a wooden frame, or the tilting of two parallel walls, or the thrust of an arch. [...] To close their vaults, the medieval builders used temporary ties in order to avoid thrusts until the piles were loaded. These ties were usually made of wood, and were sawed as closed as possible to the intrados of the base of the arches when the constructions were finished. In Reims Cathedral, these ties were made of iron, with rings at their extremities that were fixed with still existing hooks. There are only few collateral vaults where it is not possible to observe the mark of these ties." (Viollet-le-Duc, 1854-1868)

Even if this definition is very clear, Viollet-le-Duc underestimates the use of iron ties during construction, moreover even if he speaks about the use of temporary ties, not a single word can be found on the use of long-lasting ties. In Sections 2.3.2. and 2.3.3., the main differences of these two types of ties will be discussed. Also Viollet-le-Duc doesn't insist on the fact that ties were the most commonly used iron element in medieval architecture, fact that was recently highlighted by Arnaud Timbert, a French specialist of gothic architecture and researcher at the IRHIS (Historical Research Institute of the Septentrion based in France) (Timbert and Dillmann, 2010). This fact, even if not obvious, is in complete harmony with the constructing ways of these times: the use of centering should have been as restricted as possible and thus other structural techniques were developed during the construction process to counterbalance the thrust of arches and vaults.

Few documents exist on the connection between the tie and the masonry. Hooks and rings have been used in the past to connect these elements together but little is known about the anchorage between these elements and the masonry itself. Viollet-le-Duc discovered an existing means to connect them efficiently with the masonry by using wooden beams inserted longitudinally within the bearing wall (Figure 19 and Figure 20) (e.g. Basilica Saint Marie-Madeleine of Vezelay). Nevertheless parallel techniques should have been developed: the lifetime of wood inserted within masonry was considered as low and thus it seems justify that gothic builders worked on other and more durable solutions. Figure 21 and Figure 22 show examples of the long-lasting ties/masonry connections found in Milano Cathedral (Vasic, 2013).

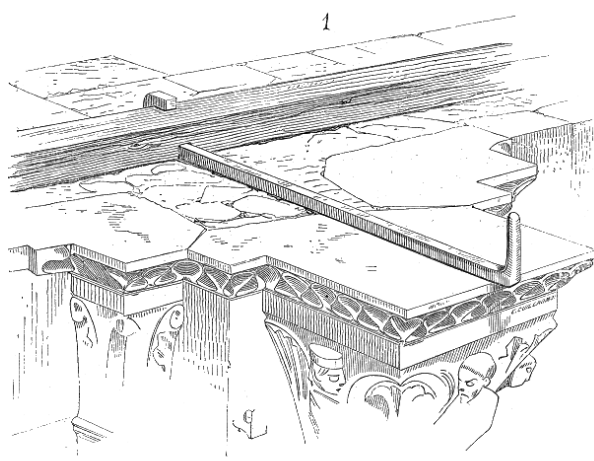


**Figure 19** – Connection of a typical iron hook with the rest of the structure. (Viollet-le-Duc, 1854-1868)

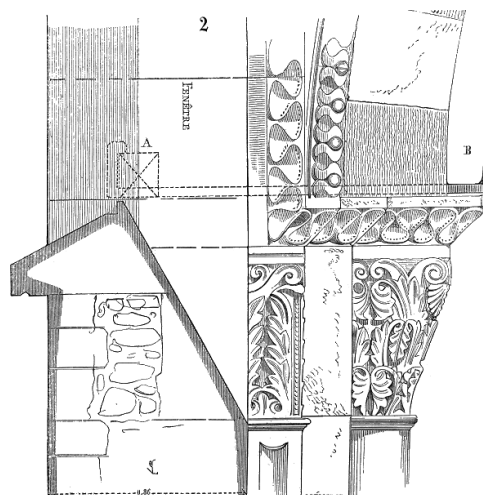


**Figure 20** – Schematic view of the connection of a typical iron hook with the rest of the structure. (Viollet-le-Duc, 1854-1868)



**Figure 21** – Milano Cathedral: typical anchorage system of the lateral naves. (Vasic, 2013)



**Figure 22** – Milano Cathedral: typical anchorage system of the main nave (Vasic, 2013)

A distinction should be done on two different kinds of ties: the temporary ties and the long-lasting ties. Even if they work in a similar way, i.e. bearing in tension horizontal forces, their purpose and thus their design is different. The next parts will explain the main differences between these two elements as well as their advantages. With an idea to show how the use of these two types of ties was widespread during gothic time and later on, several examples taken from different countries will also be given.

### 2.3.2. Temporary ties

#### *Role*

“[Before the adoption of temporary tie-rods of the side aisle vault]many interior piers of churches built at the end of the twelfth century had tilted out of the vertical, provoked by the thrust of the side-aisle vaults before the completion of the structure; for, in order to interrupt the services of worship as shortly

as possible, the builders closed in the vaults as soon as the side aisles were raised, the decentered these vaults, they established a ceiling over the central nave at the height of the triforium, and they were able to move into the church.” (Viollet-le-Duc, 1854-1868)

“The vaults of the side aisles at Amiens and at Reims preserve the mark of their tie-rods links: each of the transverse arches was undergirded by a stringer of wood engaged at one end in the masonry of the pier, at the other end in that of the wall. The metal attachments of tie-rods that were probably of iron are to be seen at Beauvais.” (Choisy, 1899)

Temporary ties were employed to withstand the horizontal thrust of the vaulting and barrel systems during the construction phases of a monument. In effect, a gothic monument is supposed to be stable at the end of its construction. Therefore temporary devices had to be designed in order to bear the existing thrust. Alternatively to the use of centerings that were expensive and difficult to uninstall, gothic builders developed other efficient tools: wooden and iron ties. The former was embedded inside the masonry and then cut after the structure or the part of the structure considered was judged stable. For iron ties, it has been already mentioned that a system of hooks and rings that allows to remove the ties after the construction process was often used. Only suppositions can be done here concerning iron ties directly built-in the masonry. It is possible that the iron was heated locally with fire until it became soft and it was possible to remove it. Once again this idea is a complete supposition. Temporary ties were also used to prevent disorders after decentering during the settlement of the masonry. Nevertheless once the construction is finished and the settlements problems in the masonry seem to have been stabilized, these ties do not present any advantage for the structure anymore: indeed the thrust line can now be taken by the complex structural system of flying arches, buttresses and additional weights such as pinnacles. Choisy and Viollet-le-Duc describe the temporary ties function in those terms:

“In the gothic era, it is employed especially to prevent disorders that occur upon removal of the centering during the period when the masonry is settling. The flying buttress makes the help of the tie-rods superfluous as permanent tension members; their role is limited to the period when the masonry is shrinking.” (Choisy, 1899)

“[Temporary ties] were placed during the course of erection between the double-centering on which the archivolts and the transverse arches were built, and were left in place until the building was completed, that is to say until the moment when the interior piers were charged to the point where the builders no longer needed to fear any buckling produced by the thrust of the side-aisle vaults.” (Viollet-le-Duc, 1854-1868)

Two assumptions can be done concerning the purpose of removing the ties: an economical reason and a subjective aesthetical one. During medieval times, materials such as iron and long wooden ties with a consequent cross-section were expansive and whenever it was possible those elements were reused in other constructions. Concerning the aesthetical reason, it was believed by numerous

persons that the presence of iron ties stopped in a way the greatness and majesty of gothic constructions. Even if this last point is a really controversial one, it might be a reason to explain why ties were removed after the construction process. Up to now, the first example of use of temporary ties has been found in the Basilica Saint Marie-Madeleine of Vezelay in France which was built around the year 1130. The presence of remaining hooks at the top of the arches of the central nave are effectively the proof that temporary ties were employed.

### Examples

The following part is mainly based on photographic evidences of the existence of temporary ties used during the construction process of several pre-gothic and gothic monuments and its main purpose is to show the widespread of this construction technique in Europe as well as interesting features such as the existing types of anchorages, the location of the ties, and how their remains look like nowadays. The sketches and pictures gathered in this part have been utilized to carry out the visual inspection of the evidences of temporary ties used in the construction of Mallorca Cathedral.

Not surprisingly, it is in France, the cradle of gothic architecture, that it is possible to observe a consequent number of gothic monuments where temporary ties were used. The principal nave of the Basilica Saint Marie-Madeleine of Vezelay rebuilt during the 12<sup>th</sup> century, the historical documents of Reims Cathedral as well as the pictures of the aisle naves of the cathedral Notre-Dame of Amiens are representative examples of the use of temporary ties in, at least, the French gothic architecture.

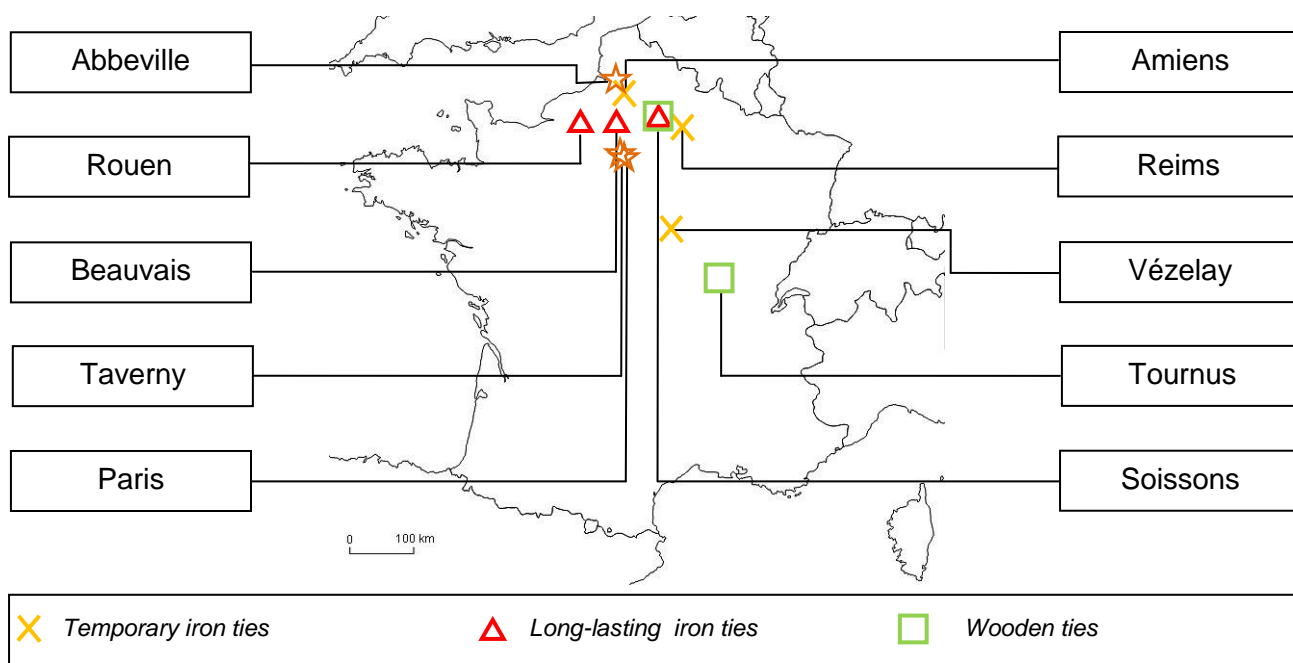


**Figure 23** – Spatial localization of some French monuments where different types of ties were used.

### *Cathedral Notre-Dame of Reims*

Reims Cathedral was built between the 13<sup>th</sup> and the 14<sup>th</sup> centuries and it is one of the gothic monuments for which historical sketches may show possible positions of temporary ties. The sketch presented on Figure 24 has been drawn by the famous medieval artist Villard de Honnecourt who lived in France during the 13<sup>th</sup> century. He is the author of a well-known portfolio of 33 sheets of parchment containing about 250 drawings dating from the first part of the 13<sup>th</sup> century. Nevertheless, even if the shapes indicating with arrows are similar to ties ends, there is no concrete proof that they actually were. One must also understand that the conception of sketches and drawings during medieval times is completely different from the one of today: sketches of a monument may have been adjusted according to the perception of its drawer. In the present case Villard de Honnecourt might have drawn them because he believed it was the good way to build, even if this solution didn't reflect reality. Despite these uncertainties, his drawings were used by authors such as Choisy to have a better understanding on the structural behavior of Reims Cathedral.

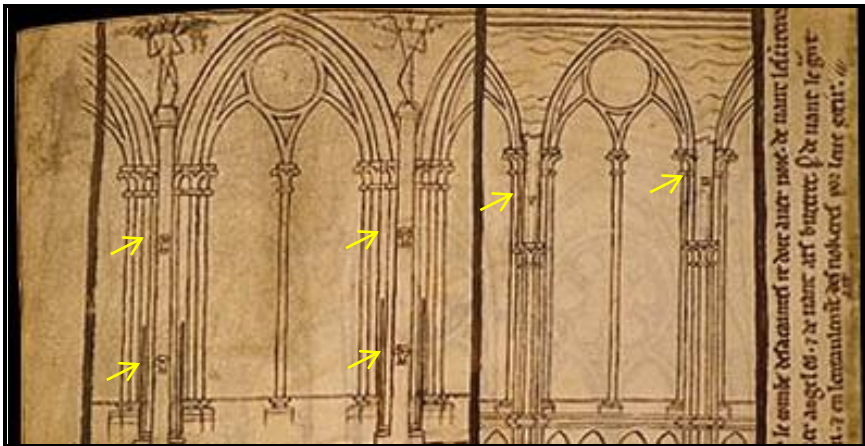


**Figure 24** – Cathedral Notre-Dame of Reims: Possible locations of temporary ties used during the construction process of one the bays highlighted with arrows. Original drawing of Villard de Honnecourt.

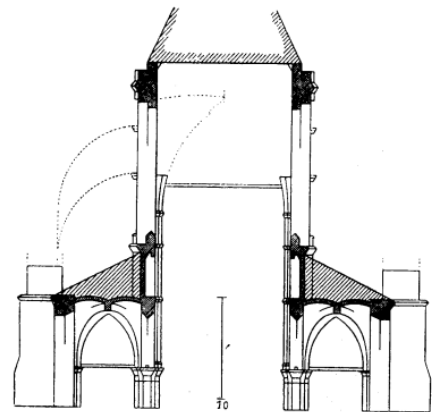
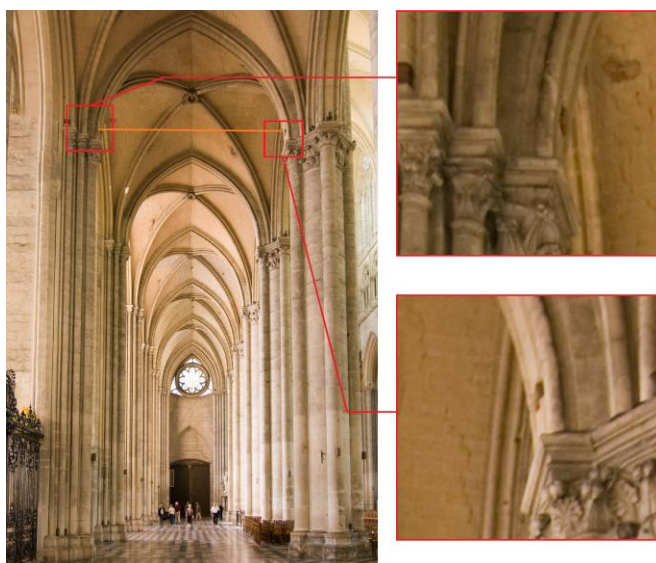
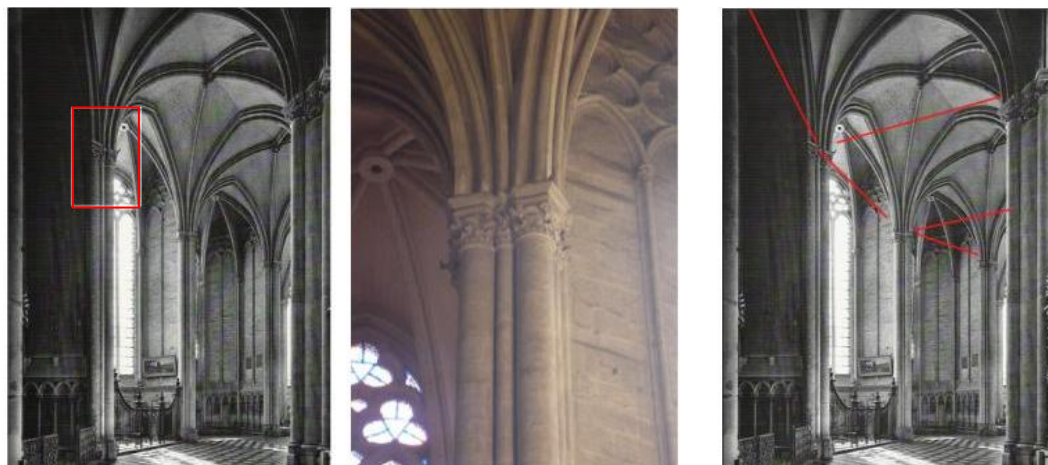


**Figure 25** – Reims Cathedral: construction process advancement. (Interpretation of a sketch of Villard de Honnecourt by Choisy, 1899).

### *Cathedral Notre-Dame of Amiens (1220 – 1288)*

From visual inspections it has been possible to localize the positions of the ties in the ambulatory of the choir and in the lateral naves of Amiens Cathedral. It is worth noticing the differences between the remaining anchorages for these two parts which are very similar to the ones found in Mallorca Cathedral: in the ambulatory they look like iron hooks whereas in the aisle naves black spots can only be seen. The later may be the remaining of ties which have been cut really closed to the masonry wall.





### Cathedral Notre-Dame of Amiens

**Figure 26** – (Up) Presence of hooks at the upper part of the columns which have been used to support temporary ties in the ambulatory of the choir.

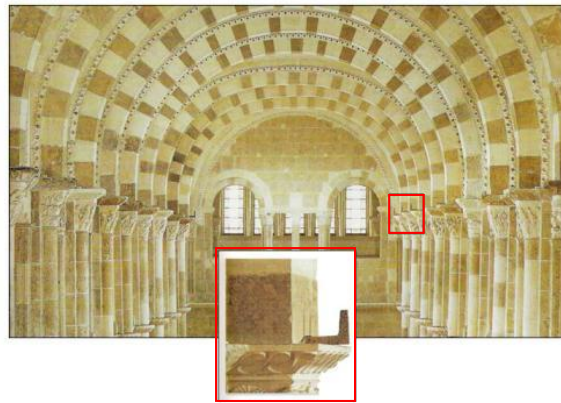
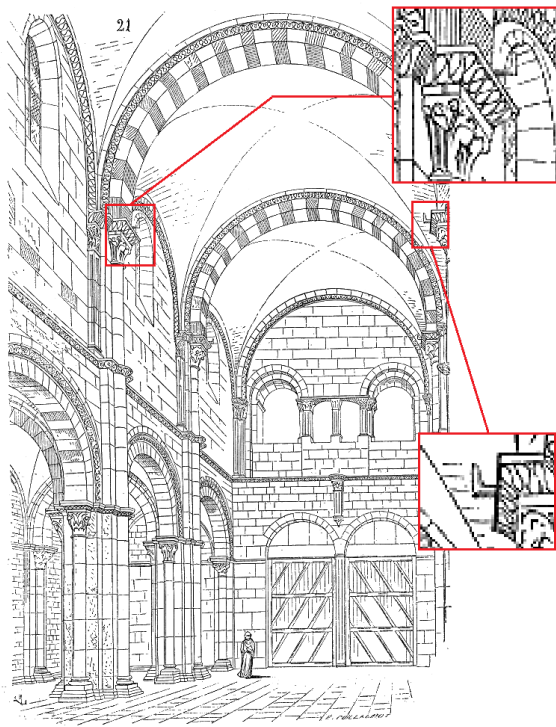
**Figure 27** – (Down) South Aisle: possible temporary ties which have been cut after the completion of the construction.

### *Basilica Saint Marie-Madeleine of Vézelay*

The Basilica of Saint Marie-Madeleine of Vézelay has really interesting features concerning the use of temporary iron ties. First of all, because their use in the main nave is undeniable: in effect it is still possible nowadays to observe the remaining hooks located at the upper part of the capital in the pillars.

“At Vézelay, the high vaults had iron transverse ties, the hooks for which still remain” (Lethaby, 1906)

Vézelay is the proof that this temporary technique was also employed during the construction of the main nave, not only for the lateral ones. Because of its important width, 23.25m, it was not possible for the builders to use normal ties. As it will be seen later in Section 2.3.5. Iron production during medieval times, before the widespread use of the indirect process for the production of iron, large iron pieces were difficult to obtain. Therefore specific iron ties, composed by small elements with a hook at an end and a ring at the other one, were installed instead. This technique is a proof of the great ingenuity of the master builders during medieval times.



**Basilica Sainte Marie-Madeleine of Vezelay, France**

**Figure 28** – Drawing of the principal nave where the hooks are shown.

**Figure 29** – Principal nave with the tie-system used.

### *Temporary ties in England*

Even if the use of temporary ties was well-developed in France, they were even more used in England. As observed by Fitchen:

“Iron was used by far more extensively to tie together the masonry members in the great English Churches than it was in those of France” (Fitchen, 1981)

The evolution of the use of ties in England is worth noticing: first were used wooden ties but due to durability problems they were progressively replaced by continuous through-the-pier iron ties attached to projecting iron hooks. Ties were finally not used anymore as though the builders' proficiency grew along with their increasing confidence.

A good example of the use of temporary ties can be found in the Chapter House of the Westminster Abbey where the remaining hooks are still present nowadays.



**Figure 30** – Westminster Cathedral, Chapter House: remaining hooks.

### 2.3.3. Long-lasting ties

#### *Role*

Concerning now long-lasting ties, they were designed to be a fully active part of the structure even after the construction was achieved. Those ties were essentially made of iron. This technique was mainly developed and used in Italy but was often applied during consolidation works realized after the construction was completed (Guadet, 1907). Examples of such ties will be given later in this part. One can mention the case of Milano Cathedral where the cross-section of the long-lasting ties varies between 35 cm<sup>2</sup> and 55 cm<sup>2</sup> (Vasic, 2013).

Another type of long-lasting ties exists: the exterior ties which we used mainly to withstand the horizontal wind forces on the lithic structure, especially flying arches and slender buttresses. The best example is Beauvais Cathedral in France (See also the following section).



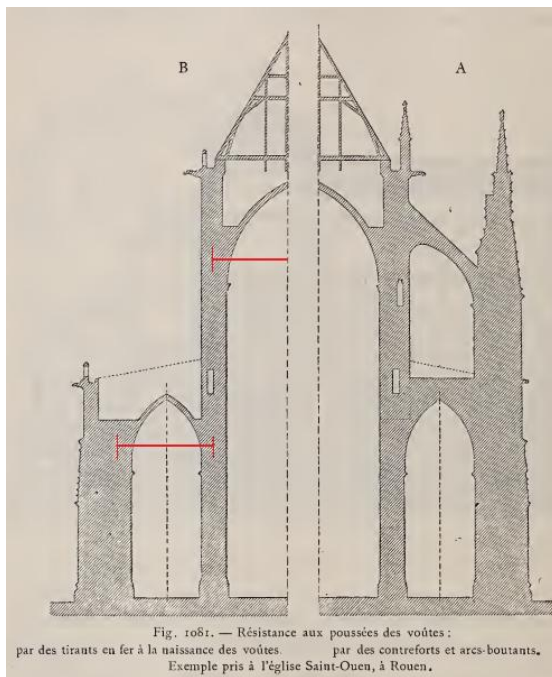


**Figure 31** – Sant-Ouen Church: architecture devices to bear the vault thrust. a) With flying arches and buttresses; b) With ties. (from Guadet, 1909)

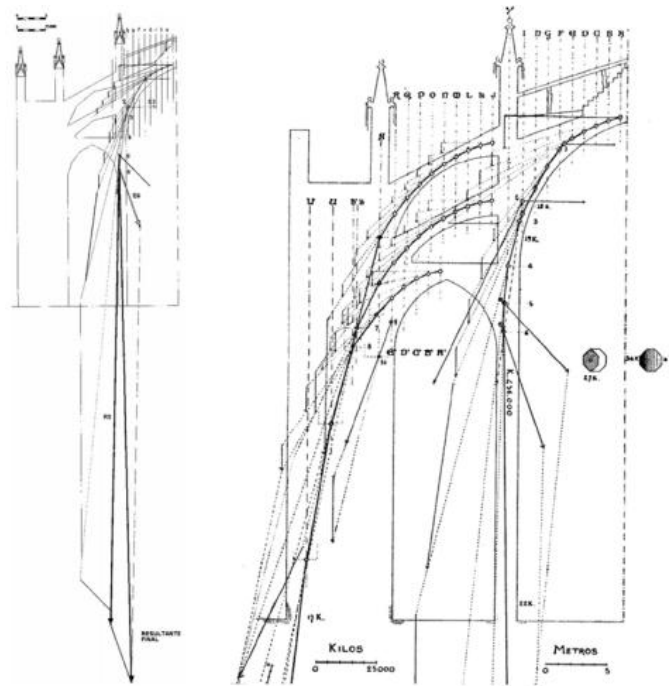


**Figure 32** – Cathedral Santa Maria de Palma: thrust line analysis. (Rubio, 1912).

### Examples

As highlighted before, long-lasting ties that can bear successfully the thrust of vaults even after the construction process were mainly employed in Italy. This technique allows essentially to save lithic material and thus significantly reduces or even replaces the flying arches and buttresses system in numerous historical Italian monuments. Nevertheless it seems that this technique was developed after the gothic era and was often used as a consolidation technique, even if it is difficult to find historical data on the subject. In the following will be shown three examples of outstanding Italian religious monuments in which long-lasting ties still remain: the Basilica San Petronio of Bologna (Figure 33), the Cathedral Santa Maria del Fiore in Firenze (Figure 34) and Milano Cathedral (Figure 35). Concerning the former, as it is shown on Figure 33, the exterior buttresses of the upper part of the nave seem small compared to the size of the central nave. The absence of external buttresses and flying arches for Santa Maria del Fiore confirms the capital structural role of the long-lasting ties which can be observed almost everywhere inside. On the plan of the Duomo of Milan, the ties pattern is represented.



**Figure 33** – Basilica San Petronio, Bologna: a) outside; b) inside. Example of combined effect of buttresses and iron ties.

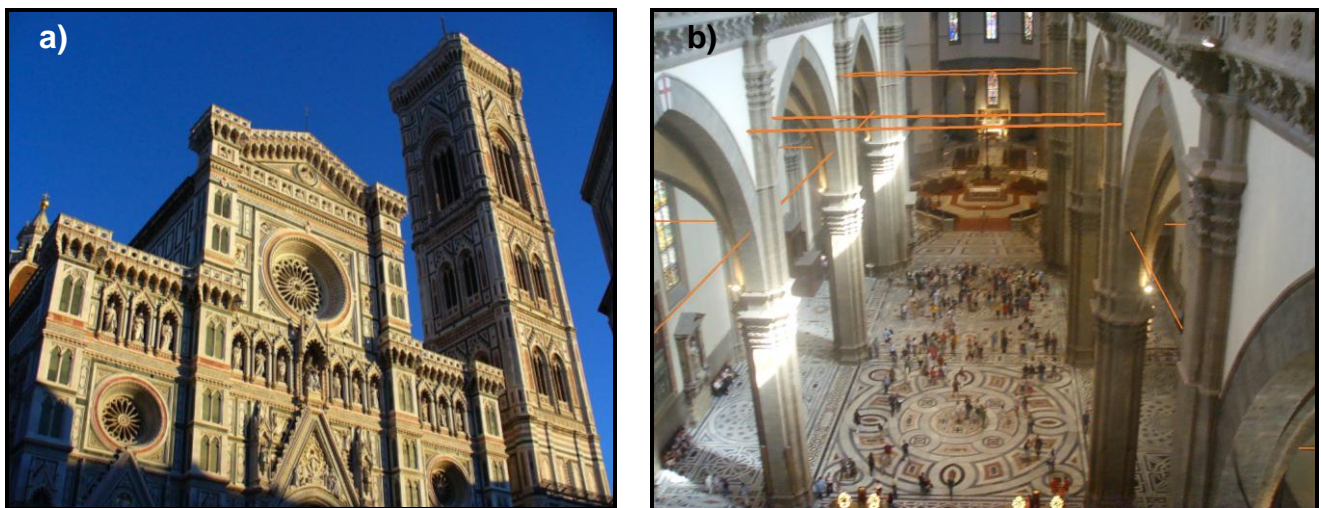


**Figure 34** – Cathedral Santa Maria del Fiore, Firenze: a) outside; b) inside. The long-lasting ties are highlighted in orange.

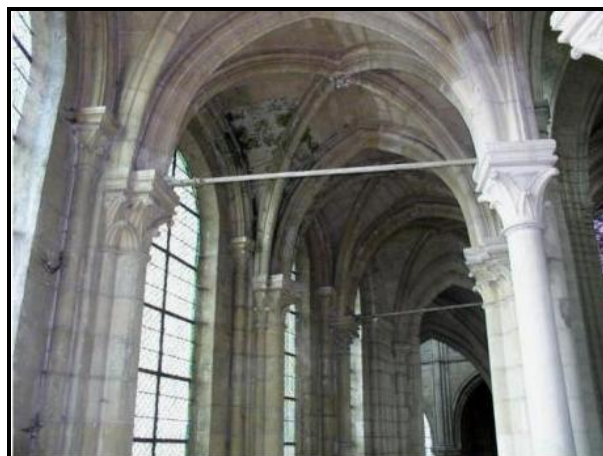


**Figure 35** – Cathedral Saint-Gervais-et-Saint-Protais of Soissons, France.

Even if this technique was fully developed and extensively used in Italy, builders from other countries used it as well: it is the case for example in the lateral naves of the cathedral Saint-Gervais-et-Saint-Protais of Soissons in France (Figure 35).

There are also long-lasting ties of smaller dimensions designed to reinforce smaller elements such as tiny columns, arches with less spans, etc. (L'Héritier, 2007).



**Figure 36** – Rouen Cathedral: iron ties of the arcs, found at the entrance of the Tour du Beurre. (L'Héritier, 2007)



**Figure 37** – Rouen Cathedral : reinforcement of the small columns of the choir. (L'Héritier, 2007)

Long-lasting ties can also have another completely different structural purpose: counterbalancing the horizontal wind forces on the external flying arches and buttresses system. External ties were used since the 13<sup>th</sup> century and one of the best examples of the use of external ties is in Beauvais Cathedral (Figure 38). Because of the slenderness of the external buttresses, it was necessary to find a way to counterbalance the wind forces on the buttresses, which has been done using external ties (Figure 39). Those ties were removed during the 60s because of aesthetical reasons and because they were found not to be active. Nevertheless the cathedral underwent some problems afterwards, and the ties were finally replaced. In effect even if these ties are not active most of the time, they play an important structural role in case of strong winds. This is a perfect example of non-fully understood restoration work which has led to the alteration of a monument.





**Figure 38** –Beauvais Cathedral : External iron ties.

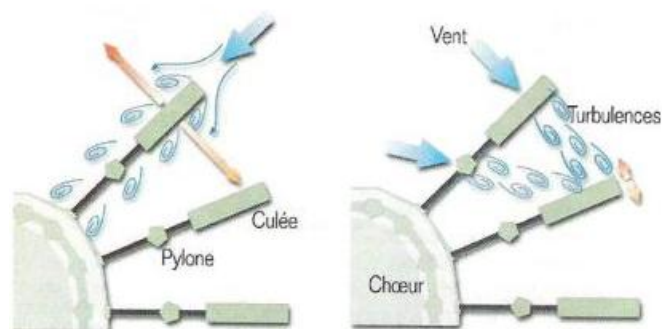


**Figure 39** – Wind forces acting on the external slender buttresses.

#### 2.3.4. Past interventions: strengthening

Ties were also utilized as a means of strengthening when the thrust of the arches and vaults was not fully taken by the system of flying buttresses and flying arches. This problem may be due to several different reasons such as: underdesign of those elements, creep behavior, addition weight added on the arch, partial destruction of the structural system, etc. In any case disorders appeared in the structure and ties were added to fix the problem. That is the case for example of Soissons Cathedral where a complete strengthening system has been added to the initial construction. On this subject Richard Brown wrote the following:

“At this time, the pillars being placed too far apart, the vaulted roof threatened to fall in, which actually took place after means had been added to support it by ‘iron braces and chains’ to hold the side walls together”. (Brown, 1845)

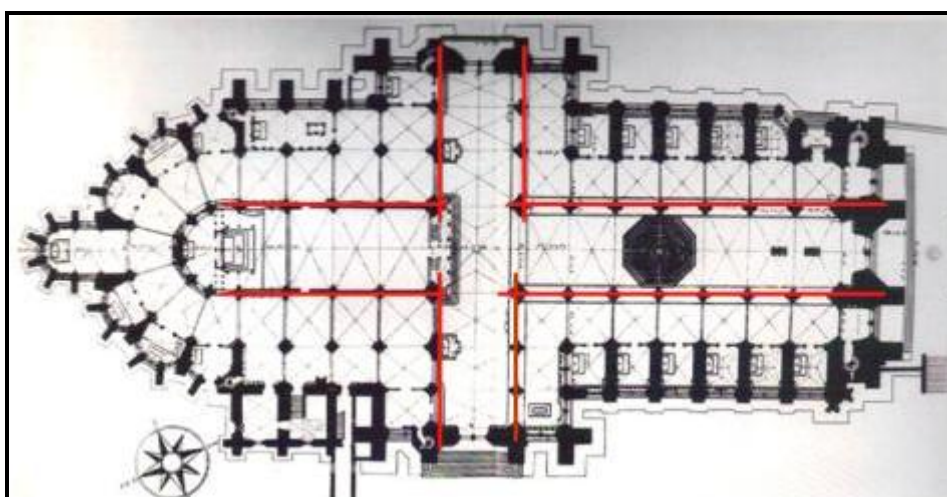


**Figure 40** – Plan view of the Cathedral Saint-Gervais-et-Saint-Protais of Soissons. The added strengthening system is shown in red.

Strengthening ties were added in modern times in numerous French historical monuments because of alarming deformations and settlements. The following list gives some examples of those buildings:

- Choir of Saint-Julien-Le-Pauvre, Paris;
- Taverny Church (Seine-et-Oise) ;
- Saint-Quentin Collegiate church;
- Great Abbey Church of Abbeville (Somme) where both iron ties (in the nave) and wooden ties (in the choir) had to be inserted under the high vaults.
- Notre-Dame of Amiens: addition of new metallic elements to stop the detachment of the two arms of the transept.

### **2.3.5. Iron properties and ties dimensions**

#### *Iron production during medieval times*

To have a better understanding of the properties of the iron employed in construction during medieval times, it is necessary to find out how iron was produced during this period. Iron in its normal state does not exist on Planet Earth; only iron ore constituted by iron, oxygen and sometimes other elements can be found. Therefore to obtain iron, this ore must be reduced first. This process consists of separating at high temperature the iron from the oxygen and possibly other elements. Two processes have been developed during medieval times: the oldest one is the direct process which after centuries was replaced progressively by the indirect one. This part is based on the works of Bernardi and Dillmann, 2005, 2002; Dillmann, 2006b; Dillmann et al., 2003; L'Héritier, 2007; L'Héritier et al., 2007, 2005; Timber and Dillmann, 2010.

#### *Direct process*

The direct process was developed during the 7<sup>th</sup> century BC and was mainly used at the beginning of the gothic era to produce iron. A shaft furnace with a blower is filled with charcoal. Afterwards the charcoal is set on fire which allowed, with the help of the blower, to reach a temperature of 1400 °C. Then the ore is added to the furnace. From this point the reduction process occurs: the oxygen elements present in the ore are combined with carbon of the burning charcoal to produce CO<sub>2</sub> and CO. During this process iron which temperature of fusion is 1527°C remains solid whereas the other ores become liquid and can therefore be evacuated at the bottom of the furnace it can also be noticed that some of the carbon of the charcoal is associated with the iron forming steel. Afterwards the bloom, a spongy and incandescent mass of iron, is taken from the furnace and worked by blacksmiths by means of human force in order to separate and homogenize the iron. The main steps of this process are given on Figure 41.

The resulting product of these two operations is an iron that presents strong heterogeneities. It is often a mix between iron and steel with sometimes phosphoric inclusions and always full of metallic

inclusions. Even the final elements produced are rudimentary, looking like the original wrought iron bars used to design them and neither special care to sort it out nor specific thermochemical treatments such as tempering or cementation were considered. Moreover the iron produced with this direct process presents several drawbacks. First of all it represents a considerable human work. Second, it consumes also a tremendous amount of charcoal. To point out the later disadvantage, it has been found in some archives that 25 sty of wood which corresponds to 25 apparent cubic meters of wooden logs were necessary for the production of 200 kg of iron (Timbert and Dillmann, 2010). It was thus a time-consuming and expensive process. Also the blacksmiths were only able to forge correctly 2.5 cm of iron under the surface.

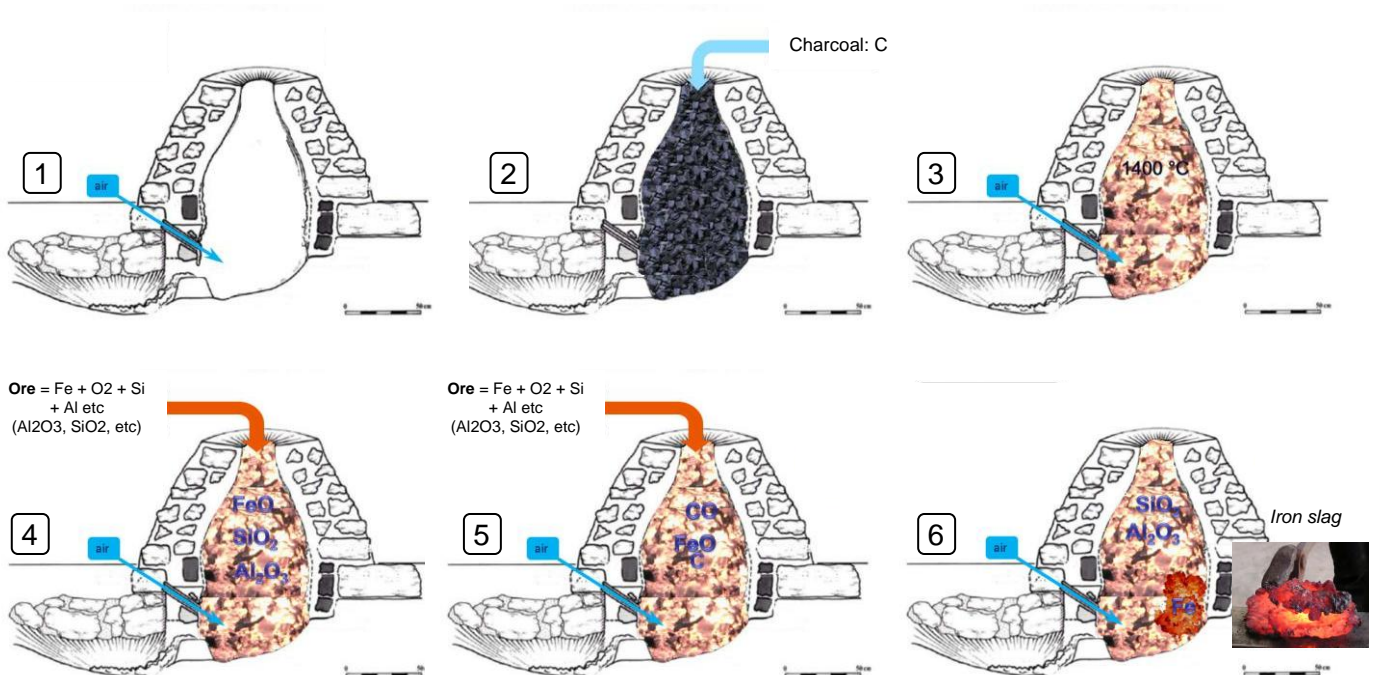


**Figure 41.** Direct Process: the transformation of ore into metal.

The highly heterogenic character of the iron produced with the direct process is of course a subject of interrogation: how elements designed with this iron were able to perform correctly their structural purposes? In effect inclusions within the iron matrix can significantly decrease the elastic properties of the iron. Also the presence of phosphor, even in extremely small quantities weakens the iron when it is cold and also during its forging at high temperature.

The heterogeneity of iron bars produced by direct process has been presented in the work of A. Juhin and I. Guillot who tested the iron of a ten of construction bars used for the construction of the dungeon

of the Vincennes castle in France. It is worth noticing that the heterogeneity is not only present among the different bars but also within a same sample. (Juhin, 2005)



**Figure 42** – Cathedral Notre-Dame of Rouen: heterogeneity of a typical iron tie observed with a microscope.

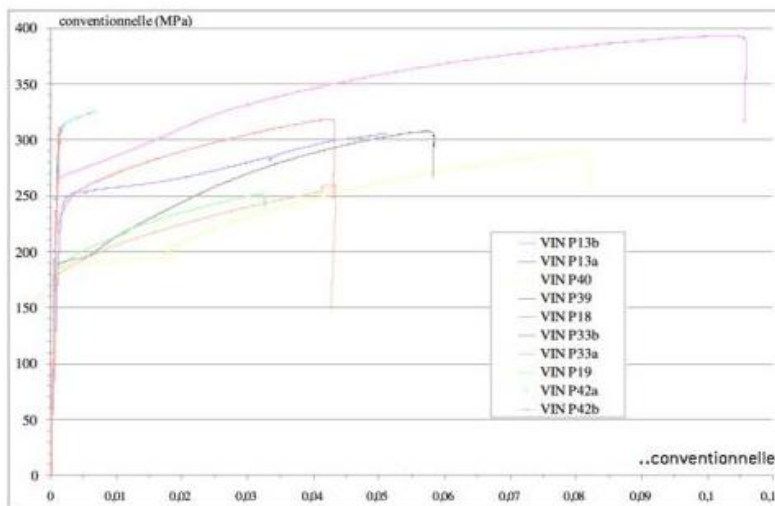


**Figure 43** – Vincennes Castle: Tensile tests on typical ties. The direct process has been used to design those ties. (Juhin, 2005)

Nevertheless the master builders of the gothic era knew how to design the metal elements with a section great enough to mechanically overcome the irregularities and heterogeneities in order to fulfill their structural role. Maxime l'Héritier shows that in the case of several churches of Rouen and Troyes most of the metallic elements used in the construction have not been broken or cracked except when those elements were rusted. It seems that a special care was taken for the design of structural iron elements. He also noticed that in case of a constant tension of the structure, the limiting factor is the strength of the stone, not the one of the iron. (L'Héritier, 2007)

### **Hydraulic hammer**

During the 12<sup>th</sup> century, the medieval world discovered how to master the hydraulic force. This discovery had tremendous consequences in several domains where the human force was mainly used: new tools and devices were created; hydraulic mills blossomed everywhere, etc. Concerning the



utilization of the amazing potential of hydraulic force for the production of iron, the first mile step was the invention of the hydraulic hammer which the first known use has been reported by Arnaud de Bonneval, Saint-Bernard de Clervaux's Biograph, on the construction site of Val d'Absinthe in 1135 (Timbert and Dillmann, 2010). In the same current years, other examples of such technique were found in England on the construction site of the Abbey of Bordesley, at Sorø in Denmark and finally in Burgundy in the abbey of Fontenay, France. This technique was a revolution for forging iron. It allowed to work more efficiently and in a quicker way leading to a higher production of iron. It was possible to forge the iron deeper under the surface and also to obtain elements with greater dimensions. Those longer metallic elements have been seen by the gothic builders as a technical answer to their desire to raise higher and lighter buildings.



**Figure 44** – Hydraulic hammer principle from Rouillard, 2003 and example of a hydraulic hammer still in use in the smith of J. Brösl at Merdzev in Slovakia.

### *Indirect process*

Even if this process seems to have been known since the 12<sup>th</sup> in Sweden, it really spread during the 14<sup>th</sup> century at the East of the Ruhr and for example was known in France during the second half of the 14<sup>th</sup> century. This new process, called indirect, introduced significant changes in the way of producing iron. First of all, with the help of hydraulic bellows, it was possible to reach 2000°C within a blast furnace which is higher than the temperature of fusion of the iron. But the product obtained after this phase was similar to cast iron and was really brittle in tension. It was necessary to refine it in order to obtain iron. This second step was performed in another furnace in oxidizing atmosphere which was able to take out the carbon contained within the ore. The final product, a bloom composed by iron and slags was compacted under a hydraulic hammer. The new process allowed to obtain an iron with no inclusions and thus with better and more homogeneous mechanical properties.





**Figure 45** – Indirect process: production of cast iron within a blast furnace with the help of hydraulic blowers. Painting of Henri Bles, “Paysage avec forges”, 16<sup>th</sup> century.



**Figure 46** – Indirect process: refining of the cast iron in order to obtain iron. Painting of Henri Bles.

In Spain, the direct process was not used until the 19<sup>th</sup> – 20<sup>th</sup> centuries (Timbert and Dillmann, 2010) and therefore it is possible to assume that the ties used in the construction process of the lateral bays of Mallorca Cathedral were made via the direct process. Figure 47 shows the difference of chemical composition of iron produced with the direct and indirect processes. This type of graph is very useful to date iron in a construction and thus to gather precious information on the date of construction, on the possible consolidation works done on the construction, etc.

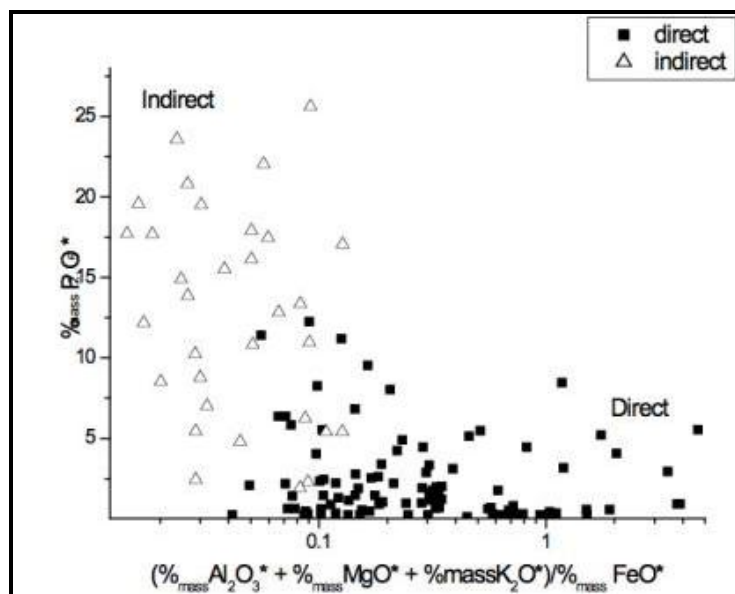


**Figure 47** – Graph that is used to differentiate iron produced with the direct process from the one produced with indirect process thanks to their different chemical composition. (Dillmann, 2006a)

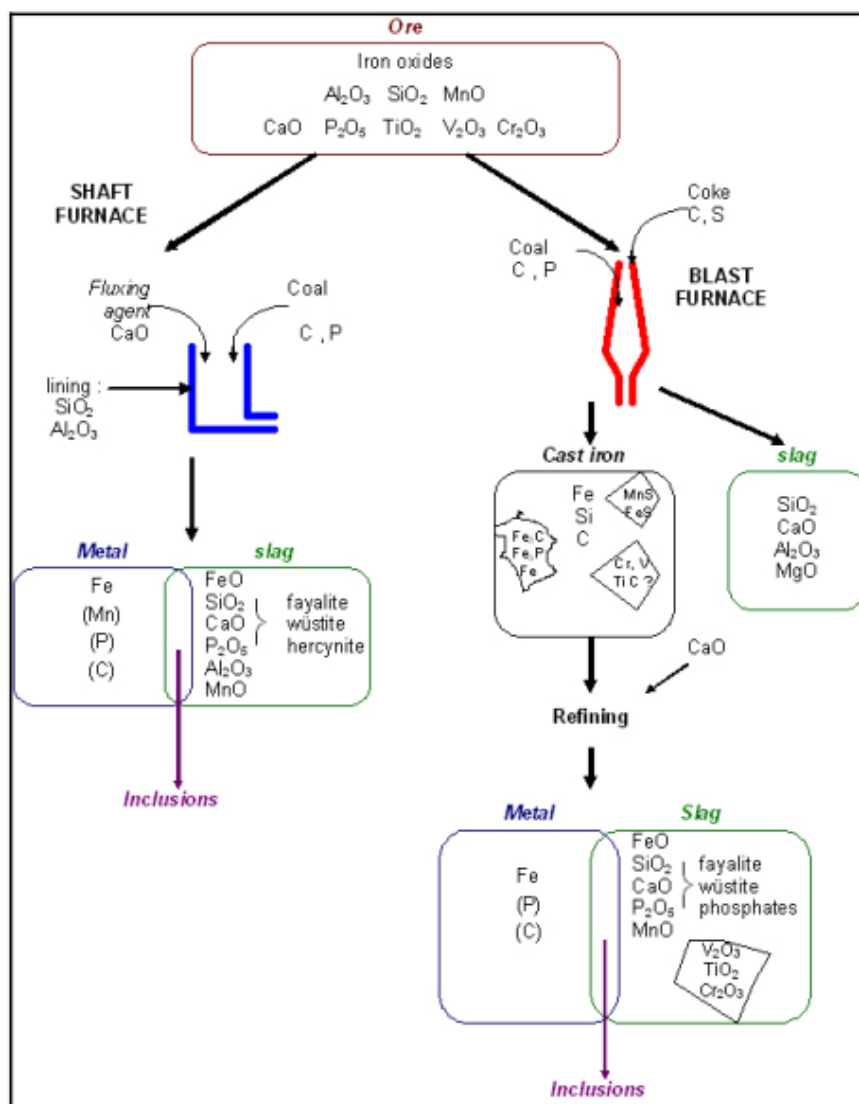


**Figure 48** – Partition of the elements and of the phases in function of the reduction process. (Dillmann et al., 2002)

### *Ties properties*

As explained above, medieval iron is a very heterogeneous material and thus it is difficult to estimate properly average values for its mechanical properties, not to add that mechanical tests on such historical elements are rare and difficult to find. Nevertheless, a thorough research has allowed to find a range for these values, especially for the 18<sup>th</sup>, 19<sup>th</sup> and 20<sup>th</sup> centuries. Table 2 gives useful values of tensile strengths, Young's moduli and Poisson ratios found in the literature.

| References: Paper/Book/Norm   | Mechanical properties         |                              |                      |
|---|-------------------------------|------------------------------|----------------------|
|   | <i>Tensile Strength (MPa)</i> | <i>Young's Modulus (MPa)</i> | <i>Poisson ratio</i> |
| Engineering materials and their properties  | 250                           | /                            | /                    |
| RT/CE/C/025 – United Kingdom  | min 285                       | /                            | /                    |
| RiL805: Guideline 805 of German railways – Germany  | min 320                       | 200 000                      | /                    |
| SBB Weisung I-AM 08/02 25/05/2002 – Switzerland   | min 320                       | 200 000                      | /                    |
| Structure métallographique et comportement des tyrants de fer du donjon du château de Vincennes, A. Juhin | min 250<br>max 390            | 243 300                      | /                    |
| Materials of Construction Rewritten, Whitney M.O., Aston J.   | /                             | 186 200                      | /                    |
| Elements of Machines design, O.A. Leutwiler, M.E.E. – McGRAW  | /                             | /                            | 0.278                |
| Mechanical Engineering  | /                             | /                            | 0.278                |

**Table 2** – Mechanical properties of wrought iron given in the literature.

As it can be observed on the Table 2 above, it is reasonable to consider a Young's modulus of 200 000 MPa and a Poisson's ratio of 0.278 for historical wrought iron. In addition, the mass density of iron can be considered as 7874 kg/m<sup>3</sup>.

One can also mention the tensile tests carried out by Mira Vasic for historical medieval iron used in the ties of the Duomo of Milan (Vasic et al., 2013):

- Average yield limit: 200 MPa;
- Average tensile strength: 300 MPa;
- Average Young's modulus: 205 GPa.

These values are very closed to the ones assumed above.

A word can be say on the appellation 'Spanish iron', a type of iron well-known during medieval times for its superior properties. This denomination does not refer to any specific geographical localization but rather to a technique of production. Therefore Spanish iron does not have any special properties during medieval times.

## 2.4. Wooden ties

Until now a special attention has been taken on iron ties. However it has already been mentioned that it exists also ties that were made of wood. Their main advantage was the possibility of sawing them

easily after their structural purposes have been achieved and they were no longer useful as a structural element for the monument. Nevertheless those elements present several important drawbacks: the need of finding a single piece of wood with dimensions great enough to carry successfully the thrust (length and cross-section), and durability problems especially at the connection of the tie with the masonry where there is a concentration of moisture. Therefore builders preferred to use iron. Concerning the use of wooden ties, Emile Brunet, the architect in charge of the work of reconstruction of the Soissons Cathedral, wrote the following lines:

“In the twelfth and the thirteenth centuries, these ties were generally of wood, subsequently sawn off flush with the stone; later they were composed of an iron rod furnished with eyes arranged to fit over strong hooks anchored in the masonry”. (Brunet, 1928)

Long-lasting wooden ties can be found for example in the barrel vault of the upper narthex of the Church of Saint-Philibert in Tournus (Figure 50). They were locked into longitudinal timber plates set in the masonry but because of its aesthetics disadvantages, this device was never used in the principal vaults. (Fitchen, 1981). The marks of the utilization of temporary ties have been found also for the Amiens Cathedral and Wetminster Abbey.

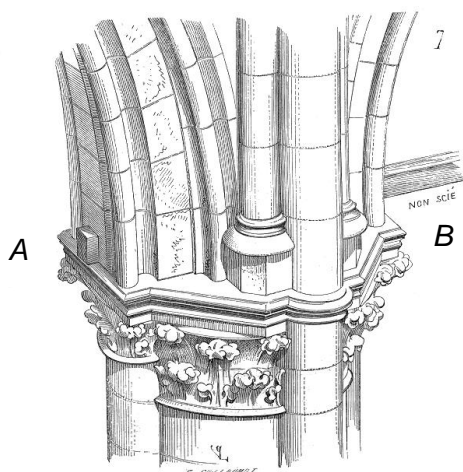


**Figure 49** – A) Cut wooden tie; B) Remaining wooden tie. Drawing by Viollet-le-Duc.



**Figure 50** – Church Saint-Philibert of Tournus: Example of remaining wooden ties in the narthex.

Another interesting feature for wooden ties is their ability to work in compression without inducing any significant buckling which allows them to be performing as an anti-seismic device. That is why ties in Byzantine and Eastern Mediterranean churches were invariably in wood because these buildings have needed to be trusted by ties that are resistant to both tensile and compressive stresses in order to bear earthquakes. (Fitchen, 1981)

This page is left blank on purpose.

### 3. MALLORCA CATHEDRAL: PAST STUDIES

The cathedral Santa Maria de Palma de Mallorca is one of the emblematic gothic monuments of the Mediterranean area and especially of Spain. The cathedral, located on Mallorca Island, has been uncontinuously constructed during more than 300 years. The construction started during the year 1306 on a place where a Mosque stood and was finished in the year 1600. The cathedral presents typical features of the so-called Catalan Gothic Style such as high lateral naves, the presence of chapels located between the buttresses and extremely slender octagonal piers resulting in a spacious and diaphanous interior space. This style is close enough to the French Gothic Style and that is one of the reasons why a focus has been done on French gothic monuments on the previous parts. One of the main features of this style in the cathedral is the presence of double batteries of flying arches spanning over the aisles. The structure of the cathedral can be divided into two parts: a large body formed by the main nave and the lateral naves and limited by the West façade and another one which includes the choir and its surrounding chapels. The cathedral was built with limestone coming from the local quarries of Santanyi. A plan of the cathedral as well as several elevations are given on Figure 52.



**Figure 51.** Picture of Mallorca Cathedral from est view.



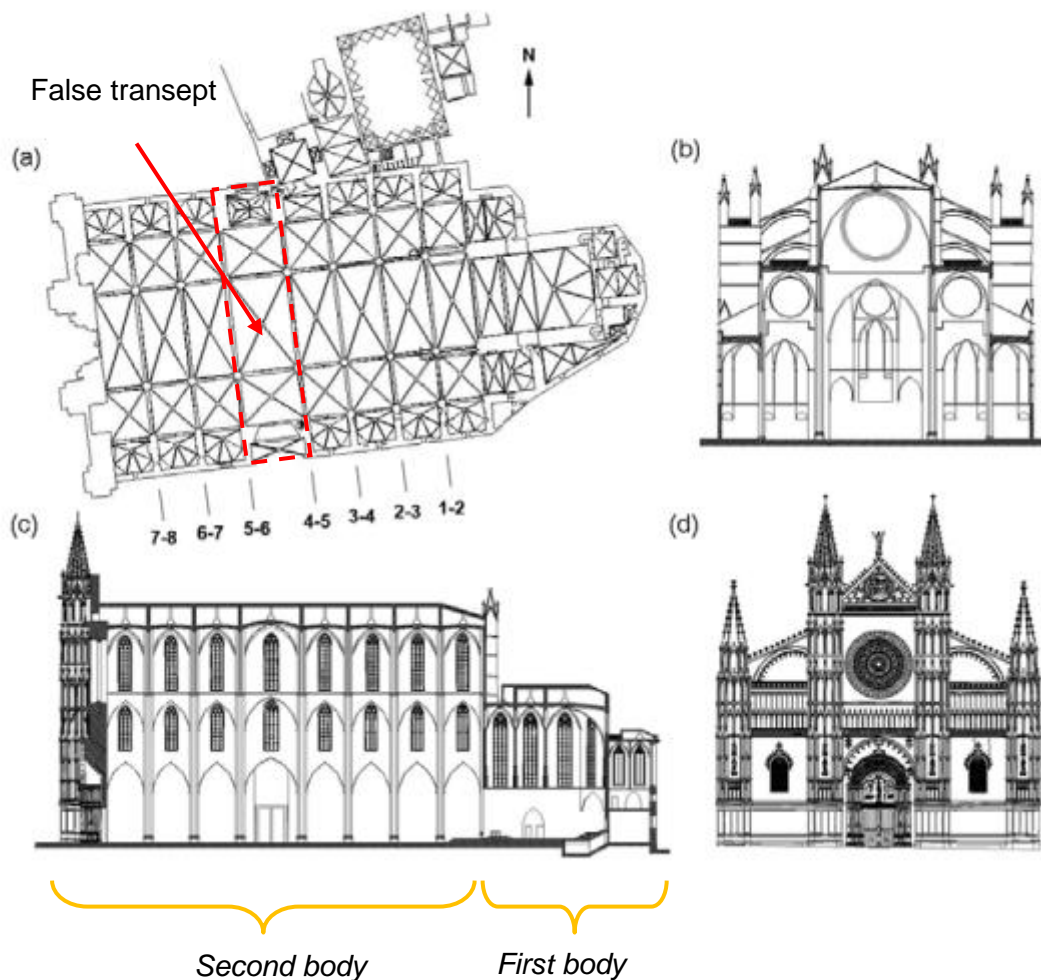


**Figure 52** – Mallorca Cathedral: plan at roof level (a), transverse section (b), longitudinal section (c) and façade (d).

### 3.1. Historical data

The following table gives the essential dates of the history of the cathedral, including its construction process, the main local collapses and the main restoration and strengthening works that have been carried out until now. It is possible to divide the history of the cathedral into five different periods of time: the Royal construction which includes specifically the construction of the first body of the cathedral from 1306 to 1368, the construction of the second body (1368 – 1601), then a period spanning over 250 years during which the cathedral has undergone several degradations. After the later period, it was decided to restore the cathedral which leads to the 4<sup>th</sup> period: the reconstruction (1851 – 1888) and finally a fifth period can be considered: the reform of the cathedral (from 1888 until now). Even if the dates that are given in Table 3 come from historical documents (original documents available at the historical files of the library of the Chapter of the cathedral) and published articles (González et al., 2008; Roca et al., 2013, 2012), some uncertainties still remain concerning some of them. In this paper the dates given are believed to be the most realistic ones. To increase the reading

of the table, the dates corresponding to reconstruction works are followed by a star whereas the ones corresponding to local collapses are shown in italics.

| Date   | Event  |
|--|--|
| <b>Previous building</b>                                 | Mosque   |
| <b>1306-1368</b>   | <b>First period: the Royal Construction</b>  |
| 1306   | Starting of the construction of the presbytery   |
| 1311   | Starting of the construction of the Royal chapel   |
| 1330   | Starting of the remaining construction according to a 3-nave plan  |
| mid 14th   | Decision of increasing the height of the vaults  |
| 1370   | Single nave presbytery is finished   |
| around 1370  | End of the construction of the Royal Chapel  |
| <b>1368-1601</b>   | <b>Second Period: the construction of the naves</b>  |
| 1368   | Decision to build the cathedral with 3 naves   |
| 1378   | Complete demolition of the Mosque  |
| mid 14th- 15th   | Construction of the main nave  |
| around 1400  | Constructions at the door of the Mirador   |
| <i>April 1490</i>  | Fall of an arch of the central nave  |
| 1498   | Almoina door is built  |
| 1460-1570  | Interruption of the construction   |
| 1594-1601  | Construction of the main façade in Renaissance style. Meanwhile the cathedral is consecrated   |
| <b>1601-1851</b>   | <b>Third Period: degradation of the cathedral</b>  |
| 1639   | First report of damage: the major vault near the façade should be dismantled and replaced. Several cracks are observed. Reconstruction                                       |
| 1655*  | The greater arch of the main nave and the first flying buttress were considered to be reconstructed due to the presence of cracks or deformation. Reconstruction of the arch |
| 1659   | Fall of an arch (no documentation about which one). Reconstruction   |
| <i>end of March 1660*</i>                                | Earthquake: fall of two arches near the façade and the origin of out-of-plumb of the façade. Reconstruction  |
| 1698*  | Vault of the second bay collapsed. Reconstruction  |
| 1699   | Collapse of the reconstructed vault  |
| 17 <sup>th</sup> , 18 <sup>th</sup> , 19 <sup>th</sup> * | Significant numbers of vaults were repaired (especially during the 18th century)   |
| 1706   | Collapse of an arch or a vault. Reconstruction   |
| 1717   | Collapse of an arch or a vault. Reconstruction   |
| 1743   | Collapse of an arch or a vault. Reconstruction   |
| 18th century   | Addition of a tile roof  |
| <i>March 1851</i>  | Decision of demolition of the original façade  |
| May 1851   | Earthquake (intensity VII-VIII)  |
| <b>1851-1888</b>   | <b>Fourth Period: the Reconstruction</b>   |
| second half of 19 <sup>th</sup> *                        | Original façade was taken down (1851) and replaced by a new one  |
| 1854*  | Restoration project is presented: Neo gothic façade, section of the buttresses of the new façade was significantly increased   |
| 1888*  | Finishing of the reformation. Finishing of the new façade designed with more robust buttresses.  |
| <b>1888-2006</b>   | <b>Fifth Period: Reforms</b>   |
| 1904-1914*   | Change of the color of the window glasses (Gaudi)  |



|                      |   |
|----------------------|---|
|                      | Several restoration and conservation works  |
| Sep. 2003 – Sep 2008 | Monitoring of the cathedral (climatic parameters, crackmeters, clinometers, extenometers) |
| 2006*                | Restoration of the towers of the west façade was concluded                                |

**Table 3** – Main chronological events of Mallorca Cathedral.

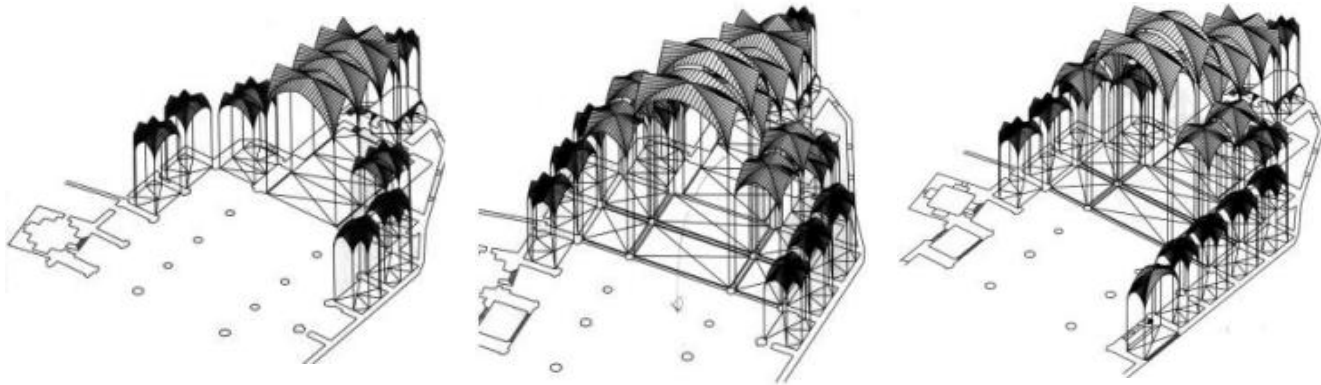


**Figure 53** – Construction stages of Mallorca Cathedral. (González et al, 2008)

### 3.2. Dimensions and interesting features

The cathedral has an overall length of 121 m and a width of 55 m and is composed by two different bodies as it has already been mentioned. The second body includes a main nave and two lateral ones. The central nave has a length of 77 m, the free span of the vaults is 17.8 m and the height from the ground to the top of the interior vaults is 44 meters. The lateral naves are smaller than the central one. In effect their height only reaches 29.4 meters which is still impressive and the vaults span is 8.75 meters. There are a total of seven bays if the false transept is included. For each of them, the thickness of the nave vault is only 20 cm.

Concerning now particular architectural features, the cathedral presents numerous but tiny windows. This architectural choice is a consequence of the strong solar exposition of the cathedral. Bigger windows would have led to luminosity and heat problems. Despite these tiny openings, the cathedral is well-known for its two gothic rose windows which include the world's largest one with a diameter of 11.5 meters.

A special attention can be taken on the design of the interior octagonal piers of the cathedral. With a circumscribed diameter between 1.6 to 1.7 meters for a height of 22.7 meters to the springing of the lateral vaults which represents a slenderness ratio between 13.35 and 14.19, they represent the most daring feature of the cathedral and can be considered as the most slender piers existing in gothic architecture. In effect for such construction this slenderness ratio is most of the time between 7 and 9. They are composed by a square block of limestone surrounding by 4 hexagonal ones (Figure 54). To counterbalance this tremendous slenderness, the dimensions of the buttresses are impressive: their

base is 7.7 meters long for 1.5 meter wide. The difference of diameter between the outer piers and the inner piers can be a consequence of the adapting design during the construction process of the cathedral: having observed some deformation for the outer piers, the master builders enlarged the remaining ones.

It is also interesting to observe the presence of additional dead loads placed over the transverse arches and central vault keystones. It has been proven that those extra loads were needed to reach a satisfactory equilibrium condition (Rubió, 1912). Lightweight pottery fill was also used for the central and lateral naves and even if it seems likely that it was removed for the central vault during the 18<sup>th</sup> century, the pottery fill of the lateral vaults still remains in place.

One can also notice the use of double battery of flying arches. Even if this feature can be regarded as a direct influence of northern gothic architecture as it can be found in the cathedrals of Amiens and Beauvais in France and Cologne in Germany, their initial purpose is still not well-known. For the afford-mentioned cathedrals, double batteries of flying arches were truly designed for a structural purpose. It is possible then that this technique was transposed in Mallorca Cathedral but without a real understanding of their structural behavior which would have led to an evident lack of structural role and the appearance of some undesired resistant effects. On the other hand, the purpose of these double batteries may have been not structural at all: they could have been designed as a draining system for the large roof of the central nave. In effect there was originally no high pitched roof for the cathedral but a flat, tiled one. This architectural characteristic may have been the consequence of the relatively dry climate of the Mediterranean area where rains are rather scarce but intense. Even if not designed to play any structural role, the upper flying arches should have been robust because of their span (more than 8 meters), which may have induced undesired secondary mechanical effects (Roca, 2001).

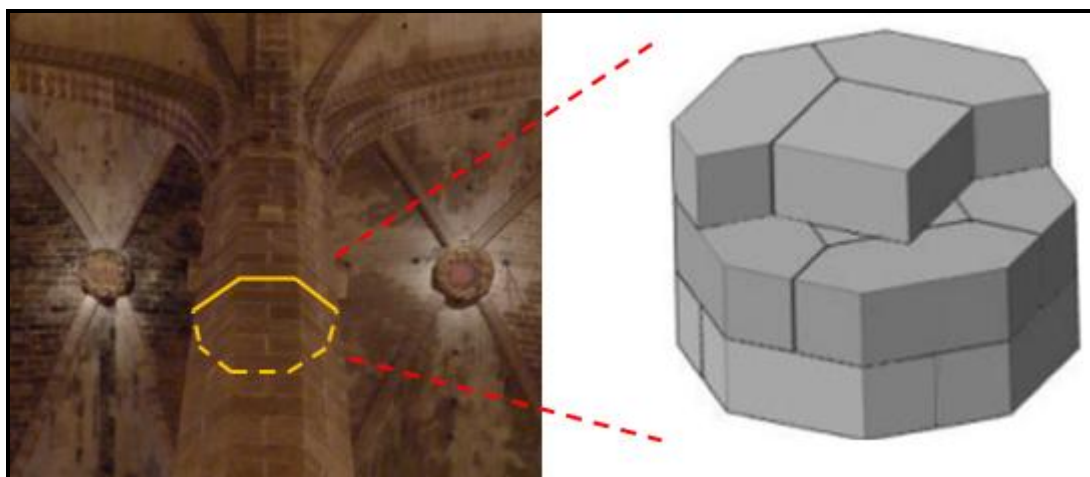


**Figure 54** – Arrangement of the stone blocks of the octagonal piers. (From Gonzáles, 2008)



**Figure 55** – Presence of dead weights placed over the transverse arches and central vault keystones. (Roca, 2001)



**Figure 56** – Double battery of flying arches. (Roca, 2001)

### 3.3. Existing damages and structural alterations

The structure of the cathedral has undergone until now mainly four different types of damages. First, consequent vertical and oblique crack patterns can be observed in some of the piers, which might be due to their overstressed state in compression. Second, it is possible to observe cracks in the arches and the vaults of the lateral naves due to differential settlements between the pier and the buttresses. For some of the arches and vaults, those crack patterns can also be due to an early or accidental removal of the centering of those structural elements during the construction process. Several cracks present along the mortar joints have also been detected for several walls and the main façade of the cathedral. Finally, the structure has undergone lateral deformations. Some of these deformations are significant, reaching the value of 30 cm for some of the piers corresponding to 1/100 of height at the springing of the lateral vaults. Those deformations vary both in magnitude in shape among the different bays as it is shown on Figure 57 and Figure 58. It is important to notice that those deformations are still not fixed nowadays (the maximum lateral deformation of piers is progressing at a rate below 0,1 mm per year). As it will be further developed in Sections 4.2.2. and 5.3.3., they are more than likely to be due to the creep behavior masonry through time associated with initial deformations that appeared during the construction process of the bays. (González, 2008; Roca, 2001, Roca et al., 2013, 2012).

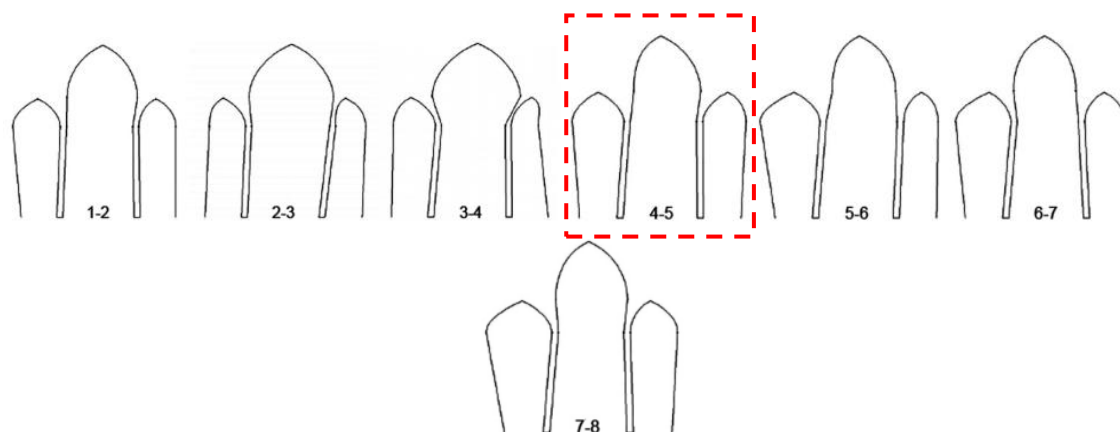


**Figure 57** – Deformed shapes of the different bays of the cathedral. The fourth bay is highlighted in red. (González, 2008)

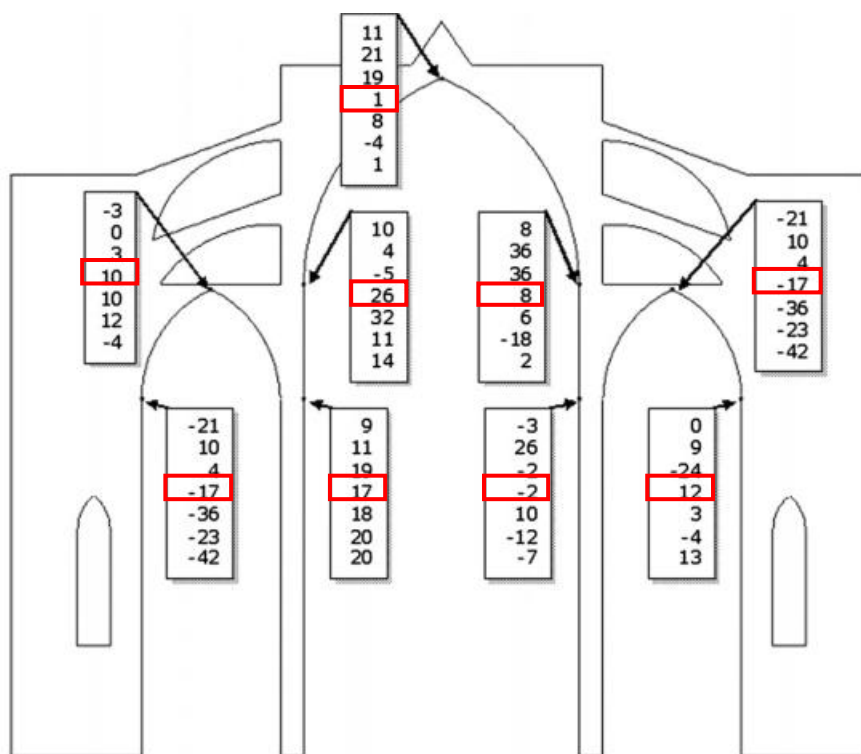


**Figure 58.** Horizontal displacements given in cm of the different bays of Mallorca Cathedral. The displacements obtained for the fourth bay are highlighted in red. (Roca, 2013)

Now that a general overview of Mallorca Cathedral has been carried out, including its history and its characteristic features, a characteristic bay of the cathedral, the fourth one, will be analyzed. As reported in the previous part, the bays of the cathedral have undergone significant deformations in the lateral direction and it is of outmost importance to understand better their structural behavior over the time. Before describing the previous studies of the 4<sup>th</sup> bay of the cathedral carried out with a finite element model, a description of the construction process of this bay will be done.

### 3.4. Construction process of the 4<sup>th</sup> bay of the cathedral

Understanding the construction process of a gothic monument is a keystone of the global understanding of its present state and structural behavior. Gothic monuments are indeed stable after the achievement of their complete construction, when the last structural element is finally added to the structure. Before that the unfinished parts of the structure undergo deformations which can be significant. To counterbalance these deformations, gothic master builders often used temporary structural devices during the construction process. The on-going construction was also adapted at each phase of the construction according to the knowledge of the builders. It was current to change the original shape of a building during the construction because of soil settlements and settlements taking place within the masonry, because of the time needed for the mortar to settle. The unbalanced horizontal thrusts of the arches and vaults system on the piers was also a possible source of deformation which must be considered.

Even if historical data on the construction process of Mallorca Cathedral are scarce, it has been possible to find documents on the construction process of its fourth bay. The whole process lasted from 1391 to 1460: first the lateral chapels of Saint Bernard and Saint Catherine were built. Then the piers were added, followed by the construction of one of the lateral vault, the so-called Epistle vault, then the second one, the Gospel Vault, and finally was added the vault of the main nave (Figure 59). The construction of each vault took around one year and because of some interruptions in the work the period of time between the completion of the first lateral vault and the one of the central nave was 5 years, meaning that the lateral thrust of the lateral naves acted on the interior piers without any permanent structural elements to counterbalance it, which corresponds here to the vault of the main nave. Three hypotheses concerning the temporary counterbalancing of this thrust during the construction process have been proposed (González et al, 2008):

- As for the construction of Santa Maria del Mar in Barcelona, already existing transverse arches might have been used to stabilize the on-going construction. This assumption requires the use of stabilizing extra weights which would have allowed the structure to resist the thrust of the lateral nave;
- As it will be studied in detail in Section 3.5.2., the non-finished structure might have been able to withstand the thrust itself without any auxiliary devices, thanks to its inner tensile strength. An interested fact is that this tensile strength is usually not taken into consideration for masonry. In effect it is more likely to vanish in the medium or long terms due to environmental cyclic effect, soil settlements, etc. Nevertheless, in the early stage of construction this tensile strength may have been enough to overcome the lateral thrust.
- The centering used for the main arches of the lateral vaults may have been active during the construction process of the bay, before the central nave was finished. Nevertheless such a technique wouldn't have let the masonry to settle properly during the construction process and

thus would have lead to difficult equilibrium conditions during their removal, causing randomly unbalanced inward or outward thrust. Figure 57 can be the consequence of such a hazardous removal.

- Finally, the use of another type of temporary devices, most likely iron ties, may have been used to overcome this thrust. This hypothesis is the core of the following analysis which will focus, after having proved that temporary iron ties were effectively installed in the lateral naves of the cathedral, on the use of such auxiliary devices during the construction process of the 4<sup>th</sup> bay of the cathedral. Because of visual evidence, this technique may have been applied to each other bay. As for the third hypothesis presented above, the quick removal of the ties may have caused rather randomly unbalanced inward or outward thrust. By the way, the removal of such iron seems far to be an easy task. As it will be fully developed in Section 5.3., remaining tensile stress within the ties is still present after the completion of the whole bay, making the ties difficult to take off. As it has been assumed before, the ties may have been heated before their removal.

Even if it will not be developed later on, another interesting point is the problem of the longitudinal stability: in effect the piers had to withstand the unbalanced longitudinal thrust of both the lateral and central vaults. One must keep in mind that the main body of the cathedral was constructed bay after bay over a long period of time which may have led to significant deformations in the longitudinal direction (González, 2008).

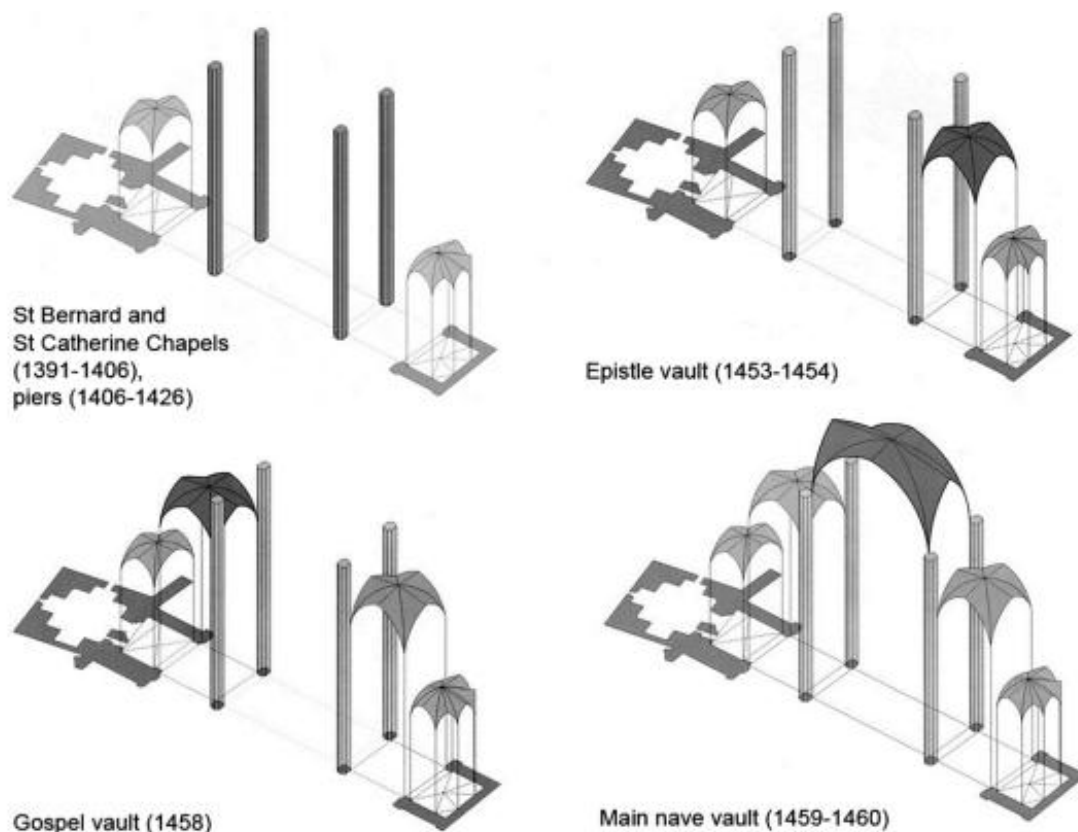


**Figure 59** – Construction process of the fourth bay from historical data. (González, 2008)

### 3.5. Previous works

Mallorca Cathedral, for it is one of the most impressive gothic monuments in Spain and also because structural alterations and deformations are clearly visible, has been the subject of numerous studies, mainly focusing on its structural behavior. Before explaining in details the Finite elements models developed for the structural analysis of the 4<sup>th</sup> bay of the cathedral, an overview of the others previous works carried out on the cathedral will be presented.

#### 3.5.1. Thrust lines and photo-elasticity studies

Until now, a rigorous thrust line analysis by means of the static graphic method has been carried out (Rubío and Bellver, 1912). During this study it was proved that the thrust line was fully contained within the thickness of the structural members. It was found also that the maximum compressive pressure was equal to 3.1 MPa within the principal arches whereas the maximum compression reached a value of 4.5 MPa within the pillars. These values, also relatively small, are closed to the resistance of the masonry work. Later on, several studies based on photo-elasticity were carried out (Mark, 1982). Unlike Rubío and Bellver' results, it was found that the maximum compression stress within the pillars was reaches a peak value of 2.2 MPa, leading to a difference of 2.3 MPa with the previous results. Nevertheless, by including a wind load to the model with a designed wind speed of



130 km/h, the maximum compressive stress within the pillars has been significantly increased to the value of 4.9 MPa. This analysis shows the existence of a significant flexural moment on the upper battery of flying arches. More recently a thorough thrust line analysis has been done by means of computer programming (Maynou, 2001). The results obtained presented a good agreement with the ones obtained by Rubío and Bellver even if both of these studies disagree on several points such as the obtaining of a satisfactory thrust line within the pillars taking into account their displacements (Maynou, 2001) and the length of the pillars that should be displaced in order to avoid their displacements.

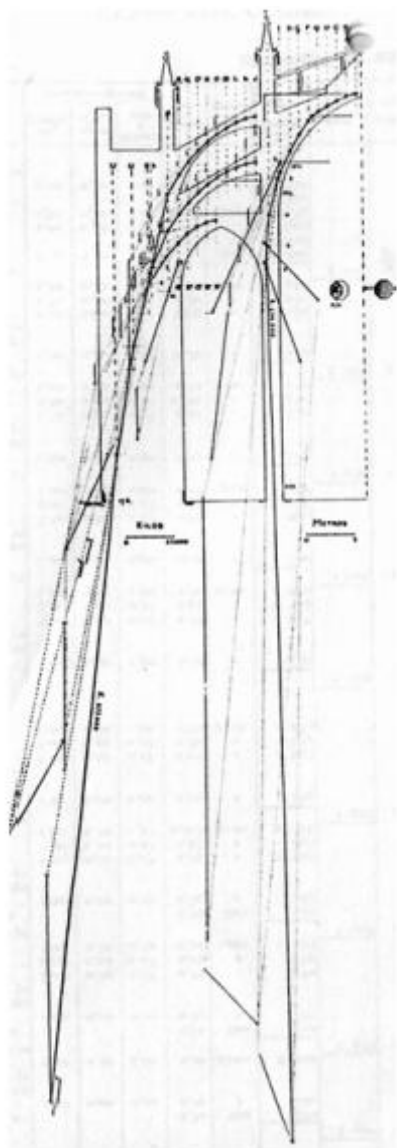


**Figure 61** – Thrust line analysis by means of the static graphic method (Rubío and Bellver, 1912).

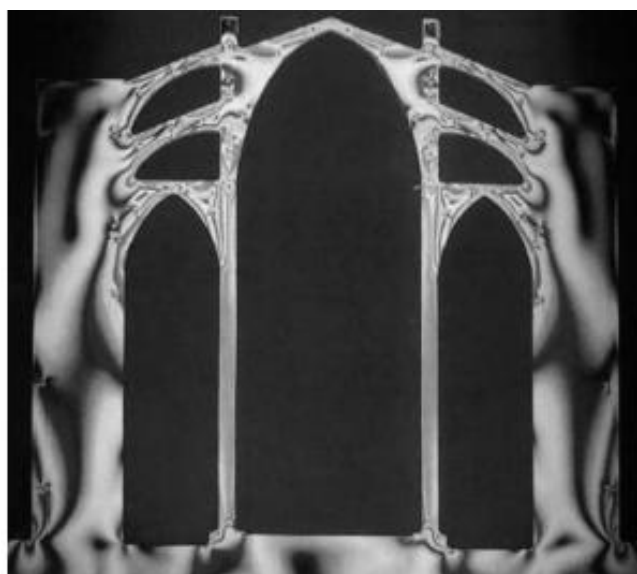


**Figure 60** – Photo-elastic analysis (Mark, 1982).

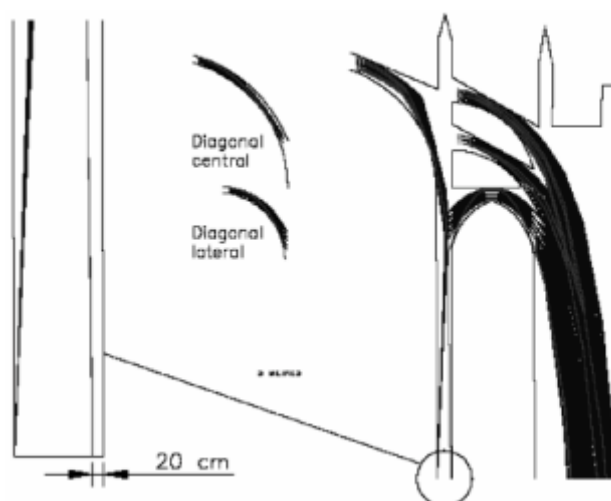


**Figure 62** – Thrust line analysis by means of computational programming (Maynou, 2001).



### 3.5.2. FEM analysis

With the increasing interest and development of finite elements models, numerous studies of Mallorca Cathedral based on this method have been carried out during the last 12 years. Because the model proposed in this work is based on the former FEM models already developed, it is of primary importance to list the previous FEM works on the cathedral and to give their principal results.

#### *Roca (2001)*

Based on a 3D Finite Element Damage continuum Model (cf. Annex A), but also on a non-linear formulation for 3D framed structures with curved members (so-called GMF), the structure of Mallorca Cathedral has been modeled as an equivalent frame with one-dimensional spatial curved elements, the model developed by Roca, 2001 showed two interesting results:

- First that the behavior of the construction is very sensitive to the ratio between the stiffness of the piers and the one of the buttresses. For similar values of stiffness for those two elements, the results obtained for the structure subjected to dead loads are closed to the ones found by Mark, 1982: mostly uniform and moderate states of compression within the piers and the other structural elements. However when the stiffness of the piers is set significantly higher than the one of the buttresses, the results obtained are closer to the ones found by Rubío and Bellver, 1912. The second hypothesis seems to be closer to reality. In effect, limestone with very good mechanical properties has been used for the construction of the piers. Moreover the filling of the piers with a non-resistant material is limited. On the contrary the masonry blocks used for the construction of the piers is of lower quality and one can notice the presence of a significant amount of non-resistant rubble infill. These first results have proved the important influence of the different stiffness values on the final results given by the model.
- Secondly that the deformed shape of the structure after the application of the dead loading, is qualitatively similar to the real one, if geometric and materials non-linearities configuration is considered: nevertheless the range of values obtained for the displacements calculated by the numerical models is ten times smaller than the ones observed in reality. The discrepancy in the results has raised many interrogations concerning their possible origins. Three hypotheses were advanced: the effect of plastic settlement of the mortar at an early age of the construction and the long term creep behavior of the masonry which may partially explained the higher displacements values found in reality but also the long terms actions on the structure such as the effect of thermal cycles, earthquakes and strong winds. Nevertheless the construction process including the possible use of auxiliary devices such as temporary wooden wedges was not considered in this analysis and was just mentioned as one of the possible explanations for the presence of vertical cracks at the base of the piers.

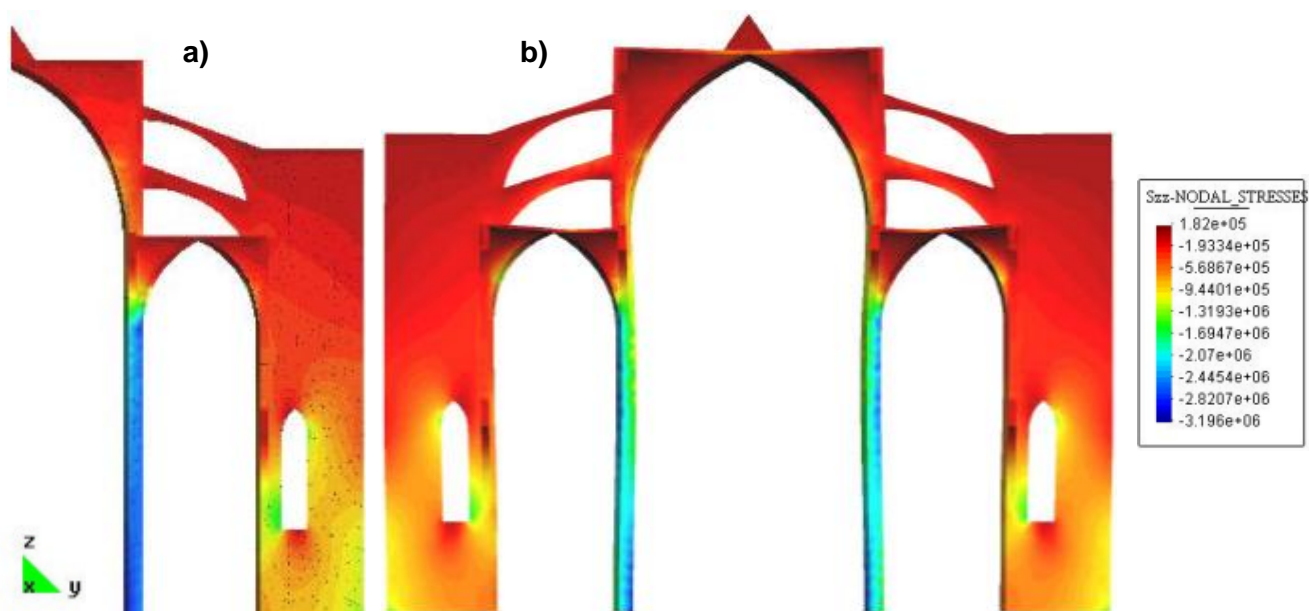


**Figure 63** – Distribution of the principal construction stresses for a typical bay of Mallorca Cathedral for two different analyses: same stiffness for the material of buttresses and piers (a) and a significant higher stiffness for the piers compared to the one of the buttresses. ( Roca, 2001)

### *Salas (2002)*

Following the work of Roca, 2001 and using the same analysis methods (FEM with an isotropic damage model the previously mentioned generalized matrix formulation GMF), Salas, 2002 performed a combined static and pushover analysis of a typical bay of Mallorca Cathedral.

Concerning the static analysis, he proved that the collapse mechanism of the structure is reached when the gravity load acting on it is multiplied by a load factor of 1.7. He also showed the importance of the presence of the extra-weight over the keystones of the vaults and the arches to stabilize the structure. In effect the structure has been found unstable without these elements (a load multiplier of 0.9 is needed to reach its collapse). He proved also that the model based on the GMF modeling is more versatile than the FEM one for indentifying the damage in the structure and predicting the possible collapse mechanisms. The models reveals that neglecting the presence of the upper battery of flying arches leads to a load multiplier of only 0.7, proving the essential structural role of this element. Nevertheless it shows also that if along with the upper battery, the additional extra weights are also neglected, the structure is stable and collapses for a load factor of 1.6.

Concerning now the pushover analysis of the bay, the models showed that the structure can stand a horizontal acceleration up to 0.12g before collapsing which is equivalent to a period of 1000 years. Wind pressures on the structure have also been studied in this analysis and Salas, 2002 has found out that the maximum pressure before collapse was equal to 1.45 kN/m<sup>2</sup>.

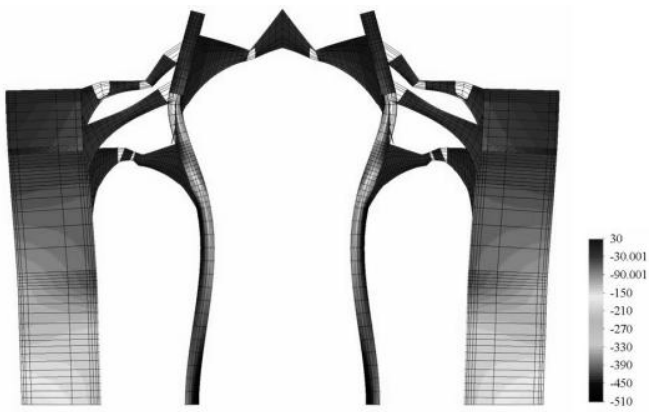


**Figure 64** – Collapse mechanism for a gravity load factor of 1.7 given with GMF (Salas, 2002).

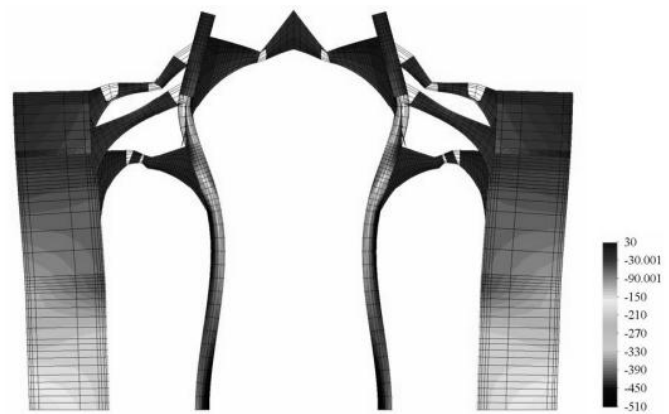


**Figure 65** – Stresses and deformed shape of the GMF model corresponding to a gravity load factor of 1.7 in the case for which the upper battery of flying arches has been neglected (Salas, 2002).

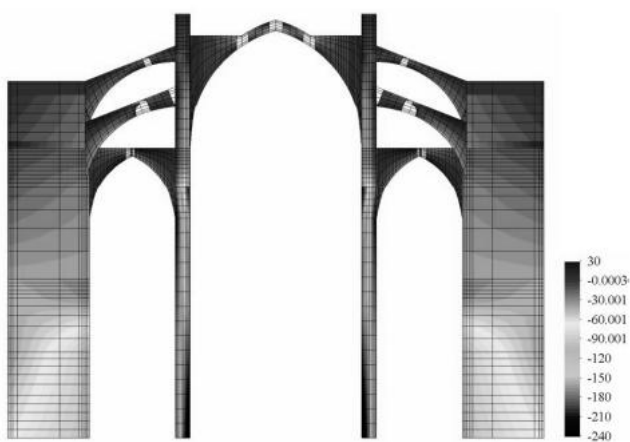


**Figure 66** – Stress distribution obtained for the GMF model where extra weights are not considered. The gravity load factor in that case is equal to 0.9 (Salas, 2002).

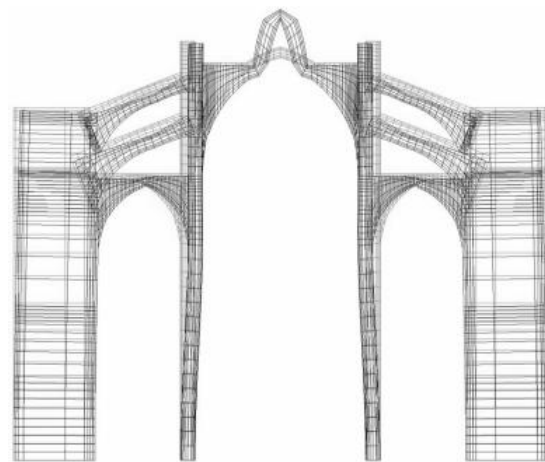


**Figure 67** – deformed shape obtained for the same model of Figure 66. (Salas, 2002).

### *Clemente (2006, 2002)*

Clemente focuses on the performance of the structure of the 4<sup>th</sup> bay of Mallorca Cathedral subjected to dead loading and the possible influence of the construction process. Clemente was indeed the first to consider the construction process of Mallorca Cathedral as a possible explanation of its actual state of deformation. Based on the model previously created by Casarin and Magagna (2001), he worked on a 2D and a 3D models of a characteristic bay of Mallorca Cathedral (the 4<sup>th</sup> one). Two different strategies were used and compared during this analysis. A smeared crack model was applied for both of the models and a localized damage model with three different radii (respectively 1 meter, 2 meters and 3 meters) were applied for the 3D model together with a small strains/small displacements formulation.

To carry out his model, Clemente has done several assumptions concerning the mechanical properties of the materials used for the different structural elements of the bay. On the one hand he considers mainly two materials with different properties: a soft limestone that has been used for the construction of the buttresses, the vaults and the walls of the bay and a harder limestone for the flying arches and the piers. The mechanical characteristics corresponding to these two different materials are presented in Table 4. These values have been deduced from experimental tests done on core samples taken from the monument. Clemente assumed a really high value for the material fracture energy in order to simulate the formation of plastic hinges with considerable ductility. He also assumed the tensile stress of the masonry to be equal to 5% of its compressive strength. The analysis was first focused on the gravity load multiplier research for the smeared crack and localized damage models for an instantaneous application of the gravity load; he found this multiplier equal to 2.0 and 2.05 for the 2D and 3D analysis respectively, considering a smeared crack configuration; and a value of 2.15 for the localized damage model. It can be also noticed that the failure mode is similar for the three cases: presence of significant damage on the buttress at the bottom left side of the window, dislocation in the main vault and presence of two hinges clearly formed on each flying arch which corresponds to the actual state of damage of the structure. Despite these interesting results, the values of displacements obtained for the pillar were too small compared to the real ones. In effect the models give a displacement of 0.76 cm whereas the real ones are comprised between 4 cm and 16 cm.

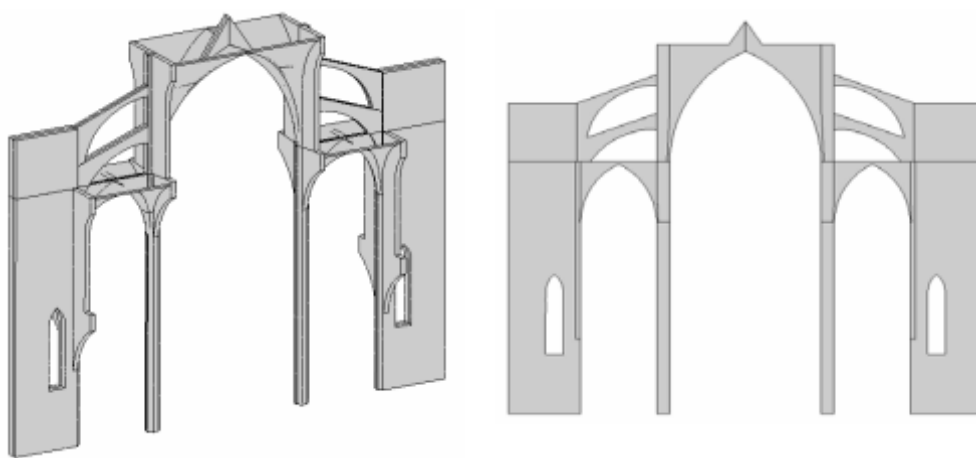


**Figure 68** – 3D and 2D geometrical models of a typical bay. (Clemente, 2002)

|            | Structural elements          | Young's modulus<br>MPa | Comp. strength<br>MPa | Tens. strength<br>MPa |
|------------|------------------------------|------------------------|-----------------------|-----------------------|
| Material 1 | buttresses, vaults, walls    | 2000                   | 2                     | 0.1                   |
| Material 2 | flying arches, arches, piers | 8000                   | 8                     | 0.4                   |

**Table 4** – Mechanical properties of the materials used by Clemente, 2002.

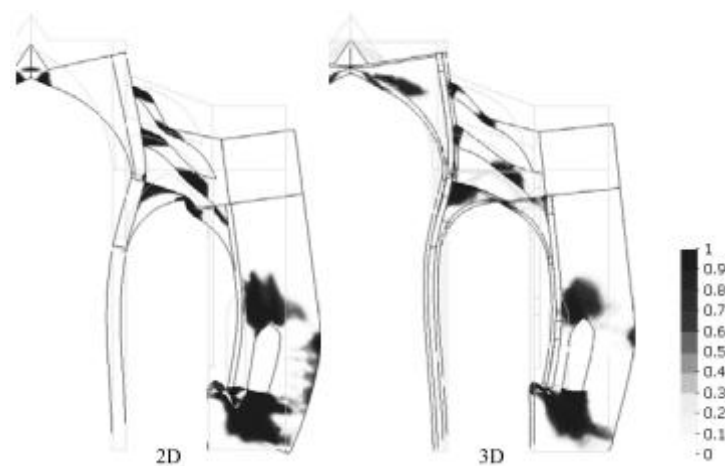


**Figure 69** – Collapse mechanism of the structure and distribution of tensile damage under gravity load considering a smeared crack model and a small strains/small displacements formulation for the 2D and the 3D models (Clemente, 2006).

A sensitivity analysis has been also carried out concerning the value of the masonry tensile strength which shows that the smeared crack model is extremely sensible to the tensile strength value adopted. The results of this analysis are given in Figure 70.

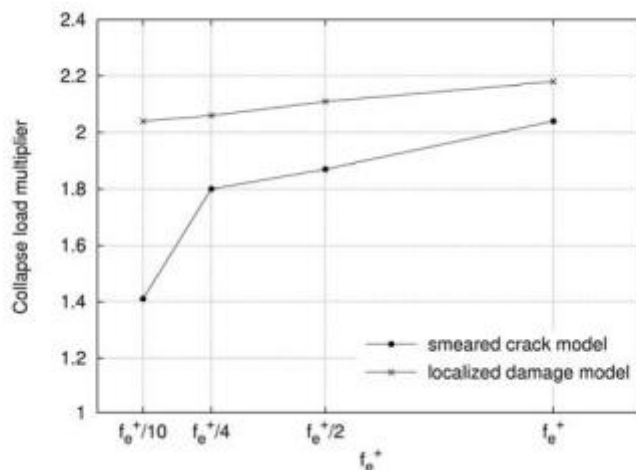


**Figure 70** – Influence of the masonry tensile strength on the collapse gravity load multiplier for 2D smeared crack model and 2D localized damage model. (Clemente, 2006)

Clemente developed later another model taking into account the construction process in order to understand the effect of a sequential loading on the structure. He divided it into 2 phases: a first phase that included the construction of the lateral vaults, the lower part of the buttress and the piers and a second phase considering the construction of the central vault together with the remainings of the buttress and the pier. the results obtained for the horizontal displacements in that case are closer to reality: in effect after the first step, the horizontal displacement of the upper part of the pillar reaches a value of 3 cm, and after the second stage of construction the horizontal displacement at this location is

equal to 1.84 cm. The results, even if they are still lower than the real ones, are encouraging and show the importance of the construction process consideration in the FEM analysis.

He also considered the influence of the creep behavior of the masonry due to long term loading during a third and final stage. The consideration of the creep behavior in the analysis led to horizontal displacements even closer to the real ones.

He repeated the analysis once again, but this time taking into account geometrical non-linearity, considering a small strains/large displacements formulation. The modeling of creep effect has also allowed to have a better understanding of the propagation of the damage within the lateral vault, the inner face of the pillar and in the clerestory.

Clemente shows that the stability of the partial structure generated during the first step is possible, but at the cost of significant deformation and certain damage.

Finally one word can be said on the pushover analysis carried out by Clemente. An assessment of the bay against seismic actions has been achieved by means of a pushover analysis. The analysis has been divided into two different steps: first the gravity load of each element was applied and then an increasing horizontal force as applied on the structure until its collapse. In that analysis, it has been observed that the type of model used, i.e. smeared crack model and localized damage models for different radii values, plays an important role on the collapse load multiplier found.

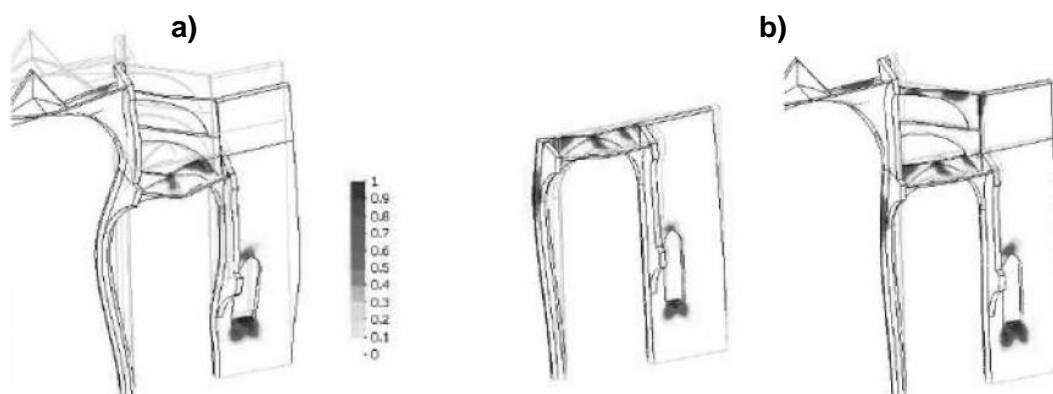


**Figure 71** – Comparison of the tensile damage state for (a) an instantaneous analysis (deformation factor of 300) and (b) a sequential analysis involving two stages (deformation factor of 50). (Clemente, 2007)

### *Roca et al. (2013, 2012)*

Based on the 3D model previously developed Roca et al. have continued to study the possible influence of the construction process and the long term deformation of the 4<sup>th</sup> bay of Mallorca Cathedral. As in the work of Clemente, 2006, the study is based on a numerical simulation taking into account the main phases identified in the construction of the bay. It has been carried out by means of

a viscoelastic and continuum damage model which has been specifically developed for this case (See also Annex A). The material viscous behavior is modeled by a Maxwell's chain type model characterized by two damage variables related to tensile and compressive stress states. A crack localization strategy has been adopted. It allowed to obtain more realistic description of the damage of the structure.

Concerning the properties of the materials, they have been implemented using experimental values. The tests have been carried out on samples from the vaults and the buttresses and from samples taken from local quarries where are originated the stones from the piers. From these tests, an average compressive strength of 6 MPa and 28 MPa were assumed respectively for the vaults and buttresses, and for the piers. The tensile strength of each lithic member has been considered to be equal to 5% of its compressive strength, allowing the structure under construction to withstand by its own the horizontal thrust of the lateral arches. Similarly to the model of Clemente, 2006, a very high value of the fracture energy has been implemented for each of the elements.

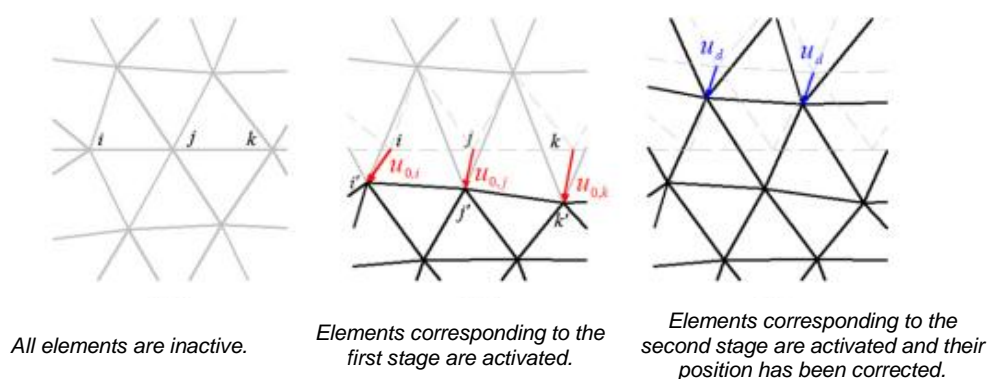
Two analyses were carried out: one only considering the material non-linearity and a second taking into account both the material non-linearity and the geometrical non-linearity (small strains/large displacements).

Considering the model, it represented actually one quarter of the bay, due to its assumed geometrical and boundary conditions symmetries. The mesh is composed of 49 979 tetrahedral elements together with 14 689 nodes. The authors have refined the mesh in locations where high stress gradients were expected: both end of the flying arches and columns, intersection between different structural elements and under the false window in the buttresses. Concerning this false widow, due to its small thickness, the authors decided to design it as a real opening. This choice has been considered as conservative. Finally, as it has already been mentioned in the previous work, additional dead loads such as pinnacles, infills and stone pyramids have not been fully modeled: only their weight has been considered.

Roca et al. added a new material within the model, the central vault backing. The mechanical properties of the three sets of materials are given in Table 5. The Young moduli of these materials have not been determined experimentally but have been calculating using the work of Martinez, 2007.

One particularity of the model is the horizontal correction of the position of the second phase of construction. In effect, after the completion of the first stage, some deformations appeared in the structure. Therefore the initial position of the upper part built during the second phase of construction has to be corrected in order to be adapted with the first stage.

| Structural element                   | $\gamma$ (kg/m <sup>3</sup> ) | $E$ (MPa) | $\nu$ (-) | $f^+$ (MPa) | $f^-$ (MPa) | $G_f^+$ (J/m <sup>2</sup> ) | $G_f^-$ (J/m <sup>2</sup> ) |
|--------------------------------------|-------------------------------|-----------|-----------|-------------|-------------|-----------------------------|-----------------------------|
| Buttresses, vaults, ribs, clerestory | 2100                          | 2000      | 0.2       | 0.10        | 2.00        | 100                         | 40,000                      |
| Columns, flying arches               | 2400                          | 8000      | 0.2       | 0.40        | 8.00        | 100                         | 40,000                      |
| Central vault backing                | 2000                          | 1000      | 0.2       | 0.05        | 1.00        | 100                         | 40,000                      |

**Table 5** – Material parameters implemented in the model.**Figure 72** – Implemented correction of the location of the upper part of the structure after the completion of the first stage.

Considering only a material non-linearity, the model gave a horizontal displacement at the top of the piers of 3 cm after the completion of the first stage of construction leading to an in-plane outward deformation of the piers if the lateral naves are taken as reference. After the completion of the second phase of construction, this displacement is reduced to the value of 1.8 cm. This is due to the fact that the vault of the main nave was able, after its finishing, to counterbalance the one of the lateral naves.

From the results of these first two stages, Roca et al. arrived to the following conclusions:

- The structure is not significantly damaged in compression;
- With the assumption of a tensile strength of 5% of the compressive strength and high fracture energy, it has been proved that the model can withstand the first construction phase without the help of any auxiliary devices but at the cost of increasing deformation and damage.
- The tensile strength of the masonry has a key role during the construction process.

This first part of the analysis reveals also that it may have been difficult to continue the construction at intermediate stages because of the deformations endured by the structure and thus the master builders seem to have constantly adapted the original design of the construction in order to take into account those deformations.

In a third stage, taking place after the structure was fully completed, the influence of the masonry creep behavior over time has been studied under the assumption of small strains/small displacements first and then small strains/large displacements. To do so, two parameters have been implemented:



the participation ratio of the Young's moduli and the retardation time (See also Annex A). Concerning the participation ratio, a parametric analysis has been carried out and compared to the results obtained by means of an on-site monitoring that lasted 5 years (from September 2003 to September 2008). Three configurations with different participation ratio have been carried out: 0.975, 0.925, 0.875. For each of these configurations, the results obtained in pseudo time have been calibrated on the monitoring data found. The monitored horizontal displacements have been decomposed into two values for each bay: an asymmetric displacement and a symmetric one, the former being attributed to an overall deformation of the rocky platform on which the building is founded and the latter being attributed to the gravity forces together with the long-term creep behavior of the structure. The authors only considered the symmetric horizontal displacements in the analysis.

For the fourth bay of the cathedral, the structure presents a symmetric horizontal displacement of about 9.5 cm at the top of the pier between the years 543 – 548 after the completion of the bay together with a deformation rate of about 0.1 mm per year for this period of time (Figure 76). With these two values in mind (horizontal displacement and displacement rate), Roca et al. modified the retardation time value in an attempt to match the experimental horizontal displacement curve with the ones obtained numerically.

Under a geometrical non-linearity assumption, it has been shown that the most representative displacement vs. time curve has been found for a participation ratio of 0.925. In effect, after the calibration of the retardation time, the modeled structure presents a horizontal displacement at the top of the pier of about 9.5 cm around the years 543 – 548 for a displacement rate of about 0.1 mm/year. In this configuration there is no failure of the structure, as it can be observed on Figure 76: the horizontal displacement at the top of the pier reaches a stable value of 24 cm after 2000 years. It has been shown that only a very high value of the participation ratio leads the model to failure in the long-term. Considering this ratio equals to 0.975, instability of the structure occurs at 1350 years. Nevertheless it is not possible to match the horizontal displacement versus time curve obtained in that case with the measured one. Also, even if it seems that the configuration with a participation ratio of 0.925 is the one closest to reality, one must keep in mind that different results might be obtained for a different constitutive equation or the change of some values adopted.

One can also note a horizontal displacement of 11 cm after 2000 years for a ratio of 0.875.

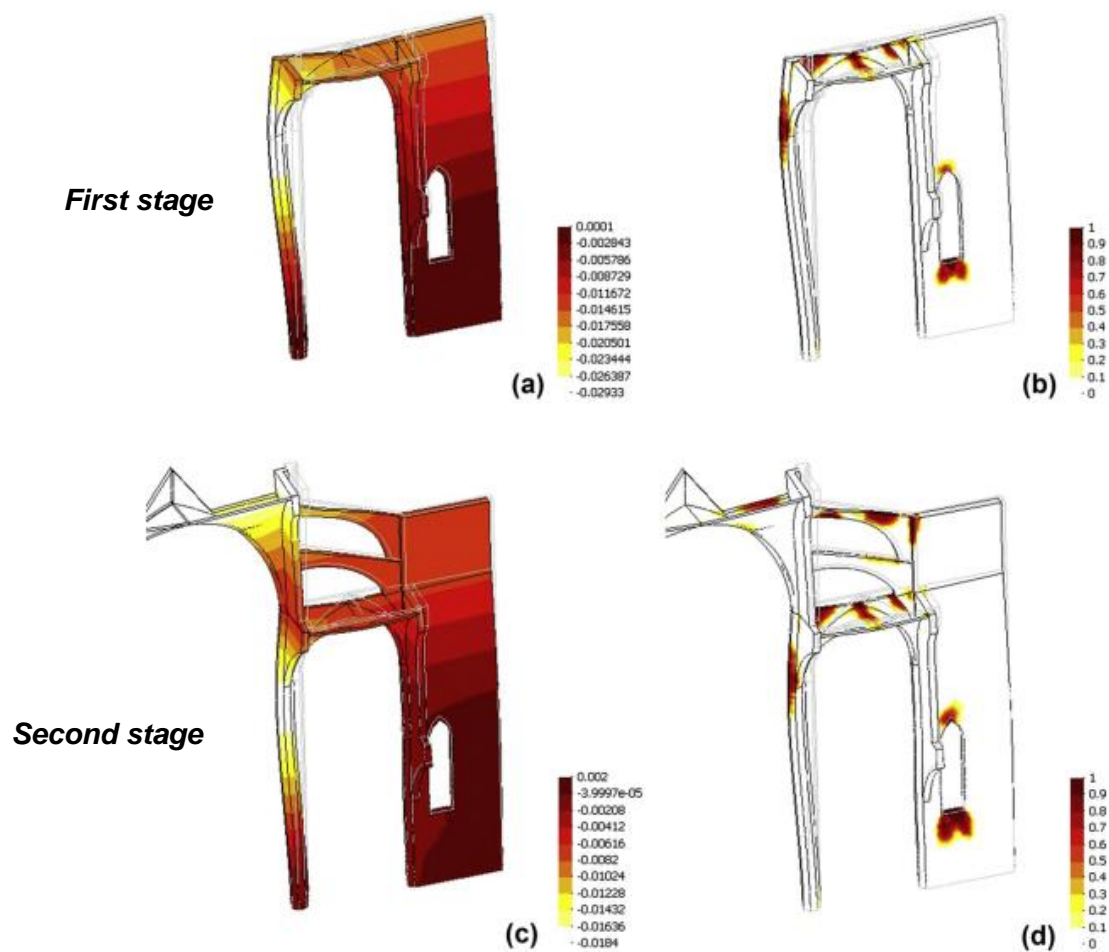


**Figure 73** – Simulation of the construction process of the 4<sup>th</sup> bay of Mallorca Cathedral. Deformed shape with horizontal displacements contours are presented on the left whereas tensile damage contours are presented on the right (Roca et al, 2013) .

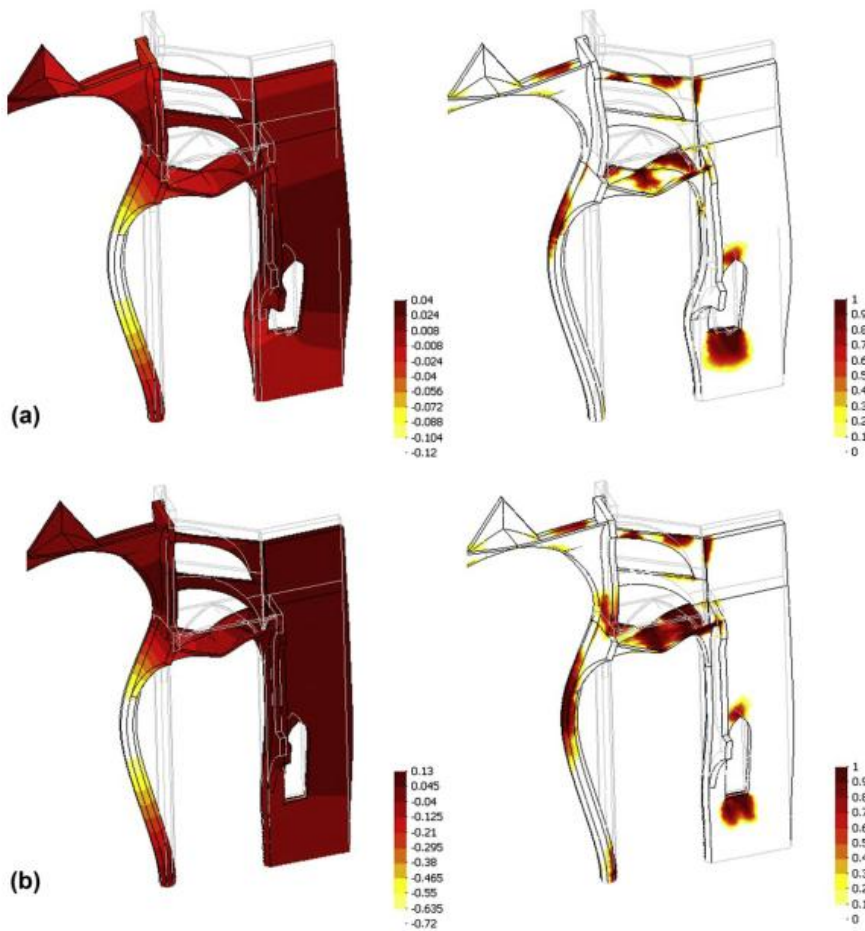


**Figure 74** – Construction process simulation with geometric non-linearity: (a) deformed shape (x50) with horizontal displacement contour (left) and tensile damage (right) for a participation ratio of 0.875, (b) deformed shape (x10) with horizontal displacement contour (left) and tensile damage (right) for a participation ratio of 0.975 (Roca et al, 2013).

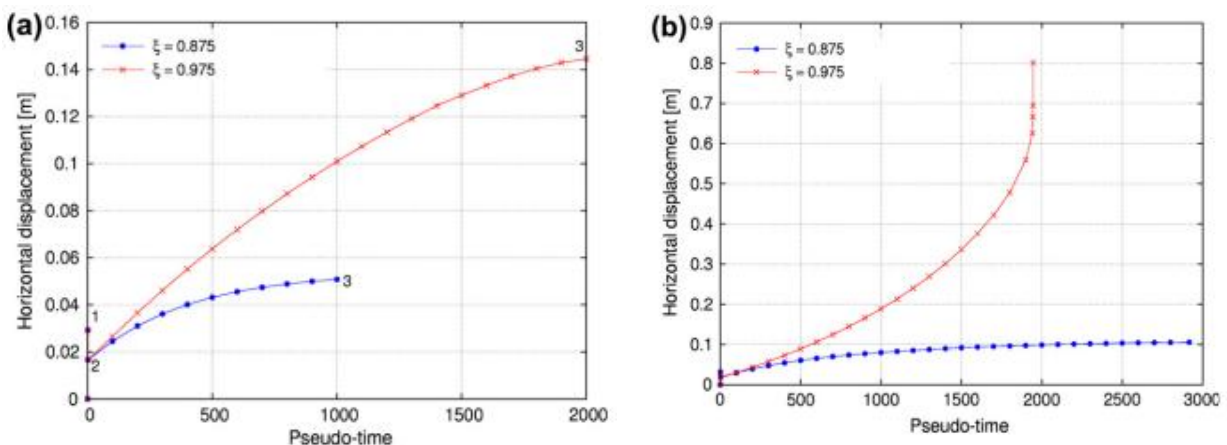


**Figure 75** – Evolution of the horizontal displacement at the top of the pier in function of pseudo-time for different participation ratios and for linear (a) and non-linear (b) geometry assumptions. (Roca et al., 2013)

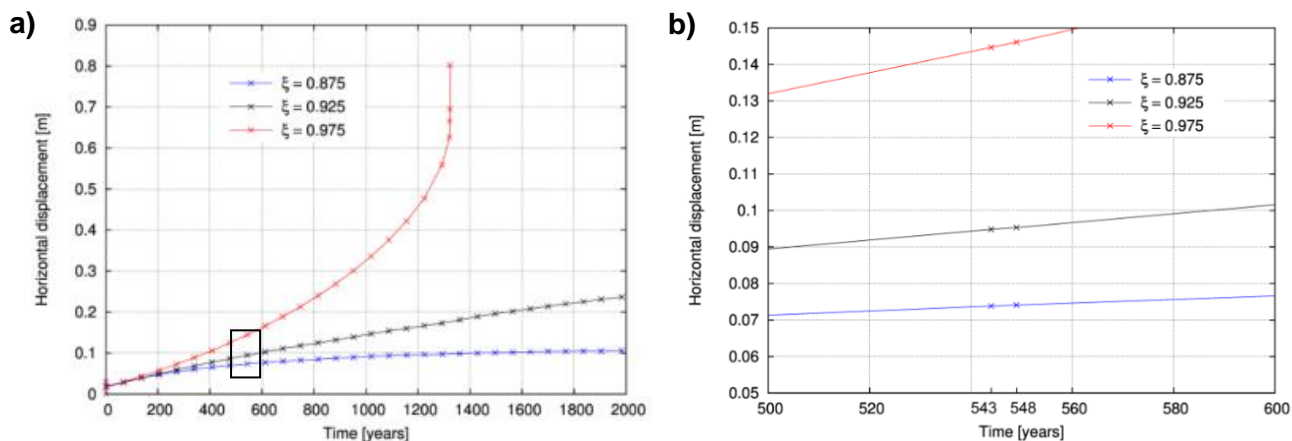


**Figure 76.** Long term creep behavior: horizontal displacements at the top of the pier vs. time obtained for three different participation ratio values a) obtained for the whole analysis; b) around the neighborhood of the monitoring period. (Roca et al., 2012)

The work of Roca et al, 2013, also included a seismic analysis of the bay by means of a pushover analysis. Shortly, this analysis has been performed on a corresponding 2D model assuming either a smeared crack formulation or a localized damage formulation (Cervera et al., 2010). It has been proved that the seismic load multiplier is influenced by the formulation used: for a smeared crack model, it is equal to 0.08, whereas for a localized damage model it can reach a value of 0.12.

This page is left blank on purpose.

## **4. ON-SITE EVIDENCES OF THE USE OF AUXILIARY TIES IN THE CONSTRUCTION PROCESS OF MALLORCA CATHEDRAL**

As it has been observed on previous works (Clemente, 2006, 2002 and Roca et al., 2013, 2012) the use of auxiliary ties during the construction process of Mallorca Cathedral cannot be disregarded. Those ties would have withstood the thrust of the vault of the lateral nave on the piers until the completion of the vault of the main nave. This technique has been used extensively during the gothic era all over Europe, as it has been proved in Section 2.3.2. and thus it is completely plausible that the master builders of Mallorca Cathedral used it as well. Nevertheless no deeper numerical study of the possible use of temporary ties must be done before a thorough investigation of the presence of ties remains in the Cathedral.

### **4.1. Investigation**

#### **4.1.1. On-site investigation**

From previously taken pictures, one can observe the presence of darker spots on the surface of the masonry, located in the lower part of the vault at two different heights. These spots seem to exist on each side of the lateral bay considered in the pictures and once the corresponding two spots of each side are linked together with fictive lines, a certain parallelism appears between the lines. Also the presence of two remaining ties for two of the bays (bays 6 – 7 and 5 – 6, see also Figure 77) has been noticed. Those ties may have been installed later as a consolidation device but they may have been placed during the construction process of the bay and then left in place.

Because of the existence of these interesting features, an on-site investigation on the existence of a possible ties remains patterns has been decided. The main objectives of this investigation were:

- to be familiar with the cathedral and its structure;
- to try to understand the origin and the nature of the darker spots;
- to carry out a thorough mapping of the presence of darker spots within the lateral naves of cathedral;
- to compare their position with the position of the two remaining ties;
- to have dense and complete photographic materials of these darker spots. These pictures have been used later to estimate the height of those spots.

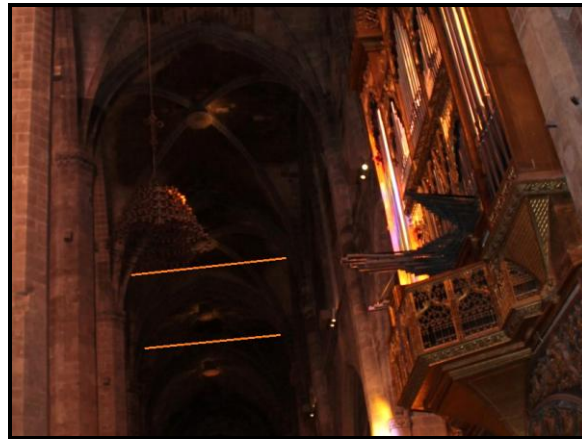
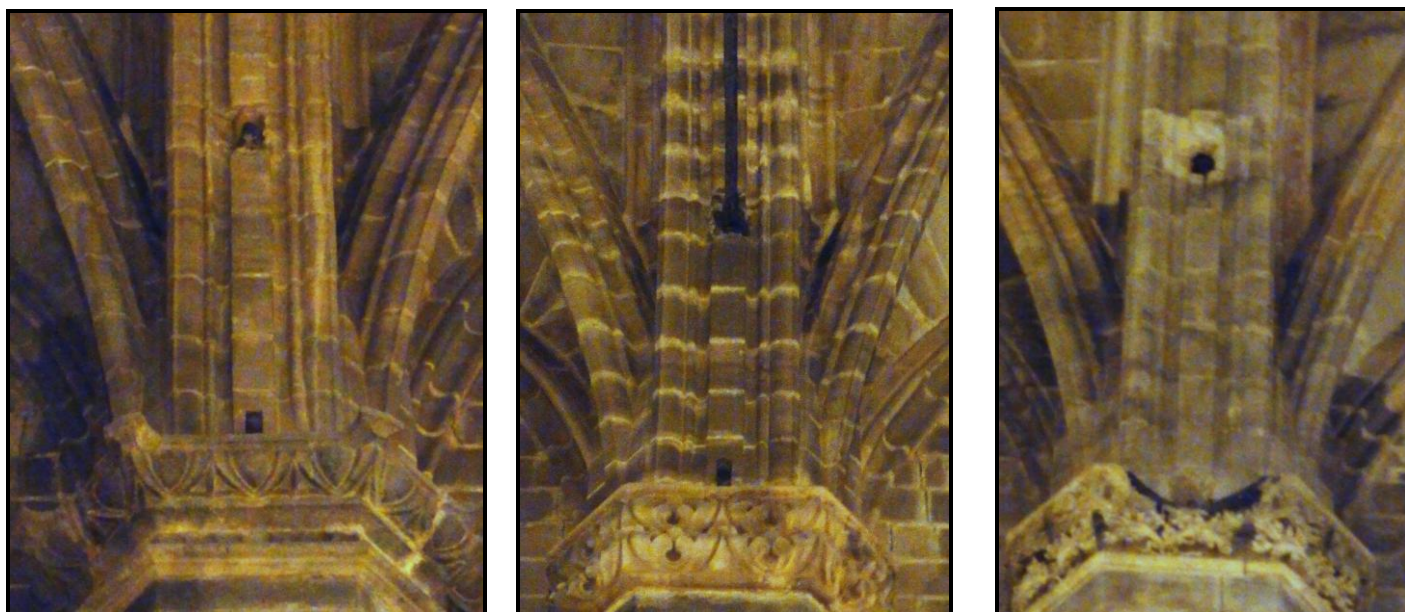


**Figure 77** – Previously taken picture where the two remaining ties in the northern lateral nave are visible (highlighted in orange).

This on-site study has been fruitful as it revealed extremely interesting features:

- The darker spots pattern has been detected for most of the bays of the cathedral. These darker spots are present in the northern lateral nave where the remaining ties are but also in the southern nave. Therefore they look like a characteristic feature of the bays of the cathedral.
- Moreover, there is a consistency of their height: in effect they always appear almost at the same heights. Concerning the upper spots, they are located at the same level as the remaining ties.
- By zooming on the spots, it has been possible to observe their real shape: concerning the upper ones, some of the pictures reveal that they are in fact remaining metallic hooks (Figure 81). The lower spots seem to be sawn rectangular metallic elements (Figure 78 and Figure 79).
- Some damages around these spots have been also observed. It seems that the masonry stone at these locations has been pulled off which may be explain by the presence of ties working in tension, leading to a concentration of tensile stresses at the location of their anchorages with the masonry. Another explanation may be that the material was damaged at such locations during the removal of the iron ties.





**Visual evidences of the double set of temporary iron ties for different locations.**

**Figure 78** – Northern nave, bay 7-8, exterior. A special interest must be taken on the almost perfect rectangular shape of the lower remain and the damage found in the surroundings of the upper one.

**Figure 79** – Northern nave, bay 6-7, exterior. Remaining upper iron tie, and lower tie remain with a rectangular shape.

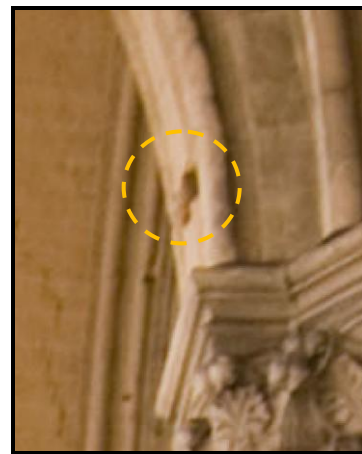
**Figure 80** – Northern nave, bay 4-5, exterior. Presence of damage in the surroundings of the ties anchorages.



**Figure 81** – Southern nave, bay 4-5, exterior. Remaining iron hook attached to the vault.

These features seem to be a proof of the use of structural iron ties during the lifetime of the cathedral. As it has been presented in Section 2.3.2., such auxiliary devices find their utilities during the

construction process of the building, when the static equilibrium of each part of the structure such as a bay, is not yet reached and unbalanced thrusts exercised on the vertical bearing elements (walls, piers, etc) by the already built vaults and arches can threaten the unstable equilibrium of the first stages of construction before the completion of the whole structure. In addition these features can be directly compared with the ties remains present in the cathedral Notre-Dame of Amiens in France and one can observe a striking similitude. First the remains found in the Amiens Cathedral seem to be positioned at the same position, i.e. the beginning of the arches of the lateral naves. Concerning the anchorage system, similar hooks have been used to bear the auxiliary iron ties in Amiens Cathedral. Also it seems that some of the ties have been sawn near the masonry, leaving rectangular darker spots contrasting with it. The strong resemblance of the two monuments with regards to these features seems to prove that the use of auxiliary ties during the construction process of Mallorca Cathedral should be highly considered.



**Cathedral Notre-Dame of Amiens, France**

**Figure 82** – Example of iron hook that linked the auxiliary iron tie with the masonry work.

**Figure 83** – Example of sawn ties located near the springing of one of lateral vaults: exterior.

**Figure 84** – Example of sawn ties located near the springing of one of lateral vaults: interior.

A thorough mapping of the location of the ties remains which includes visual evidences of the remains of temporary ties can be found on Figure 85 (interior) and Figure 86 (exterior).



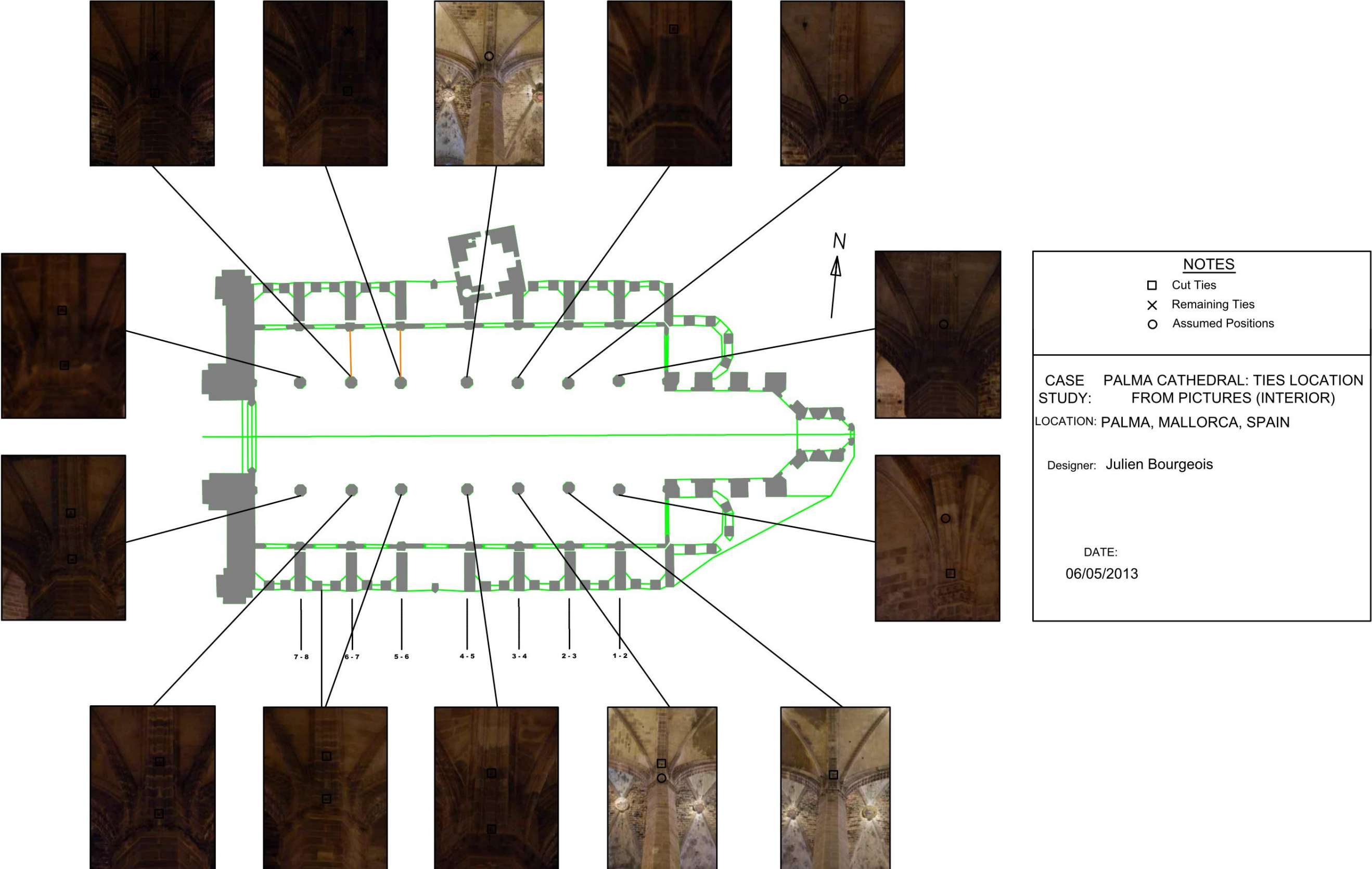


Figure 85 - mapping of the ties remains locations: interior.

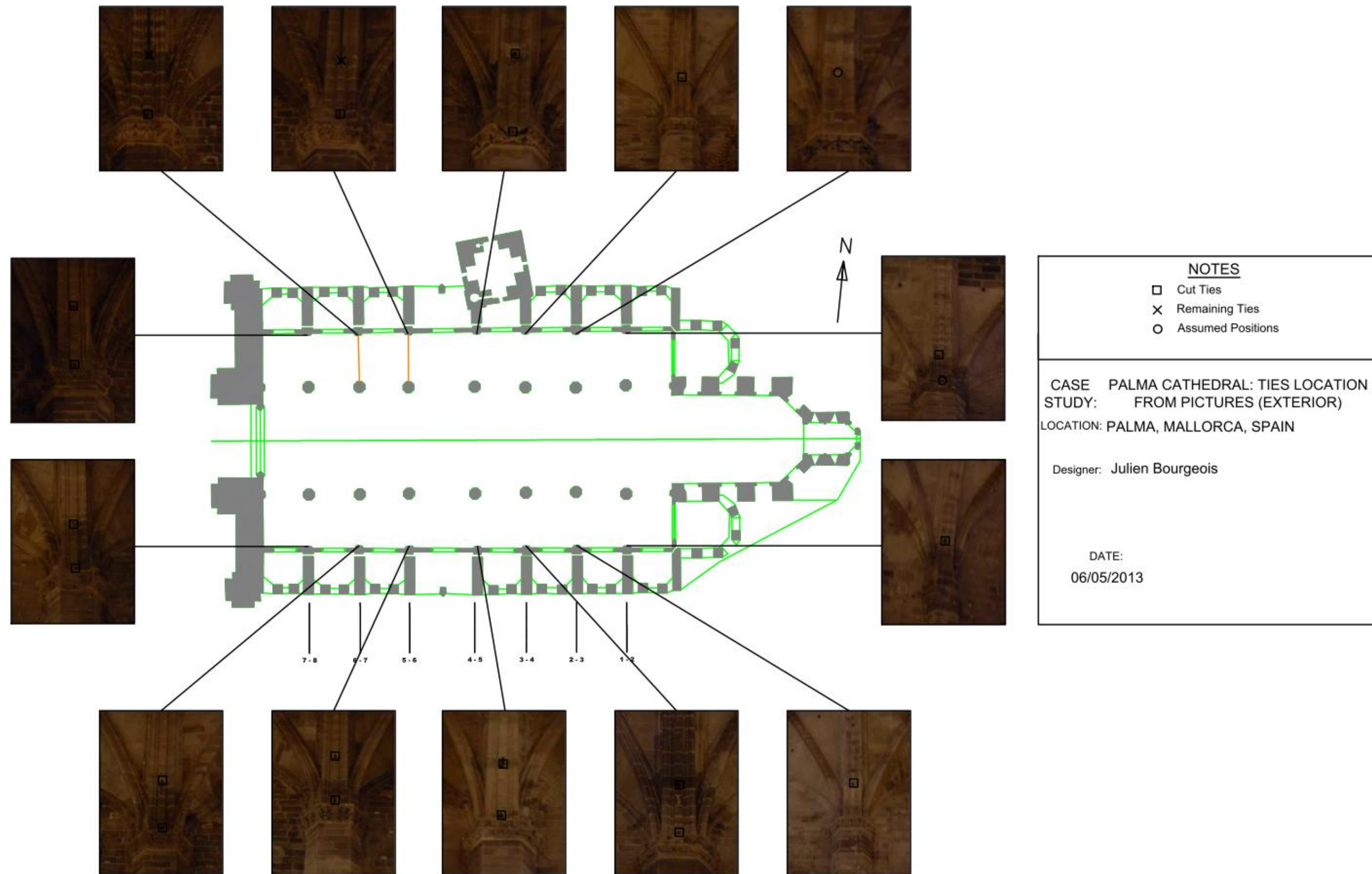
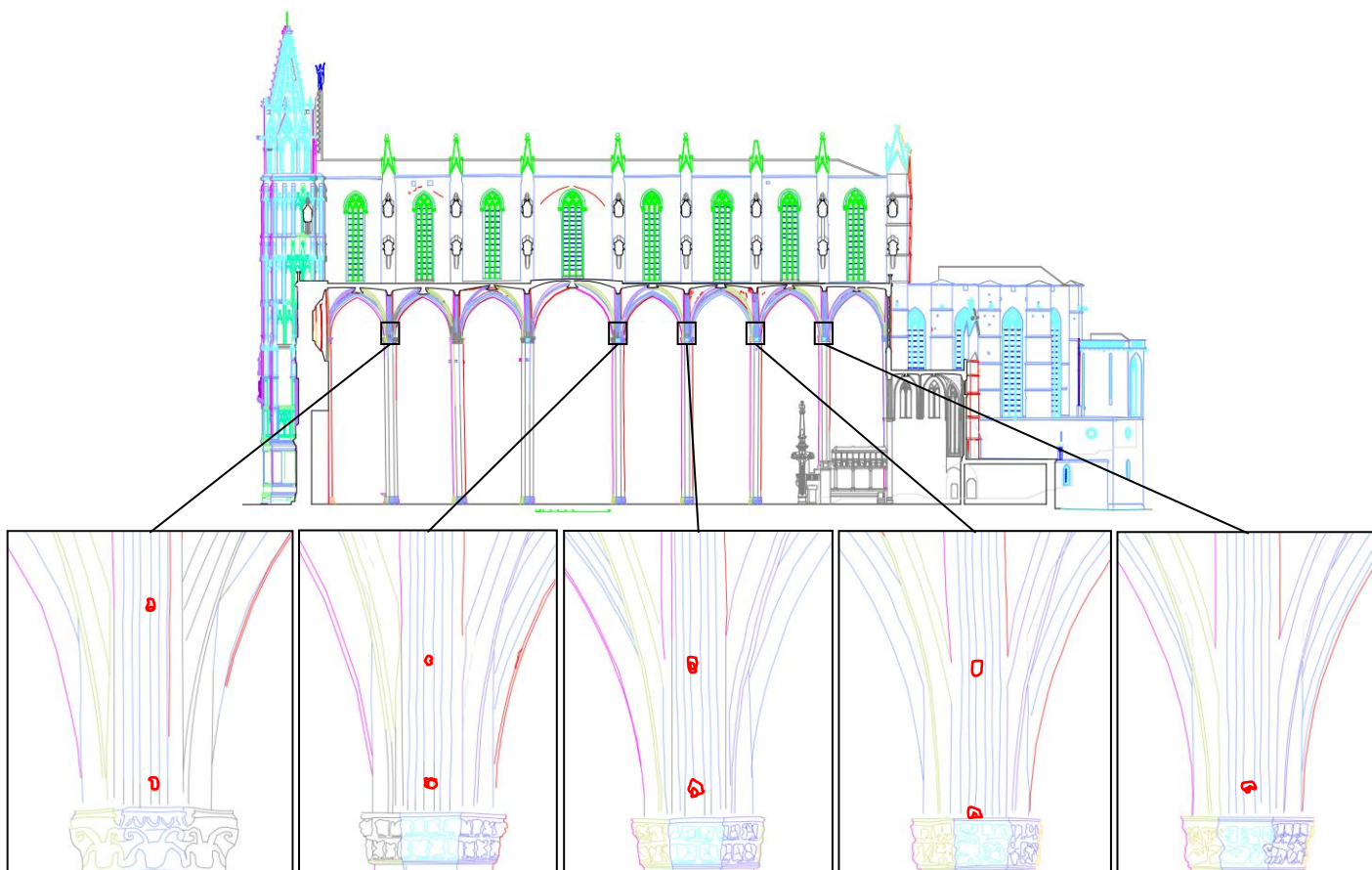


Figure 86 – mapping of the ties remains locations: exterior.



#### 4.1.2. Previous photogrammetric study

The analysis of the AutoCAD elevations of the southern lateral nave obtained after a photogrammetric study previously carried out at the beginning of the 21<sup>st</sup> century has also revealed the presence of elements that may be remains of temporary ties. As it will be developed later, the height of those elements presents a good accordance with the height found with the pictures (Figure 87).



**Figure 87** – Existing AutoCAD elevation of the south nave based on the photogrammetric study of Mallorca Cathedral. Possible remains of ties anchorages are highlighted in red on the lower pictures.

#### 4.2. Dimensions and positions

The combined study of the pictures taken during the on-site investigation, the elevation of the south nave of the cathedral resulting of its photogrammetric study as well as the use of a laser pointer, has allowed to find a good approximation of the height of the ties remains. The two former have also permitted to have an idea of the section of the missing ties.

##### 4.2.1. Ties locations

On the following elevations, the height of the remains has been measured between the top of the capital of the pier and the estimated centre of the ties remains (they are given in meters). hp, hP and hI mean respectively the height found with the pictures study, the height found with the elevations

drawn by means of the photogrammetric study and height found with the use of a laser pointer. These heights are respectively shown with a triangle, a cross and a circle. Whenever it was not possible to identify the height of the ties or even the presence of a tie, the symbol “?” was used.

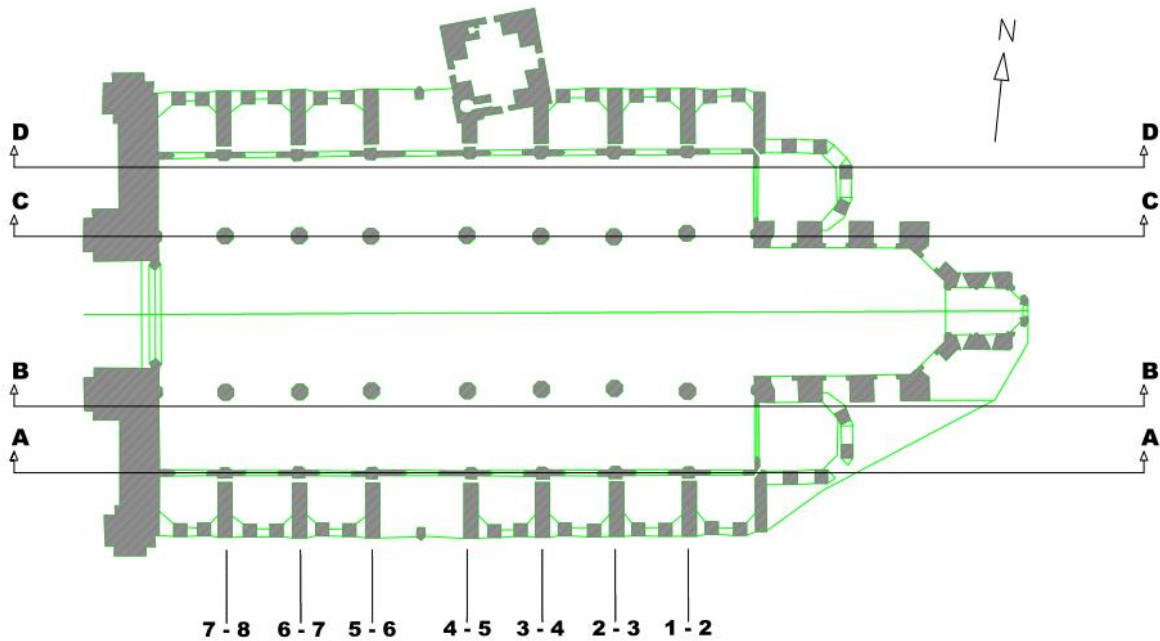


**Figure 88** – Plan view of Mallorca Cathedral with the bays designation.

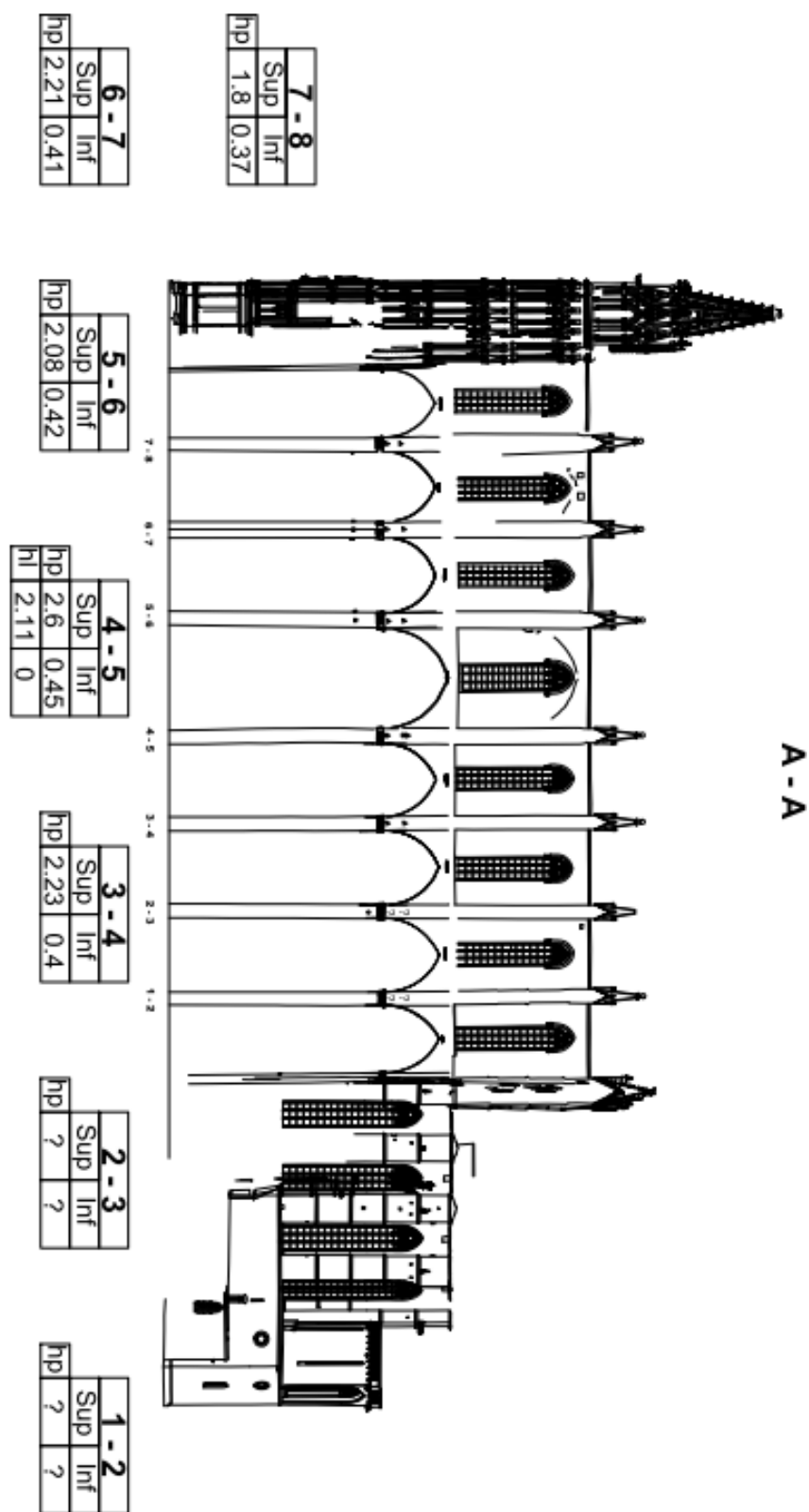


Figure 89 – Cut A-A: South lateral nave, exterior elevation



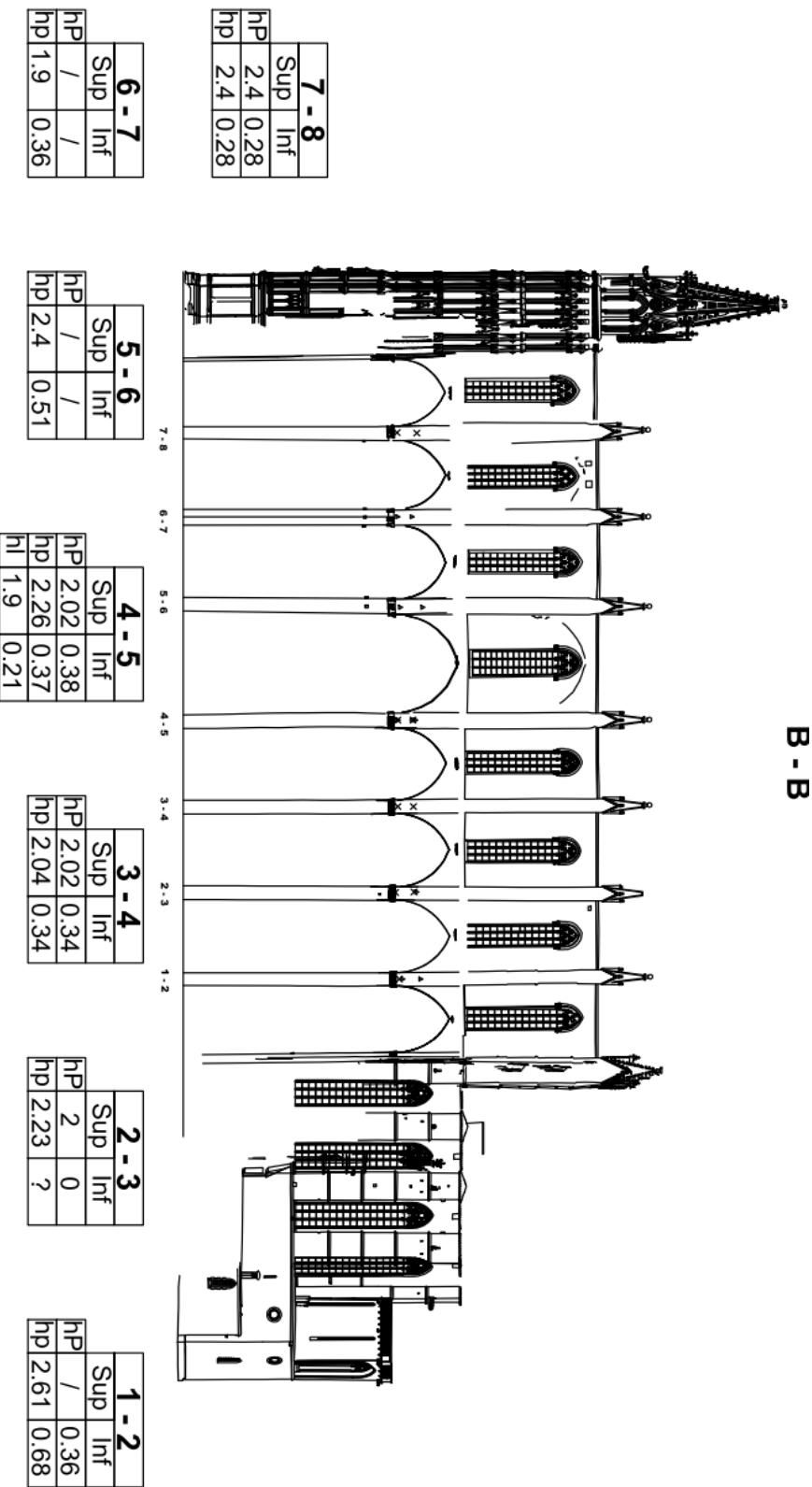


Figure 90 – Cut B-B: South lateral nave, interior elevation

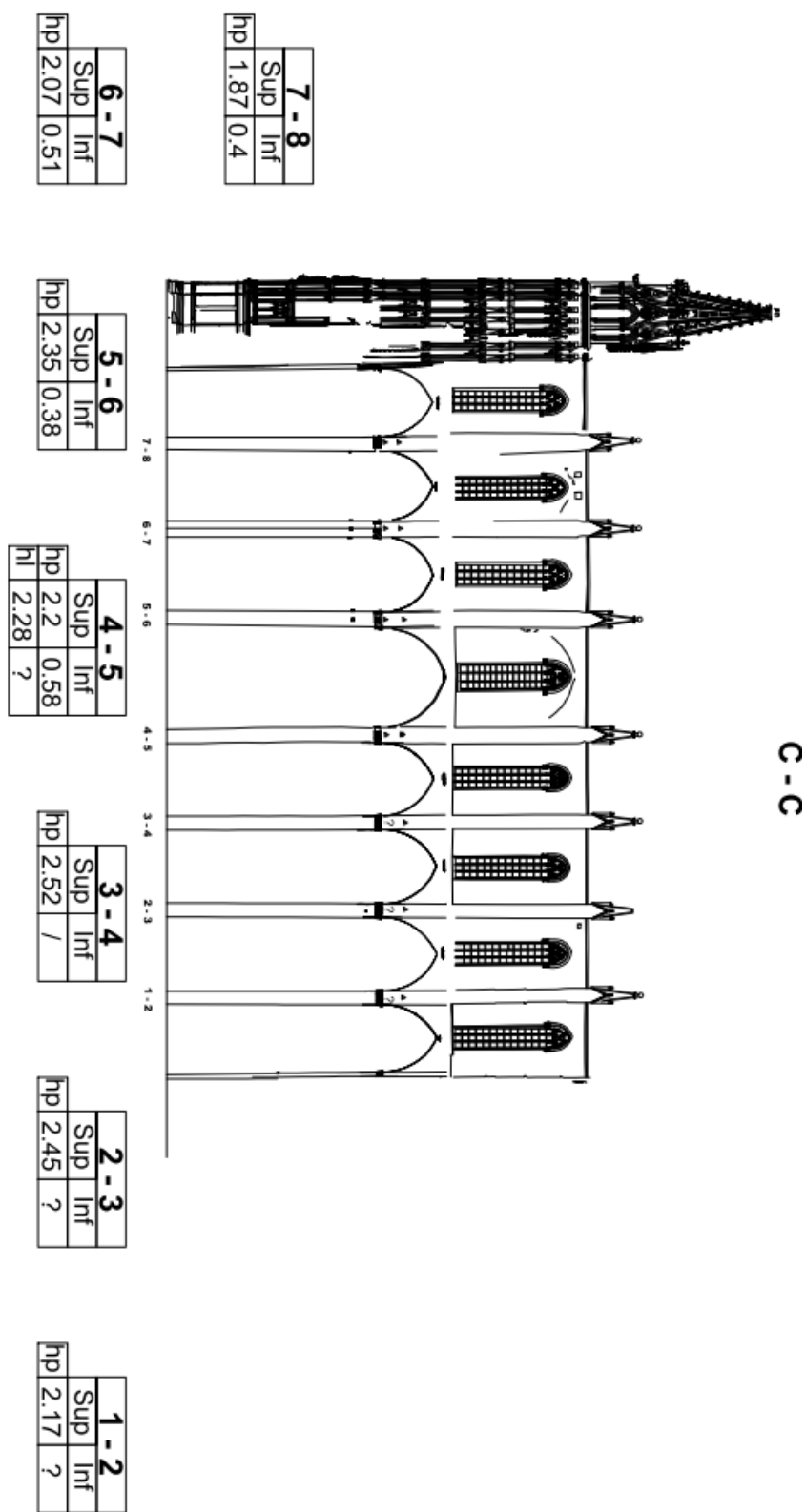


Figure 91 – Cut C-C: North lateral nave, interior elevation

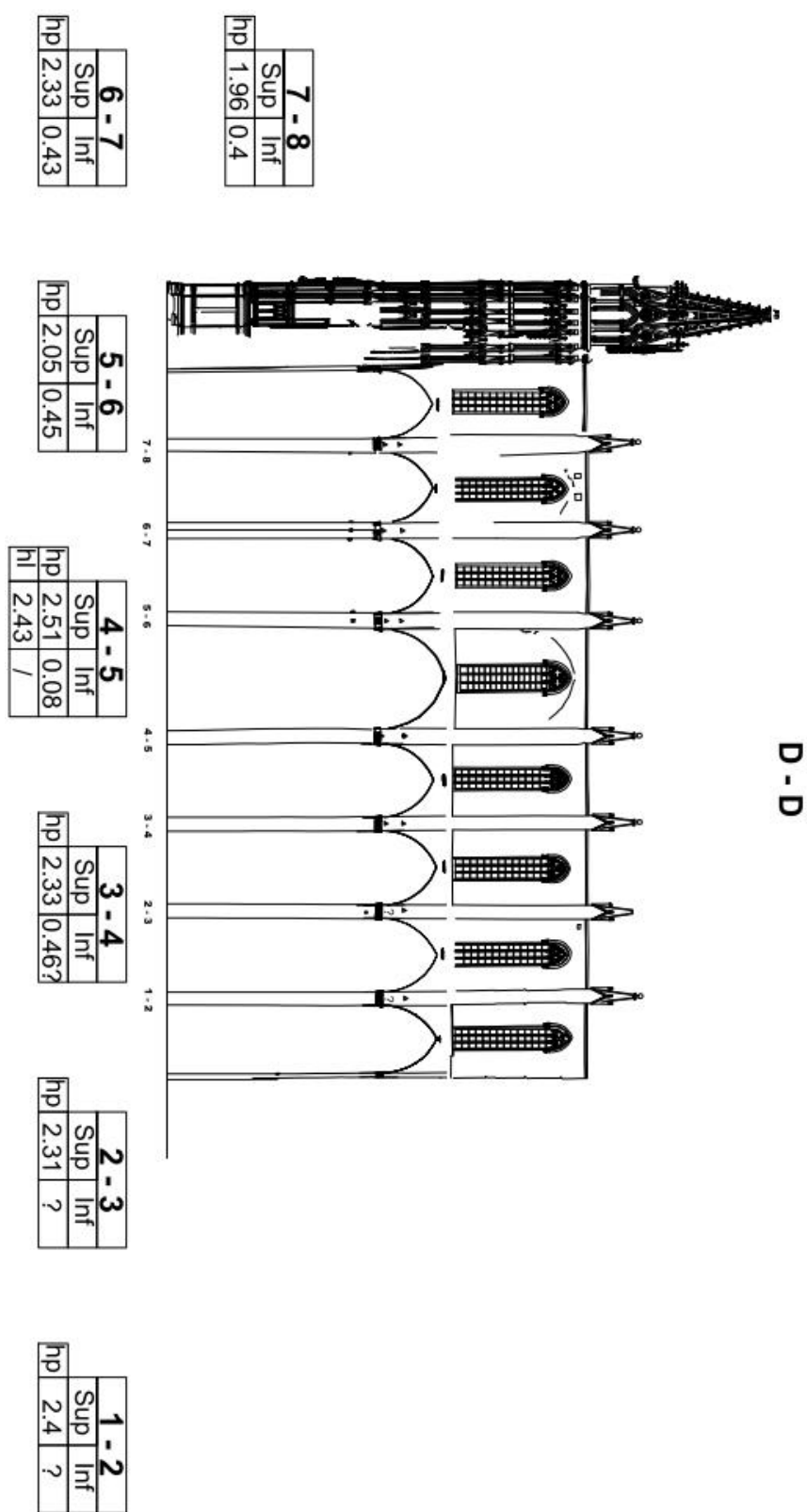


Figure 92 – Cut D-D: North lateral nave, exterior elevation

Table 6 and Table 7 summarize the results obtained with the three methods for the bay 4–5 respectively for the upper tie and the lower tie.

|                | Northern lateral nave |          | Southern lateral nave |             |
|----------------|-----------------------|----------|-----------------------|-------------|
|                | Exterior              | Interior | Exterior              | Interior    |
| Photogrammetry | /                     | /        | /                     | <b>2.02</b> |
| Pictures       | 2.51                  | 2.2      | 2.6                   | <b>2.26</b> |
| Laser          | 2.43                  | 2.28     | 2.11                  | <b>1.9</b>  |

**Table 6** – Heights of the remains of the upper ties from the capital for the 4<sup>th</sup> bay. The results are given in meters and have been measured from the top of the capital of the columns which will be the reference for the study developed later.

|                | Northern lateral nave |          | Southern lateral nave |             |
|----------------|-----------------------|----------|-----------------------|-------------|
|                | Exterior              | Interior | Exterior              | Interior    |
| Photogrammetry | /                     | /        | /                     | <b>0.38</b> |
| Pictures       | 0.08                  | 0.58     | 0.45                  | 0.37        |
| Laser          | /                     | /        | 0                     | 0.21        |

**Table 7** – Heights of the remains of the lower ties from the capital for the 4<sup>th</sup> bay. The results are given in meters and have been measured from the top of the capital of the columns.

A first observation is the dispersion of the results obtained with the different techniques. Because of the uncorrected distortion of the pictures, the heights measured on them should be greater than the real ones. Moreover the values given by the laser pointer should not be considered as completely accurate due to on-site measurements difficulties. Therefore the values given by the photogrammetry study are the most accurate and they should be used for the model.

#### 4.2.2. Ties dimensions

By considering the plans of the interior of the South aisle of the cathedral based on the photogrammetry and by considering the pictures of the sections 6-7 and 5-6 with a focus on the existing ties, it is possible to estimate the dimensions of the ties.

For the photogrammetry study, the dimensions are given on the following table. Note that the values highlighted in grey have been discarded because they were considered too small. The results are given in cm<sup>2</sup>.

|                  | (7-8) | (6-7) | (5-6) | (4-5) | (3-4) | (2-3) | (1-2) |
|------------------|-------|-------|-------|-------|-------|-------|-------|
| <b>Upper-tie</b> | 9.3   | /     | /     | 8.2   | 18.0  | 20.1  | /     |
| <b>Lower-tie</b> | 10.8  | /     | /     | 15.3  | 28.2  | 20.7  | 18.0  |

**Table 8** – Ties area assumed from the results of the photogrammetric study (unit: cm<sup>2</sup>).

The following table gives the width of the ties obtained by analyzing the pictures of the northern lateral bay for the sections 6-7 and 5-6 (where there are still remaining ties) and the corresponding area assuming a square section. The results are given in cm.

|          | (6-7)      |                                   | (5-6)      |                                   |
|----------|------------|-----------------------------------|------------|-----------------------------------|
|          | width (cm) | Area if square (cm <sup>2</sup> ) | width (cm) | Area if square (cm <sup>2</sup> ) |
| Interior | 4.5        | 20.2                              | 4.5        | 20.2                              |
| Exterior | 7.2        | 51.8                              | 6.5        | 42.2                              |

**Table 9** – Width of the remaining ties measured on the pictures and the corresponding area if a square section is assumed (unit: cm and cm<sup>2</sup>).

The results, even scattered, present the same order of magnitude: they range from 18 cm<sup>2</sup> to 51.8 cm<sup>2</sup>. This difference can be explained by the distortion of the pictures, the assumption of a square section but also by the fact that what is measured from the photogrammetry study may not be the entire section. Nevertheless an average value can be calculated: one can obtain 26.6 cm<sup>2</sup> as an approximation of the cross-section area of the lower and upper ties. If this section is assumed, the only possible material for the ties is iron. In effect, if it were wood, the section should be far greater as it is possible to observe for the Church Saint-Philibert of Tournus (Figure 50). One can also notice that the values found are of the same order of magnitude than the ones found by Mira Vasic for the long-lasting ties of Milano Cathedral (between 35 cm<sup>2</sup> and 55 cm<sup>2</sup>). (Vasic, 2013)

## 5. STRUCTURAL ANALYSIS

As it has been stated in Section 3.5.2., numerous structural analyses have already been carried out for the 4<sup>th</sup> bay of Mallorca Cathedral. The initial studies didn't take into account the construction process and the long-term creep behavior of the masonry of the bay, leading to qualitative results concerning the displacements and the deformation endured by the structure. Clemente, 2006 was the first to consider a sequential analysis of the construction process of the bay. His analysis was divided into three stages: a first stage involving the construction of the lower part of the bay (lower part of the buttresses, lower part of the piers and the lateral vaults), a second stage involving the completion of the bay (upper-part of the buttresses and piers together with the vault of the central nave) and a third stage taking into account the long-term creep behavior of the masonry. His work was continued by Roca et al., 2013, 2012 who considered a horizontal correction of the construction after the achievement of the first stage of the model. The results obtained in the study afford-mentioned were closer to the actual deformation state of the bay. It was supposed that the first stage of construction didn't require any auxiliary devices for its stability, thank to the tensile strength of the masonry. Nevertheless it was mentioned in this work that the use of such devices during the construction process of the bay couldn't be disregarded.

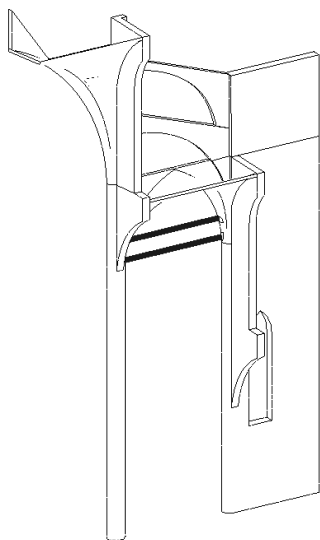


**Figure 93** – Overview of the model with the two auxiliary ties.

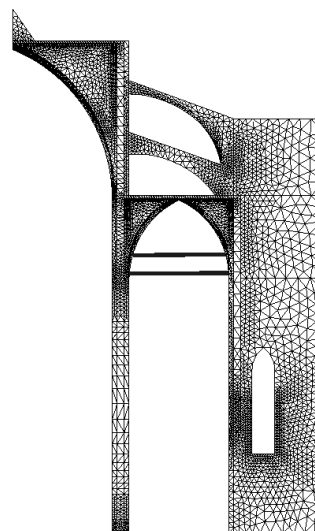


**Figure 94** – Corresponding FEM mesh: 3D tetrahedral elements for the masonry, 2D truss elements for the ties.

The purpose of the present analysis is to consider the use of temporary iron ties within the already developed model of Roca et al., 2013, 2012 and to analyze the consequences of the use of such auxiliary devices on the construction process stages as well as the their influence on the actual state of the bay taking into account the long-term creep behavior of the masonry. This work will contribute to

gain a better understanding of the structural problems linked to the construction stages of the 4<sup>th</sup> bay of Mallorca Cathedral and to have a better understanding on how gothic master builders dealt with the existence of unbalanced forces such as thrusts during its construction process. The pre-post processor GID (CIMNE, 2002) and the FE software COMET (Cervera et al., 2002), both developed at the CIMNE (UPC), have been utilized for this study. These softwares have been applied in many recent studies for the FE analysis of masonry structures, see also Pelà, 2009 and Pelà et al., 2013.

### 5.1. Model description

The original FE model developed by Roca et al., 2013, 2012 has been carefully modified in this work to include the iron ties in the structure discretization. The model is composed by 49 979 tetrahedral elements, 2 2D truss elements and 14 689 nodes. The new model includes 4 new material sets (2 sets for the ties and 2 others for the different anchorages) which increase the number of sets to a total of 17. The different material sets are presented on Figure 95.

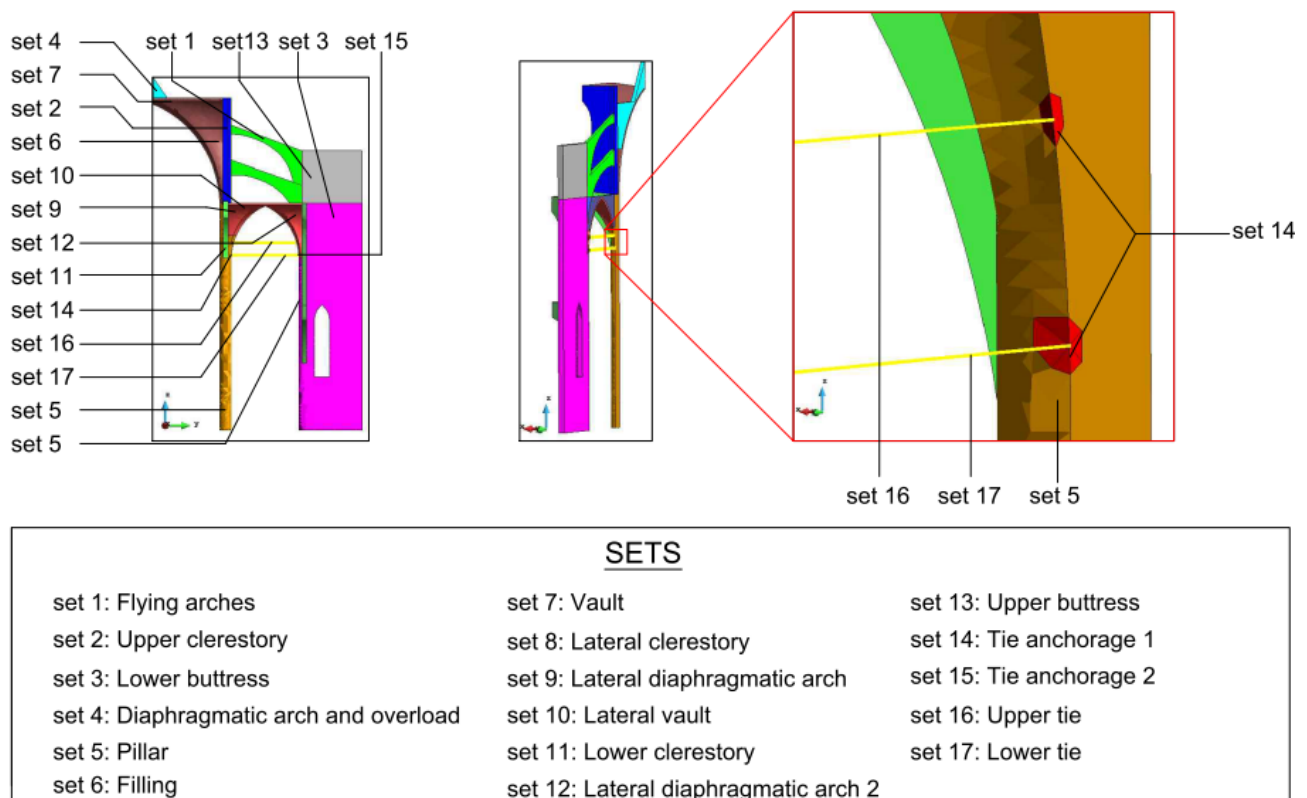


**Figure 95** – Definition of the different sets of the present model and their localization.

#### 5.1.1. Integration of the ties

As previously explained, due to an assumed geometrical symmetry, only a quarter of the bay has been modeled (Roca et al, 2013). Each tie has been modeled with a 2D truss element. From the results obtained previously in Section 4.2.2., the total cross-section of the ties has been assumed to be equal to 25 cm<sup>2</sup>, leading to a section to implement of 12.5 cm<sup>2</sup> (only half of each tie is modeled).



The ties are considered elastic since they are made of relatively ductile iron compared to the masonry ductility in tension.

### *Location of the ties*

From the data collected in Section 4.2.1., it has been possible to estimate the height from the upper part of the capital of the piers to the ties anchorages location. Combining the data collected with photogrammetry, pictures and laser pointer and assuming that the photogrammetric data are more relevant than the others, the following heights have been considered for the present work:

- 0.40 meter from the top of the capital of the pier to the center of the lower tie;
- 2.06 meters from the top of the capital of the pier to the center of the upper tie, corresponding to the average value of the height given by each of the three methods.

Those heights have been considered for both sides of the bay and the ties are believed to be horizontal. In order to insert the ties inside the model without significantly modifying the finite element mesh already developed by Roca et al., 2013, it has been decided to connect the ties with the masonry at already existing nodes of the mesh. As a way of consequences, the chosen heights had to be slightly modified. Table 10 gives the final heights chosen for each side of the lateral vault and the corresponding nodes of the mesh. In the table, "inside" indicates the anchorage with the pillar, i.e. towards the main nave, while "outside" indicates the anchorage with the buttress, i.e. towards the outside the cathedral.

|       |                     | Upper tie |         | Lower tie |         |
|-------|---------------------|-----------|---------|-----------|---------|
|       |                     | Inside    | Outside | Inside    | Outside |
| Model | Assumed height      | 2.06      |         | 0.4       |         |
|       | Height from capital | 2.031     | 2.081   | 0.412     | 0.435   |
|       | Corresponding node  | 5682      | 4044    | 5050      | 3803    |
|       | Height from capital | 1.985     | 1.999   | 0.402     | 0.404   |
|       | Corresponding node  | 8845      | 12443   | 8647      | 11966   |

**Table 10** – Assumed heights from photogrammetric, photographic and laser data and the final heights chosen in the model. All the values are given in meters.

Concerning their horizontal position, the ties have been inserted in the middle of vault.

### *Anchorage system*

It was first assumed that the ties were connected to the exterior part of the masonry. In order to avoid a stresses concentration within the elements surrounding the nodes of connection which may have led to unwanted local failures, those elements have been considered as elastic. Because this modification of the original model was very localized, it was assumed that the overall structural behavior of the bay

would not be affected. A second model has been implemented in which the lower tie only was considered and was this time inserted within the masonry according to some sketches drawn by Viollet-le-Duc (Figure 97). This location is purely hypothetical and was arbitrarily chosen only to compare the results of the two models with different locations of the anchorages. Note that all the other parameters, laws and mathematical formulations for the two models are exactly the same.

The differences of the results for the displacements as well as for the deformed shape of the structure are negligible. Only the tensile damage contour for the two models is different (Figure 98). In effect while tensile damage can be observed at the anchorages locations of the ties for the first model, no tensile damage at this very location is observed for the second one. Those tensile damage patterns seem to reflect the real behavior of the structure: as it has been observed in Section 4.1.1., the masonry is damaged in the surroundings of the ties remains for numerous bays. Even if these damages may be linked to iron corrosion problem or to the ties removal, they may be due also to a localized concentration of tensile stresses in this area. Therefore the ties have been assumed to be anchored to the exterior side of the masonry.

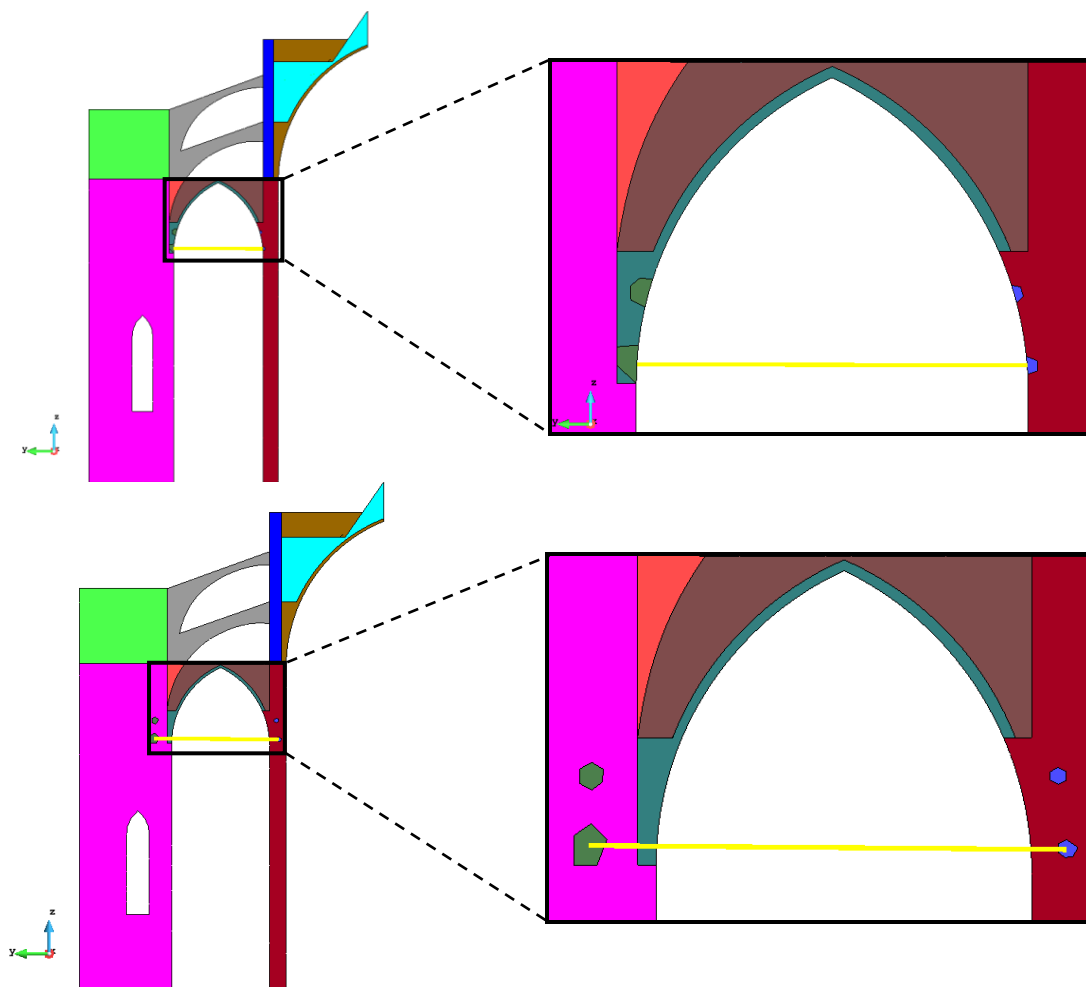


**Figure 96** – Location of the ties anchorages: (a) outside the masonry; (b) inside the masonry (they are represented in dark green and blue).

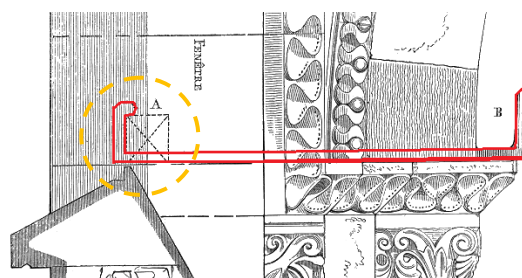


**Figure 97** – Schematic view of the anchorage system of an iron hook within the masonry (from Viollet-le-Duc, 1854-1868).

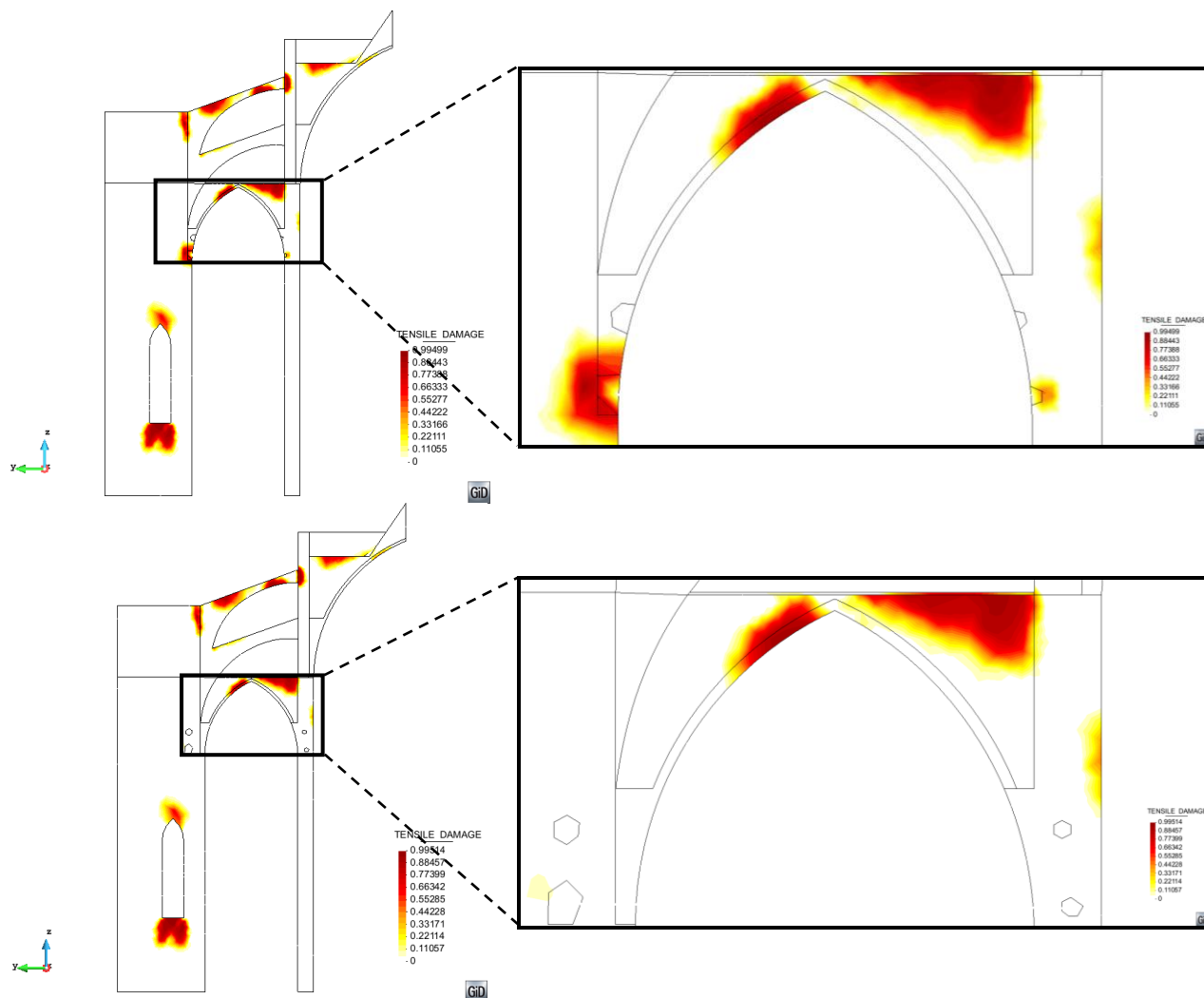


**Figure 98** – Localization of the tensile damage after the second stage of construction for 2 different positions of the anchorage: (a) outside the masonry; (b) inside the masonry. Only the lower tie is activated.

### 5.1.2. Materials parameters

The materials parameters that have been used for the present study are presented in Table 11. Note that the tensile strength of the masonry has been taken equal to 5% of the compressive strength and both the tensile fracture energy and the compressive fracture energy of the masonry are assumed to

be really high in order to simulate a proper distribution of damage in the most critical locations of the structure (Clemente, 2006).

| Model                            | Structural Element                         | $\gamma$ (kg/m <sup>3</sup> ) | E (MPa) | $\nu$ (-) | $f_t$ (MPa) | $f_c$ (MPa) |
|----------------------------------|--|-------------------------------|---------|-----------|-------------|-------------|
| Tension<br>compression<br>damage | Flying arches,<br>piers                    | 2400                          | 8000    | 0.2       | 0.40        | 8.00        |
|                                  | Clerestory,<br>buttresses,<br>vaults, ribs | 2100                          | 2000    | 0.2       | 0.10        | 2.00        |
|                                  | Central vault<br>backing                   | 2000                          | 1000    | 0.2       | 0.05        | 1.00        |
| Elastic                          | Iron ties                                  | 7874                          | 2.00E5  | 0.278     | /           | /           |
|                                  | Tie anchorage<br>(Pillar)                  | 2400                          | 8000    | 0.2       | /           | /           |
|                                  | Tie anchorage<br>(Vault)                   | 2100                          | 2000    | 0.2       | /           | /           |

**Table 11** – Materials properties used in the model

The properties of the iron ties used here are the ones found in the literature (Section 2.3.5. Ties properties). Two sets for the ties anchorages have been defined due to the different properties of the masonry they are connected with.

### 5.1.3. Additional weights

As the models developed before (Clemente, 2006, Roca et al, 2013, 2012) the pinnacles, the infills and the stone pyramids over the lateral vaults have not been modeled as elements in the model. Instead only their self-weight have been considered.

### 5.1.4. Boundary conditions

Because only one quarter of the bay has been considered, it was necessary to defined boundary conditions taking into accounts the effects of the rest of the bay and the effects of the adjacent bays. The boundary conditions have been implemented in the previous models (Roca et al., 2013, 2012), and no change has been done for the present model.

## 5.2. Modeling strategy

Several models have been computed in order to gain a better understanding of the consequences of the use of auxiliary ties during the construction process of Mallorca Cathedral.

### 5.2.1. Different configurations

From the studies developed in Section 4.2.1., two potential locations for the ties exist: an upper tie located at 2.06 meters from the top of the piers capital, and a lower one located at 0.40 meter from

this reference height. Nevertheless, even if visual evidences on the existence of ties remains have been found for each bay, only suppositions can be done concerning their use and the duration of their use. Four different ties configurations have been studied:

- Activation of the upper tie only;
- Activation of the lower tie only;
- Activation of the two ties;
- No tie (this model has been used to compare the results previously obtained by Roca et al., 2013, 2012 as well as a reference to compare the results obtained with the other configurations).

### **5.2.2. Formulation**

Two different formulations have been considered in the following: a small strains/small displacements formulation and a small strains/large displacements one which takes into account the geometrical non-linearity effects in the structure.

### **5.2.3. Sequential analysis**

The sequential analysis has been divided into 4 different stages and an intermediate step. Each of them has a significant importance on behavior of the structure:

- First stage: beginning of the construction. During this stage, only the sets corresponding to the lower part of the bay have been activated in the analysis. These sets include: the lower part of the buttress, the pier, the lateral clerestory, the lateral diaphragmatic arches, the lateral vault, the lower clerestory, the ties anchorages, and the ties (if their activation is considered in the analysis);
- Correction of the upper-part of the structure before its activation. Because the lower part of the structure has undergone deformations during the first step, the coordinates of the nodes of the upper part have to be corrected in order to take into consideration these deformations. This correction plays an important role when a small strains/large displacements formulation is considered. Based on the two following assumptions: maintenance of the direction of the vertical and horizontal lines and negligence of the total elongation of the line at the boundary between parts corresponding to different phases (Roca et al., 2013), an average displacement vector taking into account the horizontal and vertical deformations of the first stage has been applied to the nodes of the upper part of the structure.

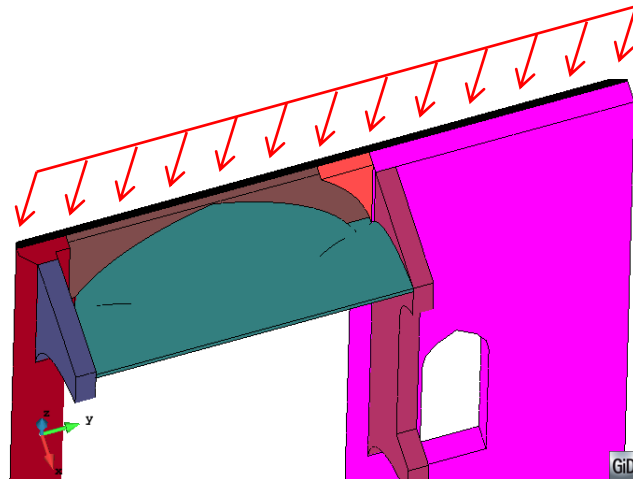


**Figure 99** – Nodes considered to calculate the averaged correction of the upper part (black line below the arrows).

- Second stage: construction of the rest of the bay. During this stage, the bay is completed. In addition to the sets of elements previously activated, the upper part of the bay is added. This includes the upper buttress, the upper clerestory, the flying arches, another diaphragmatic arch with its overload, the vault of the main nave and its filling.
- Third stage: removal of the ties. If the ties are considered as auxiliary devices, their quick removal may have led to an increase of deformations. Therefore it is of primary importance to consider this step as an entire stage.
- Fourth stage: long-term creep behavior of the masonry.

#### 5.2.4. Parallel studies

Two parametrical studies have been developed in parallel, respectively on the influence of the ties cross-section and on the influence of the tensile strength value of the masonry.

### 5.3. Study of the use of auxiliary ties during the construction of the bay

#### 5.3.1. General assumptions and outcomes

In this part, the following assumptions have been adopted:

- A tensile strength of the masonry equal to 5% of its compressive strength;
- An exponential softening law for the masonry (Figure 100);
- High fracture energies in tension and compression in order to simulate the formation of plastic hinges with considerable ductility as it has been assumed in the work of Clemente, 2006;
- A total cross-section of the ties assumed to be equal to 25 cm<sup>2</sup>;
- A small strains/large displacements formulation for the first and second parts of the study.

The study will focus on the horizontal and vertical displacements of three characteristic nodes of the model:

- node 5383 corresponding to the top of the pier;
- node 5682 corresponding to the connection of the upper tie with the pier (note that in the model the set “Pier” also includes the lower part of the lateral arch);
- node 5050 corresponding to the connection of the lower tie with the pier.

The state of stresses within the ties after the first two steps will be also considered and finally a special attention will be done on the tensile damage within the structure and especially at the ties anchorages locations.

The study of the fourth step of the sequential analysis, i.e. the long-term creep behavior of the masonry, will be treated in a separate part. In this part the evolution of the horizontal displacement at the top of the pier (node 5383) with time will be analyzed, considering a lower tie configuration and a configuration with no tie.

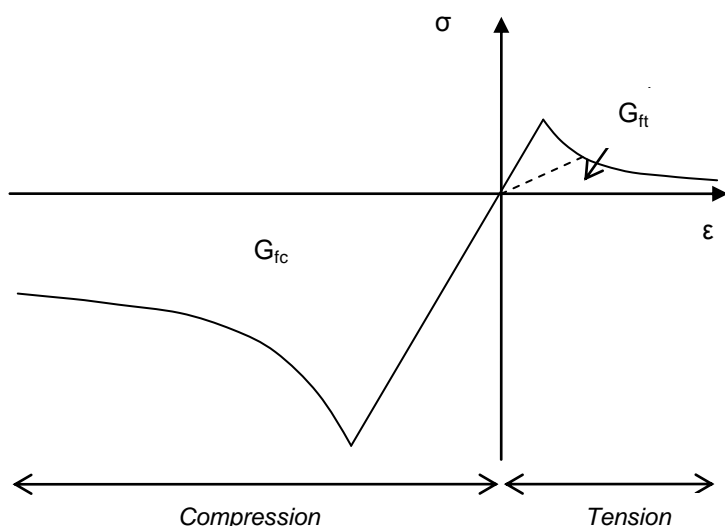


**Figure 100** – Exponential softening law in tension and compression considering finite fracture energies in tension and compression.

### 5.3.2. Construction process and ties removal

The following study has been carried out considering both small strains – small displacements and small strains – large displacements formulations. Nevertheless because the difference between the obtained results in both cases are negligible, only the results obtained with the latter formulation will be presented here. It is logical that the results are really close because the deformations are rather small which will not be the case for the 4<sup>th</sup> step of the analysis taking into account the long-term creep behavior of the masonry. Note that the deformed shapes for the first stage as well as the horizontal displacements contour for each configuration are given in Annex B.



### Displacements and correction

Figure 101 gives the evolution of the horizontal displacement in function of the length of the upper part of the construction after the completion of the first stage. From these data it has been possible to calculate the average horizontal correction to apply for each tie configuration (Table 12). Table 13, Table 14 and Table 15 give the results obtained for the vertical and horizontal displacements at node 5383, 5682, and 5050 after each sequential stage of the analysis.

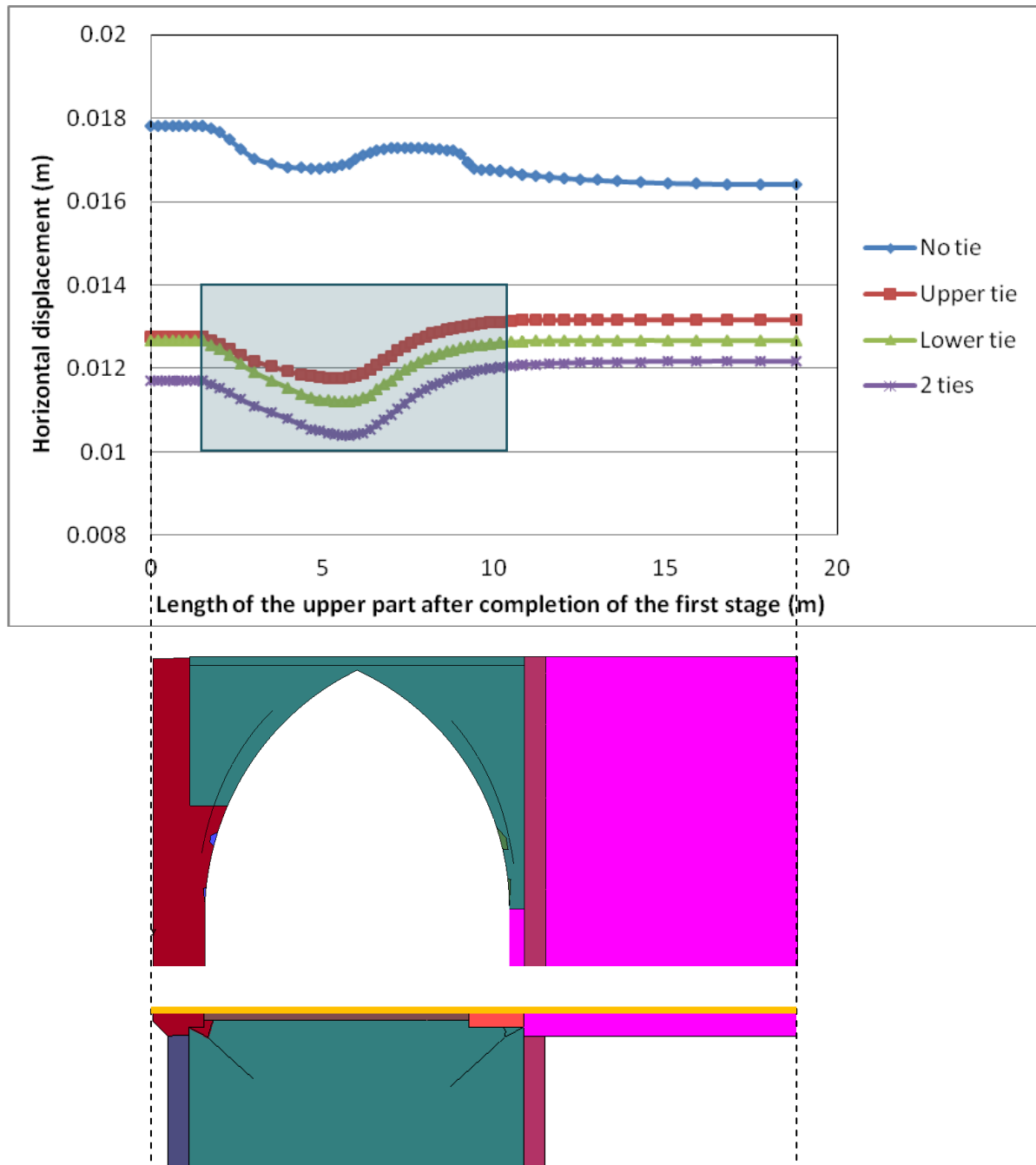


**Figure 101** - Evolution of the absolute horizontal displacement of the nodes on the orange line in function of the length of the upper part of the construction after the completion of the first stage (m).

One can notice the smaller horizontal displacements at the level of the arch when ties are added to the model (Figure 101, highlighted in grey) which is logical: this location is stiffened by the presence of the ties and thus is less subjected to displacements.

| No tie |        | Upper tie |        | Lower tie |        | 2 ties |        |
|--------|--------|-----------|--------|-----------|--------|--------|--------|
| Y      | Z      | Y         | Z      | Y         | Z      | Y      | Z      |
| -0.017 | -0.010 | -0.013    | -0.008 | -0.012    | -0.008 | -0.012 | -0.007 |

**Table 12** – Horizontal and vertical corrections applied on the nodes of the upper-part after the first stage of the sequential analysis with respect to the reference axis of GID.

|              |  | Node 5383 |        |           |        |           |        |        |        |
|--------------|--|-----------|--------|-----------|--------|-----------|--------|--------|--------|
|              |  | No tie    |        | Upper tie |        | Lower tie |        | 2 ties |        |
| First Stage  |  | Y         | Z      | Y         | Z      | Y         | Z      | Y      | Z      |
|              |  | -0.030    | -0.003 | -0.016    | -0.003 | -0.014    | -0.003 | -0.012 | -0.003 |
| Second stage |  | Y         | Z      | Y         | Z      | Y         | Z      | Y      | Z      |
|              |  | -0.017    | -0.007 | -0.008    | -0.007 | -0.005    | -0.008 | -0.004 | -0.008 |
| Third stage  |  | Y         | Z      | Y         | Z      | Y         | Z      | Y      | Z      |
|              |  | -0.017    | -0.007 | -0.014    | -0.007 | -0.013    | -0.007 | -0.012 | -0.007 |

**Table 13** – Horizontal and vertical displacements found at the top of the pier after each stage for different ties configurations (the results are given in meters).

|              |  | Node 5682 |        |           |        |           |        |        |        |
|--------------|--|-----------|--------|-----------|--------|-----------|--------|--------|--------|
|              |  | No tie    |        | Upper tie |        | Lower tie |        | 2 ties |        |
| First Stage  |  | Z         | Y      | Z         | Y      | Z         | Y      | Z      | Y      |
|              |  | -0.004    | -0.015 | -0.003    | -0.014 | -0.003    | -0.012 | -0.003 | -0.004 |
| Second stage |  | Z         | Y      | Z         | Y      | Z         | Y      | Z      | Y      |
|              |  | -0.010    | -0.006 | -0.009    | -0.005 | -0.008    | -0.004 | -0.008 | -0.010 |
| Third stage  |  | Z         | Y      | Z         | Y      | Z         | Y      | Z      | Y      |
|              |  | -0.010    | -0.012 | -0.009    | -0.011 | -0.009    | -0.011 | -0.009 | -0.010 |

**Table 14** – Horizontal and vertical displacements found at the connection between the upper tie and the pier after each stage for different ties configurations (the results are given in meters).

|              | Node 5050 |        |           |        |           |        |        |        |
|--------------|-----------|--------|-----------|--------|-----------|--------|--------|--------|
|              | No tie    |        | Upper tie |        | Lower tie |        | 2 ties |        |
| First Stage  | Y         | Z      | Y         | Z      | Y         | Z      | Y      | Z      |
|              | -0.030    | -0.003 | -0.016    | -0.003 | -0.014    | -0.003 | -0.012 | -0.003 |
| Second stage | Y         | Z      | Y         | Z      | Y         | Z      | Y      | Z      |
|              | -0.017    | -0.008 | -0.008    | -0.008 | -0.005    | -0.008 | -0.004 | -0.008 |
| Third stage  | Y         | Z      | Y         | Z      | Y         | Z      | Y      | Z      |
|              | -0.017    | -0.008 | -0.013    | -0.008 | -0.013    | -0.008 | -0.012 | -0.008 |

**Table 15** – Horizontal and vertical displacements found at the connection between the lower tie and the pier after each stage for different ties configurations (the results are given in meters).

First of all, it can be observed that the model without ties gives similar results to the ones found by Roca et al., 2013: the magnitude of order of the difference is less than 1 mm which can be explained by the upgrades of the software used to process the data: COMET. They can also be explained by the presence of a vertical correction in the model studied here. Nevertheless the difference is really small and the new model is therefore calibrated on the one developed previously.

- Vertical displacements

The addition of the ties, whatever the configuration, does not affect the vertical deformation of the structure. This observation is logical: in effect the role of the ties is to prevent the piers to undergo high horizontal displacements because of the thrust of the lateral vaults, not to stop the settlement of the structure due to the application of the self-weight.

- Horizontal displacements

During the first two steps, the presence of ties reduces significantly the horizontal displacements within the pier: the insertion of the ties within the model stops effectively the deformations caused by the horizontal thrust of the lateral vault. Figure 102 and Figure 103 give respectively the horizontal displacement at the top of the pier at each stage and for the four different configurations and the ratio  $\frac{\text{horizontal displ. with no tie} - \text{horizontal displ.}}{\text{horizontal displ. with no tie}}$  for each configuration. Once the construction of the bay is completed the assumed quick removal of the ties affects significantly the horizontal displacements for the configuration with ties. Nevertheless at the end of this stage, the horizontal displacements within the pier are still less than the ones found in the configuration with no tie. The evolution of the horizontal displacement at the top of the pier follows the same tendency for the three different tie configurations. Comparing now the three different tie configurations, the two ties configuration is the best to restrain the drift at the top of the pier; nevertheless the displacements obtained in that configuration are really closed to the ones obtained for the lower tie configuration (Figure 102 and Figure 103). Only the upper tie configuration seems to be less effective than the other two for the first two stages. After the removal of the ties, the results for the three cases are very similar.

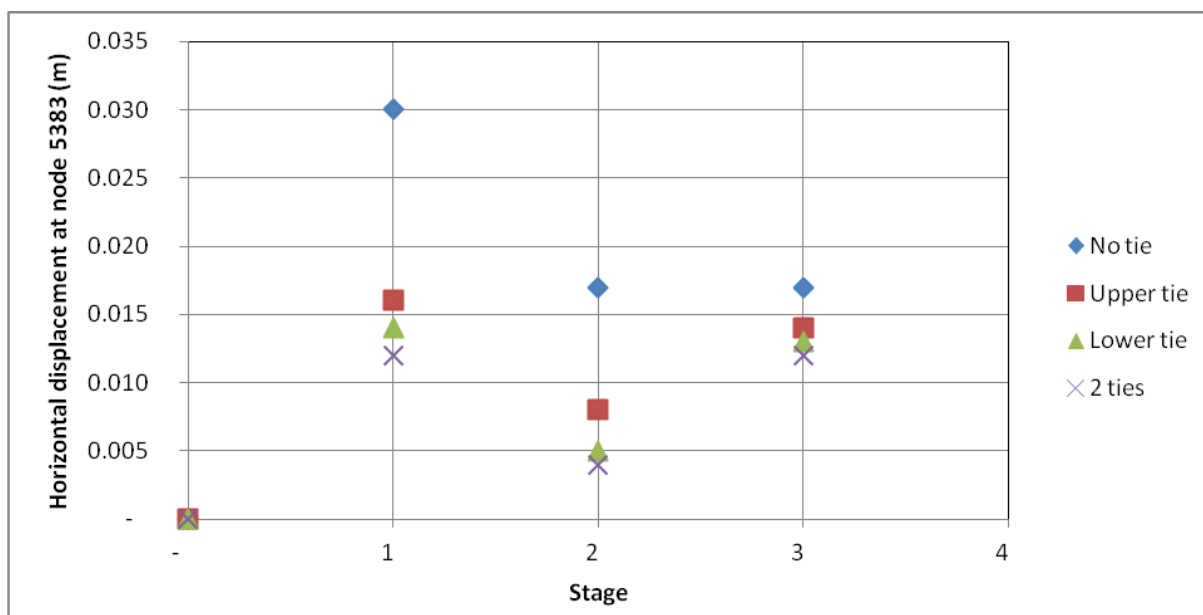


**Figure 102** – Evolution of the horizontal displacement (absolute value) at node 5383 after each step four the four different configurations.

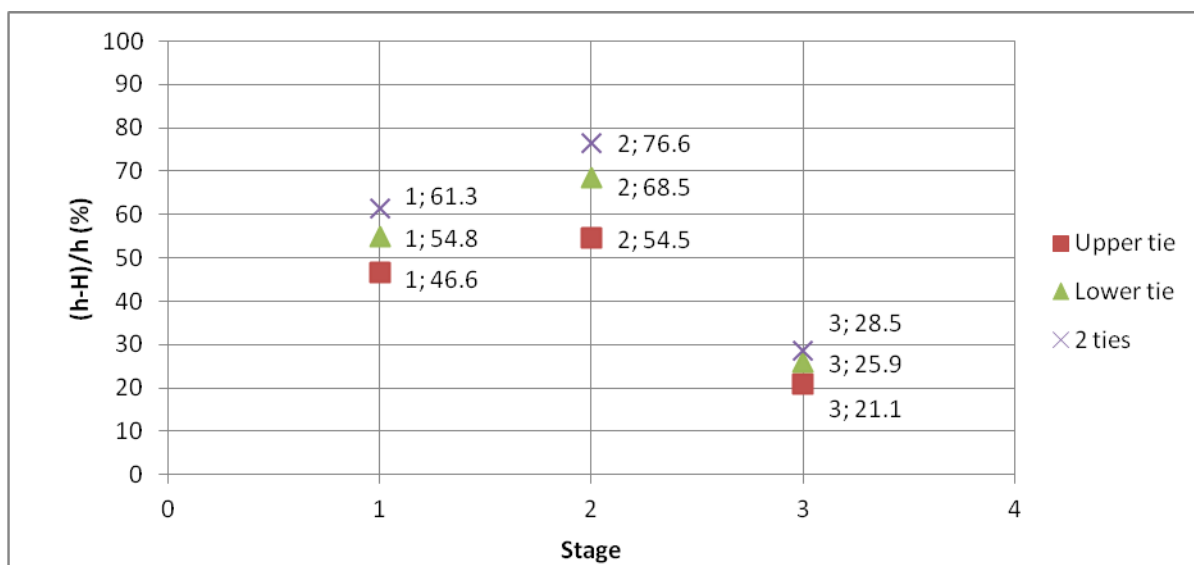


**Figure 103** – Ratio  $\frac{\text{horizontal displ. with no tie} - \text{horizontal displ. with tie}}{\text{horizontal displ. with no tie}}$  expressing the restrain effectiveness of each ties configuration. The values are given in %.

### *Mechanical behavior of the ties*

In order to understand how the ties work during the first stages of construction of the bay, their structural behavior has been studied. Due to the fact that they have been modeled as elastic elements, it has been possible to use Hook's law to find the stresses inside them. For the lower tie configuration, the stresses have been compared afterwards with the ones calculated with GID and the

difference between them has been found as negligible. The results are summarized in Table 16. In this table one can find:

- the initial distance between two corresponding anchorages:  $l_1$ ;
- the final distance after the end of the current stage:  $l_2$ ;
- the total elongation between  $l_1$  and  $l_2$  after the end of the current step:  $E_t$ ;
- the relative elongation between the final distances at the end of the current stage and the end of the previous stage:  $E_{r_i}$ ;
- The tensile stress within the ties, calculated using Hook's Law:  $\sigma_t$  (MPa);
- The corresponding force for a tie cross-section of  $12.5 \text{ cm}^2$  (half of the tie):  $F_t$  (kN).

| Config.          | Stage  | Tie Position | Small strains – Large displacements |              |              |              |                     |               |
|------------------|--------|--------------|-------------------------------------|--------------|--------------|--------------|---------------------|---------------|
|                  |        |              | $l_1$<br>(m)                        | $l_2$<br>(m) | $E_t$<br>(m) | $E_r$<br>(m) | $\sigma_t$<br>(MPa) | $F_t$<br>(kN) |
| <b>No tie</b>    | First  | <i>Upper</i> | 8.280                               | 8.296        | 0.016        | 0.016        | /                   | /             |
|                  |        | <i>Lower</i> | 8.851                               | 8.870        | 0.019        | 0.019        | /                   | /             |
|                  | Second | <i>Upper</i> | 8.280                               | 8.291        | 0.011        | -0.005       | /                   | /             |
|                  |        | <i>Lower</i> | 8.851                               | 8.865        | 0.014        | -0.005       | /                   | /             |
|                  | Third  | <i>Upper</i> | 8.280                               | 8.291        | 0.012        | 0.000        | /                   | /             |
|                  |        | <i>Lower</i> | 8.851                               | 8.865        | 0.014        | 0.000        | /                   | /             |
| <b>Upper tie</b> | First  | <i>Upper</i> | 8.280                               | 8.284        | 0.004        | /            | 95.416              | 119.270       |
|                  |        | <i>Lower</i> | 8.851                               | 8.858        | 0.007        | /            | /                   | /             |
|                  | Second | <i>Upper</i> | 8.280                               | 8.283        | 0.003        | -0.001       | 77.057              | 96.322        |
|                  |        | <i>Lower</i> | 8.851                               | 8.857        | 0.006        | -0.001       | /                   | /             |
|                  | Third  | <i>Upper</i> | 8.280                               | 8.289        | 0.009        | 0.006        | /                   | /             |
|                  |        | <i>Lower</i> | 8.851                               | 8.863        | 0.012        | 0.006        | /                   | /             |
| <b>Lower tie</b> | First  | <i>Upper</i> | 8.280                               | 8.284        | 0.004        | /            | /                   | /             |
|                  |        | <i>Lower</i> | 8.851                               | 8.855        | 0.004        | /            | 97.165              | 121.457       |
|                  | Second | <i>Upper</i> | 8.280                               | 8.283        | 0.003        | -0.001       | /                   | /             |
|                  |        | <i>Lower</i> | 8.851                               | 8.854        | 0.003        | -0.001       | 78.862              | 98.578        |
|                  | Third  | <i>Upper</i> | 8.280                               | 8.289        | 0.009        | 0.006        | /                   | /             |
|                  |        | <i>Lower</i> | 8.851                               | 8.862        | 0.011        | 0.008        | /                   | /             |
| <b>2 ties</b>    | First  | <i>Upper</i> | 8.280                               | 8.282        | 0.002        | /            | 56.283              | 70.354        |
|                  |        | <i>Lower</i> | 8.851                               | 8.854        | 0.003        | /            | 66.660              | 83.325        |
|                  | Second | <i>Upper</i> | 8.280                               | 8.281        | 0.002        | -0.001       | 40.582              | 50.727        |
|                  |        | <i>Lower</i> | 8.851                               | 8.853        | 0.003        | 0.000        | 56.717              | 70.897        |
|                  | Third  | <i>Upper</i> | 8.280                               | 8.288        | 0.009        | 0.007        | /                   | /             |
|                  |        | <i>Lower</i> | 8.851                               | 8.862        | 0.011        | 0.008        | /                   | /             |

**Table 16** – Mechanical behavior of the ties, considering a small strains/large displacements configuration.

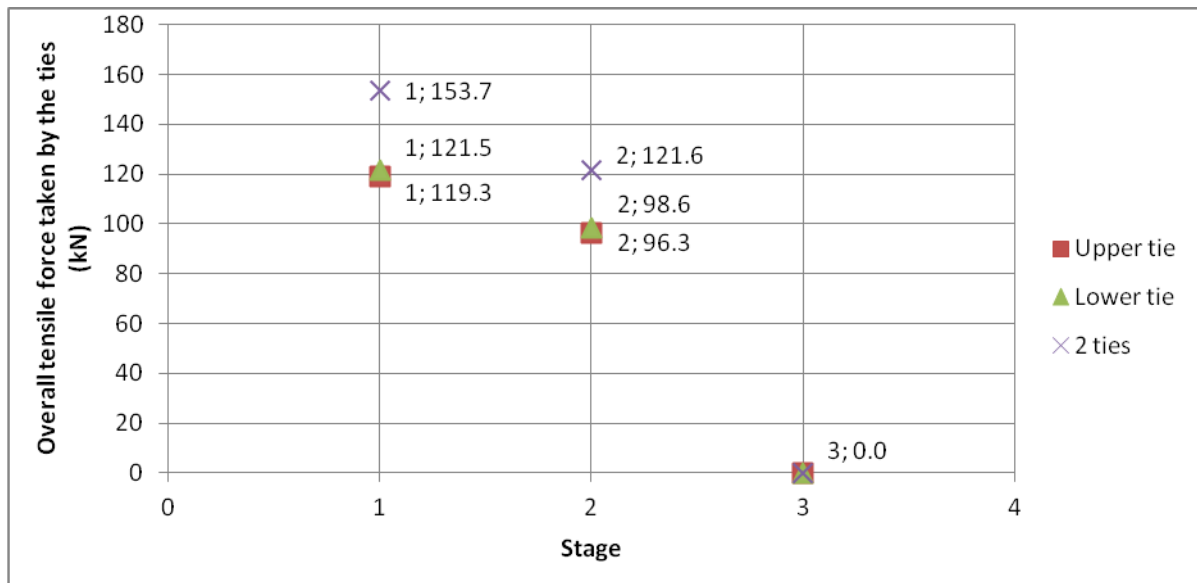


**Figure 104** – Overall tensile force taken by the ties in each configuration and after each phase of construction.

The computed behavior of the ties is in good adequacy with the assumed one: the ties effectively work in tension and resist the tensile stresses due to the horizontal thrust of the lateral vault. The stress state is constant for the whole length of the ties and in any case the maximal tensile stress found (97.165 MPa for the first stage of the lower tie configuration) is far less than the minimum tensile strength found for iron in the literature (Section 2.3.5. Ties properties), meaning that the ties don't reach the threshold between the elastic and the plastic domains.

The two configurations with one tie present almost the same results concerning the tensile force taken by the ties, meaning that the ties in the two different configurations work in a similar way. The configuration with two ties allows to take more tensile force nevertheless, when comparing the obtained results for the lower tie configuration with the 2 ties configuration on Figure 102 and Figure 103, one can observe that the horizontal displacements within the piers are almost the same for these two configurations. From these observations, it can be assumed that the lower tie configuration is the best compromise between structural response and material use, taking into account the horizontal displacement reduction and the mechanical behavior of the ties together with the cost of wrought iron during the gothic era, time and labor as well as the uncertainties concerning the removal of the ties. Therefore, the long-term creep behavior analysis as well as the different parametric studies will be based on this configuration.

### *Tensile damage*

All the tensile damage contours for each configuration at each stage is given in Annex C. Figure 105 and Figure 106 show the existing difference between the tensile damage contour respectively at the

end of the first stage and at the end of the third stage for the configuration with no tie and the one with lower tie. These two examples have been used to illustrate visually the differences between a configuration with ties and a configuration without ties.

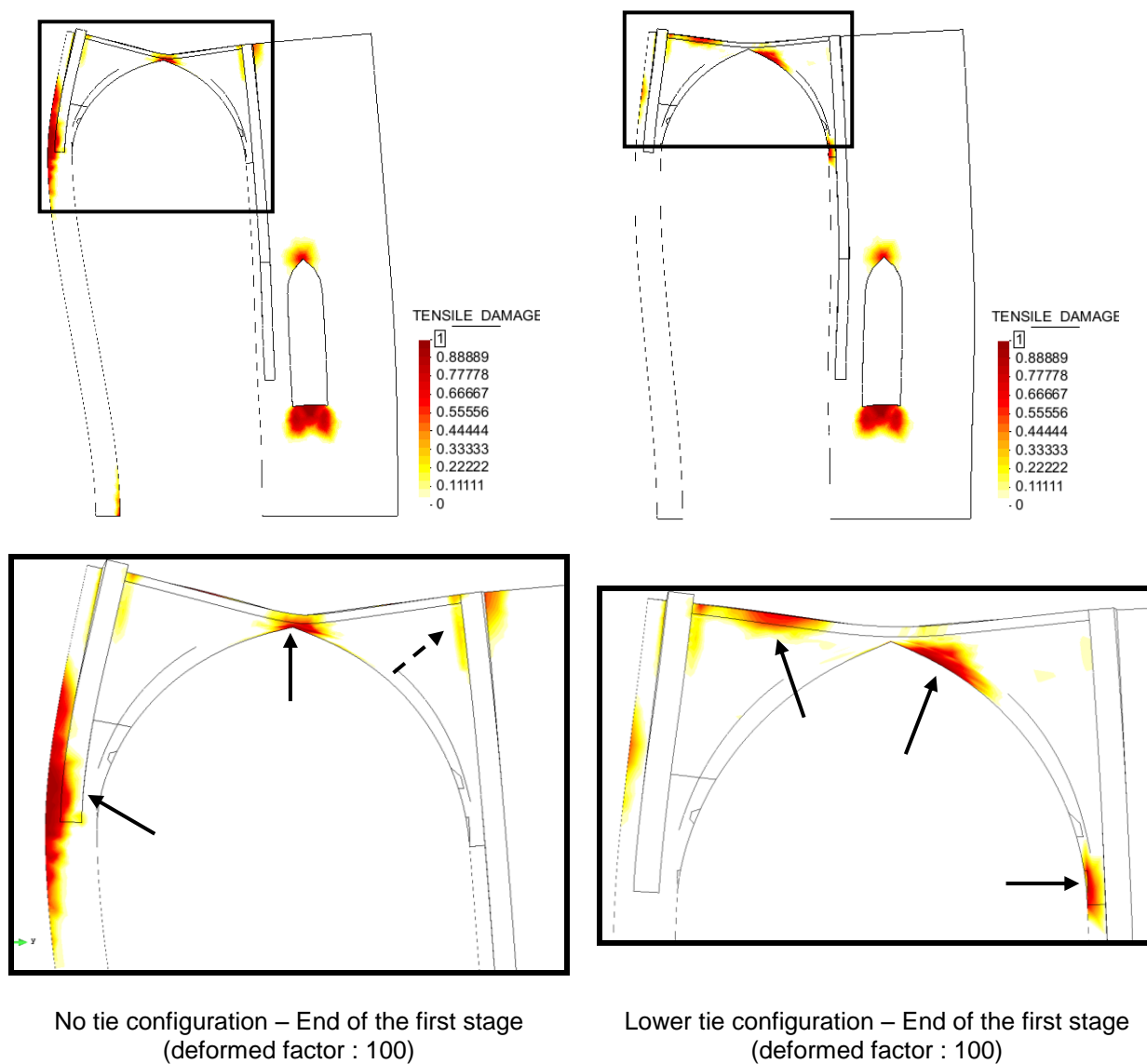
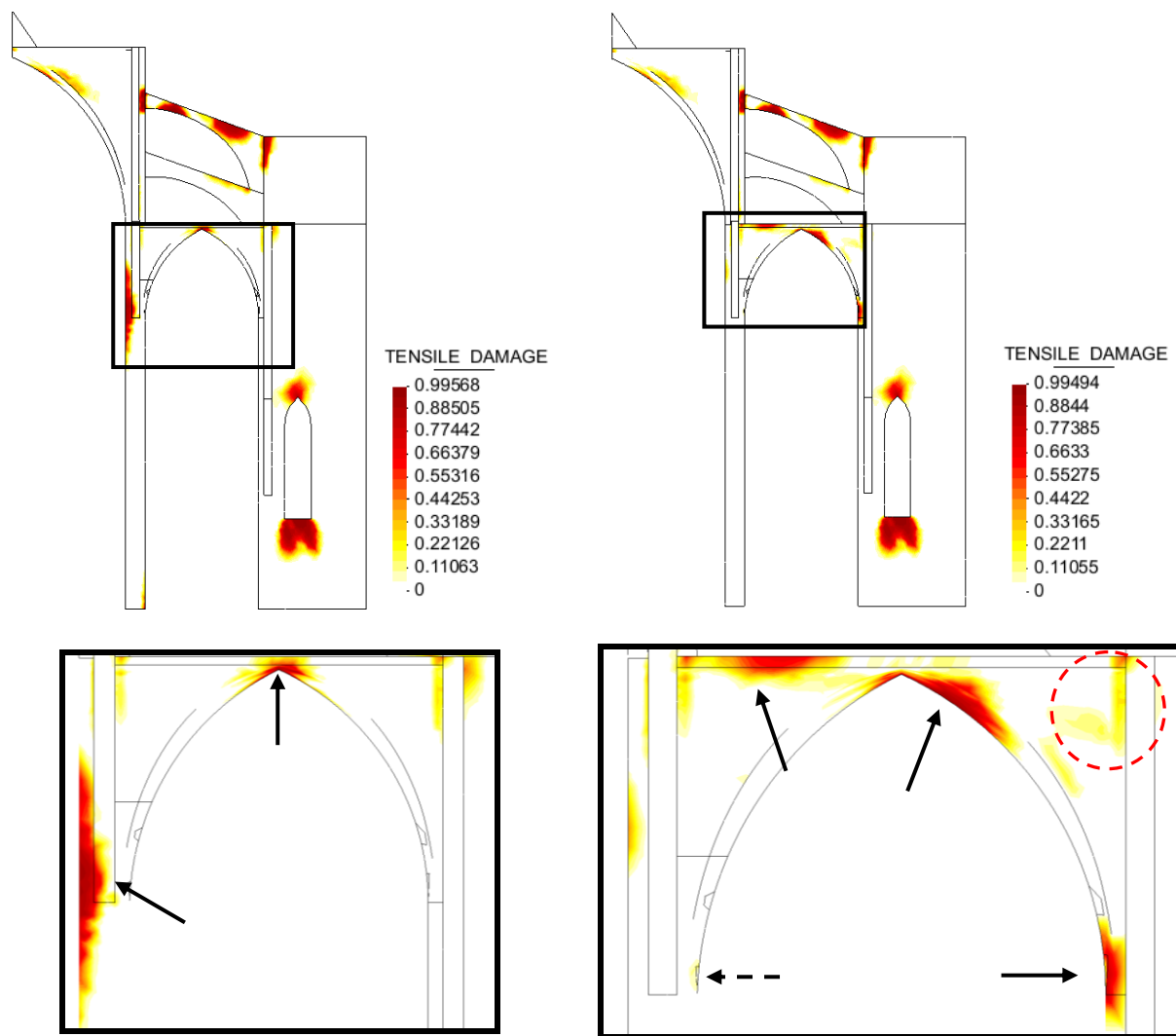


**Figure 105** – Comparison of the tensile damage contour and the deformed shape at the end of the first stage for two different configurations. The principal differences are shown by an arrow.





No tie configuration – End of the third stage

Lower tie configuration – End of the third stage

**Figure 106** – Comparison of the tensile damage contour at the end of the third stage for two different configurations. The principal differences are shown by an arrow.

- Tensile damage contour for a configuration without ties

Mainly there are four locations where the structure is affected by tensile damage in this configuration after the completion of the structure: the top outer part of the pier, the lower middle part of the arch, the upper flying arch and the masonry below the opening. One can notice the overall symmetry of the tensile damage repartition within the arch. Also it is important to point out the widespread tensile damage at the top outer part of the pier. Considering now the evolution of the tensile damage of the lower part of the structure with the construction stages, no new significant tensile damage appears after the completion of the structure, and the already existing ones are slightly extended.

- Tensile damage contour for a configuration with auxiliary ties

As expected, the structural behavior of the bay is changed in the region of the lateral arch. The tensile damage distribution is no longer symmetric within the arch and presents mainly two zones where tensile damages are concentrated (Figure 106, right). The tensile damage at the top outer part of the pier does no longer exist, thank to the structural action of the ties. Nevertheless new localized zones of tensile damages have appeared at the ties anchorages, especially at the connections between the ties and the lateral vault (on the right). This phenomenon is more remarkable for the upper tie where important tensile damage also appears at the connection between the tie and the pier. Considering now the evolution of the tensile damage of the lower part of the structure with the construction stages, the already existing tensile damages are slightly amplified except in the outer-upper part of the pillar. Also some tensile damage appears near the connection between the lateral arch and the buttress after the removal of the ties (highlighted in red on Figure 106).

Otherwise, the overall tensile damage contour is similar to the one in the configuration with no tie for the rest of the structure.

### **5.3.3. Fourth step: long-term creep behavior of the masonry after the ties removal**

#### *Preliminary considerations*

Now that the construction process of the different ties configurations has been carefully analyzed, a long-term behavior of the lower tie configuration taking into account the creep behavior of the masonry has been carried out. Nevertheless this part is left incomplete due to the long time needed for the analysis to be ran entirely and should be regarded as an introduction to further studies.

This analysis has been done considering a participation ratio  $\xi$  of 0.975 (The definition of this parameter is given in Annex A). This participation ratio, that sets the amount of material stiffness susceptible to creep, has been chosen in order to compare the results obtained with the ones found by Roca et al., 2013, 2012. In this previous work, as it has been resumed in Section 3.5.2, the authors proved that the instability of the structure occurs for such a high participation ratio after 1350 years. Thus it is interesting to see if such instability occurs for a configuration with temporary lower tie and if so, to evaluate the elapsing time before the collapse. Even if only the beginning of the analysis has been carried out due to a lack of time, it has been possible to reach the monitoring period (From September 2003 to September 2008, corresponding to the years 543 and 548) and thus to draw some conclusions.

Thank to the monitored data, it has been possible to calibrate the curve horizontal displacement at the top of the pier versus time by adjusting the value of the retardation time. The main idea was to find an

absolute displacement at the top of the pier closed to the one measured in reality for that period of time and to compare the rate of the deformation found according to the model with the one measured on-site. It was possible to find the following values with the monitor system:

- A symmetrical horizontal displacement at the top of the pier equal to 9.5 cm between the years 543 and 548;
- A deformation rate equal to 0.1 mm/year at this location for the same period of time.

Figure 107 shows graphically that a retardation time value equal to 48 is needed to obtain a horizontal displacement of 9.5 cm between the years 543 and 548. Considering this retardation time, the deformation rate is found equal to 0.18 mm/year which is almost the double of the one wanted.

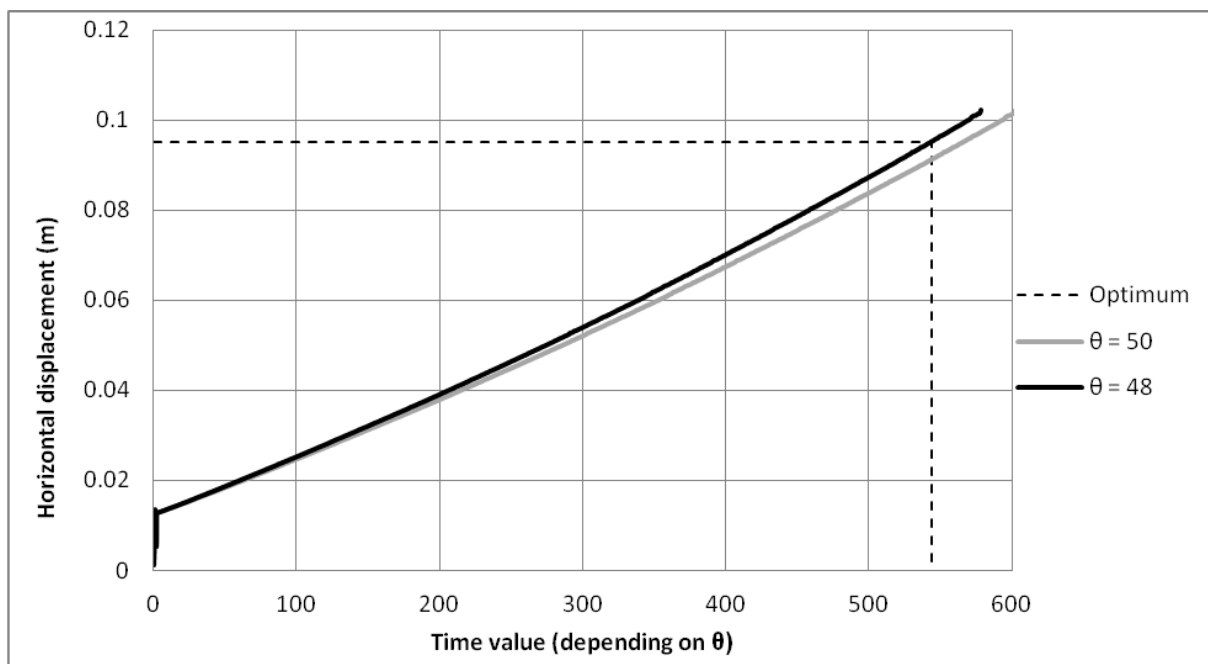


**Figure 107** – Calibration of the retardation time for the lower tie configuration.

## Results

Once the calibration has been achieved, the curve obtained has been compared with the one drawn by Roca et al., 2012 (Figure 108). Table 17 summarizes the different values of horizontal displacements as well as the deformation rates at the top of the pier found during the monitoring period and with the models. A retardation time equal to 48 has been considered for the models.

|                               | Monitoring system | No tie | Lower tie |
|-------------------------------|-------------------|--------|-----------|
| Horizontal displacement* (cm) | 9.5               | 10.1   | 9.6       |
| Deformation rate (mm/year)    | 0.1               | 0.183  | 0.179     |

\*Average value for the years 543 and 548

**Table 17** – Outcomes of the models calibration together with the data collected on-site.

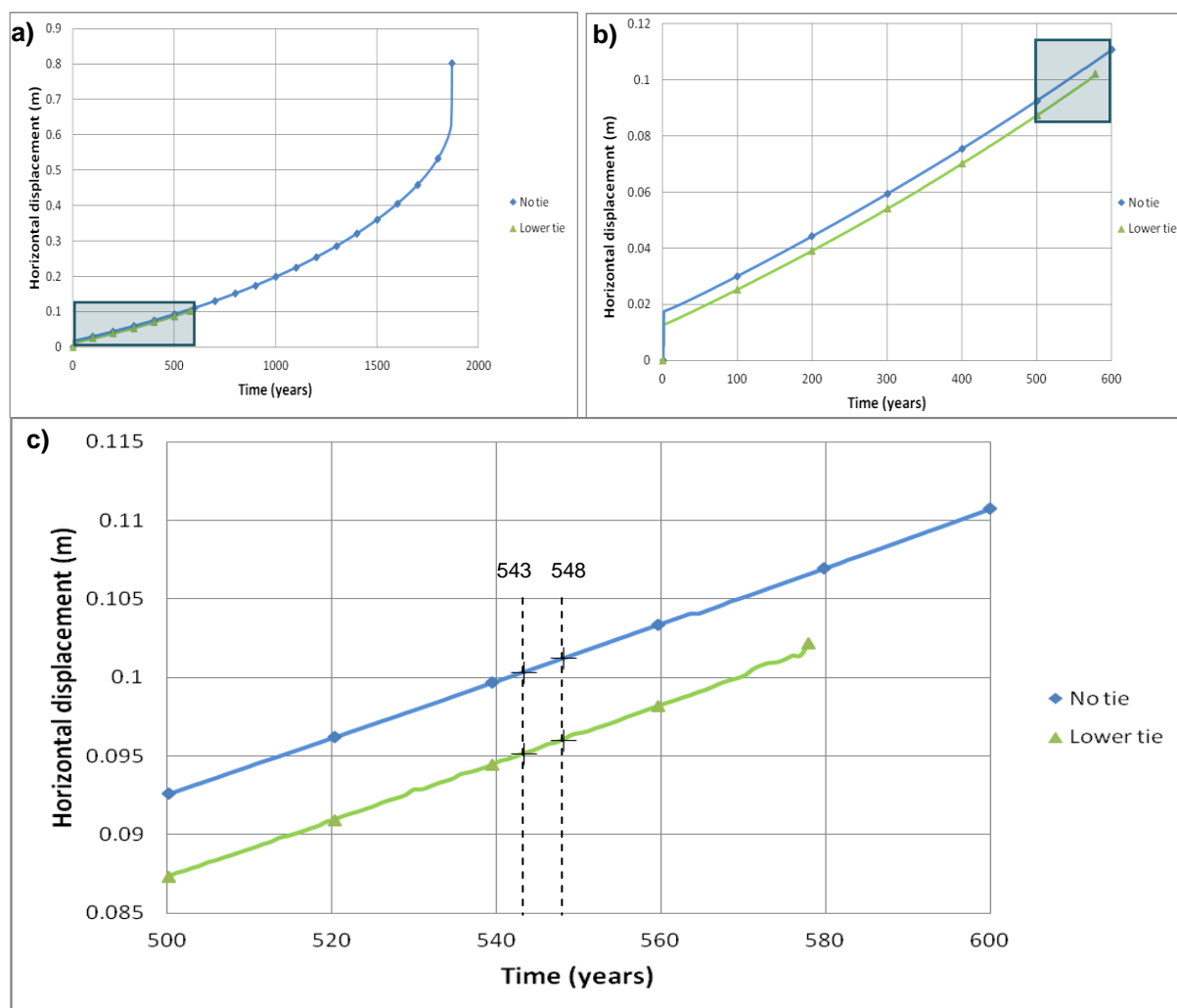


**Figure 108** – FE simulation of long-term creep deformation: comparison of the increase of the horizontal displacement at the top of the pier for the lower tie configuration and for the one with no tie. a) Overall results; b) zoom of the curves between 0 and 600 years; c) zoom of the curves on the neighborhood of the monitoring period.

## Observations

Except from the different initial displacements due to the utilization of temporary ties, the two curves seem to follow a similar trend. Nevertheless one has to be careful not to draw rapid conclusions: in effect, as it has been observed in Section 5.3.2, the tensile damage contour for the two configurations

is very different in the neighborhood of the arch and especially in the surroundings of the top of the pier. These different damage contours should lead to a different long-term behavior for the two models. Also, even if the two curves seem parallel, their respective deformation is not exactly the same. From the results obtained so far, one can assume an instability that might take place after 1850 years (500 years more than the configuration without tie) but only a deeper analysis would allow to conclude on the role of temporary ties when a long-term creep behavior is considered. In effect, the dissimilar structural states of the two models after the construction process should lead to two distinct structural behaviors. Instability for the lower tie configuration can only be assumed for the moment.

### *Further works*

In order to draw solid conclusions concerning the effect of the use of auxiliary ties during the construction process on the long term behavior of the structure, the work presented above should be pursued:

- First of all, the analysis previously developed should be completed extending the time duration;
- Still considering a lower tie configuration, several other analyses with different participation ratios should be ran in order to find the one that matches the data collected on-site. One should focus first on the values of the participation ratios of 0.925 and 0.875 in order to compare the results with the ones obtained by Roca et al., 2012;
- The whole long-term creep behavior study should be carried out again for the two remaining ties configuration (upper tie and two ties) in order to assess whether or not the structural behavior of the structure is same for different ties configurations.
- Finally, it may be interesting to perform another analysis considering this time a long-lasting tie configuration. An upper tie configuration should be particularly interesting because of the fact that some of these ties still remain nowadays in Mallorca Cathedral.

## **5.4. Parametric study: influence of the tie cross-section**

It is interesting to consider the influence of the ties cross-section on the final displacements and tensile damage contour. In effect even if an average value closed to 25 cm<sup>2</sup> has been found during the investigation previously carried out, some of the cross-sections found were closed to the double of this value. Therefore another study has been carried out, considering this time a total cross-section of the ties equal to 50 cm<sup>2</sup>. The results for the intermediate correction after the first stage are given in Table 18 whereas the displacements found at the end of each stage for node 5383 are given in Table 19.

| No tie |        | Upper tie |        | Lower tie |        | 2 ties |        |
|--------|--------|-----------|--------|-----------|--------|--------|--------|
| Y      | Z      | Y         | Z      | Y         | Z      | Y      | Z      |
| -0.017 | -0.010 | -0.012    | -0.008 | -0.012    | -0.007 | -0.011 | -0.007 |

**Table 18** – Horizontal and vertical corrections applied on the nodes of the upper-part after the first stage of the sequential analysis considering a tie cross-section of 50 cm<sup>2</sup>.

|              |  | Node 5383 |        |           |        |           |        |        |        |
|--------------|--|-----------|--------|-----------|--------|-----------|--------|--------|--------|
|              |  | No tie    |        | Upper tie |        | Lower tie |        | 2 ties |        |
| First Stage  |  | Y         | Z      | Y         | Z      | Y         | Z      | Y      | Z      |
|              |  | -0.030    | -0.003 | -0.015    | -0.003 | -0.012    | -0.003 | -0.010 | -0.003 |
| Second stage |  | Y         | Z      | Y         | Z      | Y         | Z      | Y      | Z      |
|              |  | -0.017    | -0.007 | -0.007    | -0.007 | -0.004    | -0.008 | -0.003 | -0.008 |
| Third stage  |  | Y         | Z      | Y         | Z      | Y         | Z      | Y      | Z      |
|              |  | -0.017    | -0.007 | -0.013    | -0.007 | -0.012    | -0.007 | -0.012 | -0.007 |

**Table 19** – Horizontal and vertical displacements found at the top of the pier after each stage for different ties configurations considering a tie cross-section of 50 cm<sup>2</sup> (the results are given in meters).

Comparing the results with the ones found in Section 5.3.2, one can observe that horizontal displacements are slightly smaller when a higher tie cross-section is considered (the difference is between 1 and 2 mm). The vertical displacements do not seem affected by the change of section. The overall structure is therefore only slightly affected by this change of cross-section which has an influence only locally, when one considers the stresses acting in the ties. In effect, because of the greater cross-section, the stresses developed within the ties for a section of 50 cm<sup>2</sup> are more or less 2 times less than the ones found for a section of 25 cm<sup>2</sup> (Table 20).

All the graphical results concerning horizontal displacement patterns as well as tensile damage contour for each tie configuration and each step are given respectively in Annex D and Annex E.

| Config.   | Stage  | Tie Position | Cross-section: 25 cm <sup>2</sup> |         | Cross-section: 50 cm <sup>2</sup> |         |
|-----------|--------|--------------|-----------------------------------|---------|-----------------------------------|---------|
|           |        |              | $\sigma_t$                        | $F_t$   | $\sigma_t$                        | $F_t$   |
| Upper tie | First  | Upper        | 95.416                            | 119.270 | 52.418                            | 131.046 |
|           |        | Lower        | /                                 | /       | /                                 | /       |
|           | Second | Upper        | 77.057                            | 96.322  | 42.997                            | 107.494 |
|           |        | Lower        | /                                 | /       | /                                 | /       |
| Lower tie | First  | Upper        | /                                 | /       | /                                 | /       |
|           |        | Lower        | 97.165                            | 121.457 | 55.362                            | 138.404 |
|           | Second | Upper        | /                                 | /       | /                                 | /       |
|           |        | Lower        | 78.862                            | 98.578  | 44.967                            | 112.418 |
| 2 ties    | First  | Upper        | 56.283                            | 70.354  | 29.953                            | 74.883  |
|           |        | Lower        | 66.660                            | 83.325  | 37.284                            | 93.211  |
|           | Second | Upper        | 40.582                            | 50.727  | 20.532                            | 51.331  |
|           |        | Lower        | 56.717                            | 70.897  | 32.539                            | 81.348  |

**Table 20** – Comparison of the mechanical behavior of the ties considering a tie cross section of 25 cm<sup>2</sup> and a tie cross-section of 50 cm<sup>2</sup>.

### 5.5. Parametric study: influence of the tensile strength of the masonry in the lower tie configuration

On the previous models, a masonry tensile strength equal to 5% of its compressive strength has been assumed. This value has been considered principally to allow the structure to withstand the construction process without the use of auxiliary devices such as ties (Clemente, 2006, Roca et al., 2013, 2012). Now that ties were added to the model, a parametric study of the influence of the masonry tensile strength on the structural behavior of the bay can be computed. This approach has been carried out using the configurations without ties (reference case) and with lower tie. Several tensile strength values have been computed:  $f_t = 5\%f_c$ ,  $f_t = 2.5\%f_c$ ,  $f_t = 1.25\%f_c$  and  $f_t = 0.5\%f_c$ , where  $f_c$  is the compressive strength of the masonry.

The analysis has been carried out under the following assumptions:

- Small strains/large displacements configuration to take into account the geometrical non-linearity.
- Ties section of 50 cm<sup>2</sup>.
- Very high tensile and compressive fracture energies (almost infinite).

The displacements obtained at node 5383 at each stage for each configuration are given in Table 21 and Table 22.

|                     | Node 5383 No tie  |        |                     |        |                               |         |                               |         |
|---------------------|-------------------|--------|---------------------|--------|-------------------------------|---------|-------------------------------|---------|
|                     | 5% f <sub>c</sub> |        | 2.5% f <sub>c</sub> |        | 1.25% f <sub>c</sub>          |         | 0.5% f <sub>c</sub>           |         |
| First Stage         | Y                 | Z      | Y                   | Z      | Y (0.6)                       | Z (0.6) | Y (0.3)                       | Z (0.3) |
|                     | -0.030            | -0.003 | -0.039              | -0.003 | -0.030                        | -0.002  | -0.022                        | -0.001  |
|                     | convergence       |        | convergence         |        | No convergence after step 0.6 |         | No convergence after step 0.3 |         |
| Correction to apply | Y                 | Z      | Y                   | Z      |                               |         |                               |         |
|                     | -0.017            | -0.010 | -0.020              | -0.011 |                               |         |                               |         |
| Second stage        | Y                 | Z      | Y                   | Z      |                               |         |                               |         |
|                     | -0.017            | -0.007 | -0.015              | -0.007 |                               |         |                               |         |
| Third stage         | Y                 | Z      | Y                   | Z      |                               |         |                               |         |
|                     | -0.017            | -0.007 | -0.151              | -0.007 |                               |         |                               |         |

**Table 21** – Horizontal and vertical displacements at node 5383 obtained either until the end of the third stage, or either until divergence of the solution. Configuration with no tie.

|                     | Node 5383 Lower tie |        |                     |        |                               |         |                               |         |
|---------------------|---------------------|--------|---------------------|--------|-------------------------------|---------|-------------------------------|---------|
|                     | 5% f <sub>c</sub>   |        | 2.5% f <sub>c</sub> |        | 1.25% f <sub>c</sub>          |         | 0.5% f <sub>c</sub>           |         |
| First Stage         | Y                   | Z      | Y                   | Z      | Y (0.8)                       | Z (0.8) | Y (0.5)                       | Z (0.5) |
|                     | -0.012              | -0.003 | -0.014              | -0.003 | -0.017                        | -0.003  | -0.009                        | -0.002  |
|                     | convergence         |        | convergence         |        | No convergence after step 0.8 |         | No convergence after step 0.5 |         |
| Correction to apply | Y                   | Z      | Y                   | Z      |                               |         |                               |         |
|                     | -0.012              | -0.003 | -0.013              | -0.008 |                               |         |                               |         |
| Second stage        | Y                   | Z      | Y                   | Z      |                               |         |                               |         |
|                     | -0.004              | -0.008 | -0.002              | -0.008 |                               |         |                               |         |
| Third stage         | Y                   | Z      | Y                   | Z      |                               |         |                               |         |
|                     | -0.012              | -0.007 | -0.011              | -0.007 |                               |         |                               |         |

**Table 22** – Horizontal and vertical displacements at node 5383 obtained either until the end of the third stage, or either until divergence of the solution. Configuration with lower tie.

From Table 21 and Table 22, it appears that for each configuration, the solution diverges for  $f_t < 2.5\% f_c$  because of tensile damage occurring on the whole cross section of a structural element.

- In the configuration with no tie, this occurs at the top of the pier;
- In the configuration with lower tie, this seems to occur at the anchorage between the tie and the lateral vault (right side on Table 23).

It can also be noticed that more tensile damages have been developed within the lateral arch for the configuration with no tie than for the configuration with lower tie.

Comparing the results for the two configurations, the structure with lower tie can resist higher tensile stresses and thus bear more loads. Nevertheless the behavior of the model with a lower tie configuration wasn't supposed to be that weak for tensile strength values less than  $2.5\% f_c$  but the



results are logical: due to the concentration of tensile stresses in the surrounding of the tie anchorages, the masonry still needs some tensile strength.

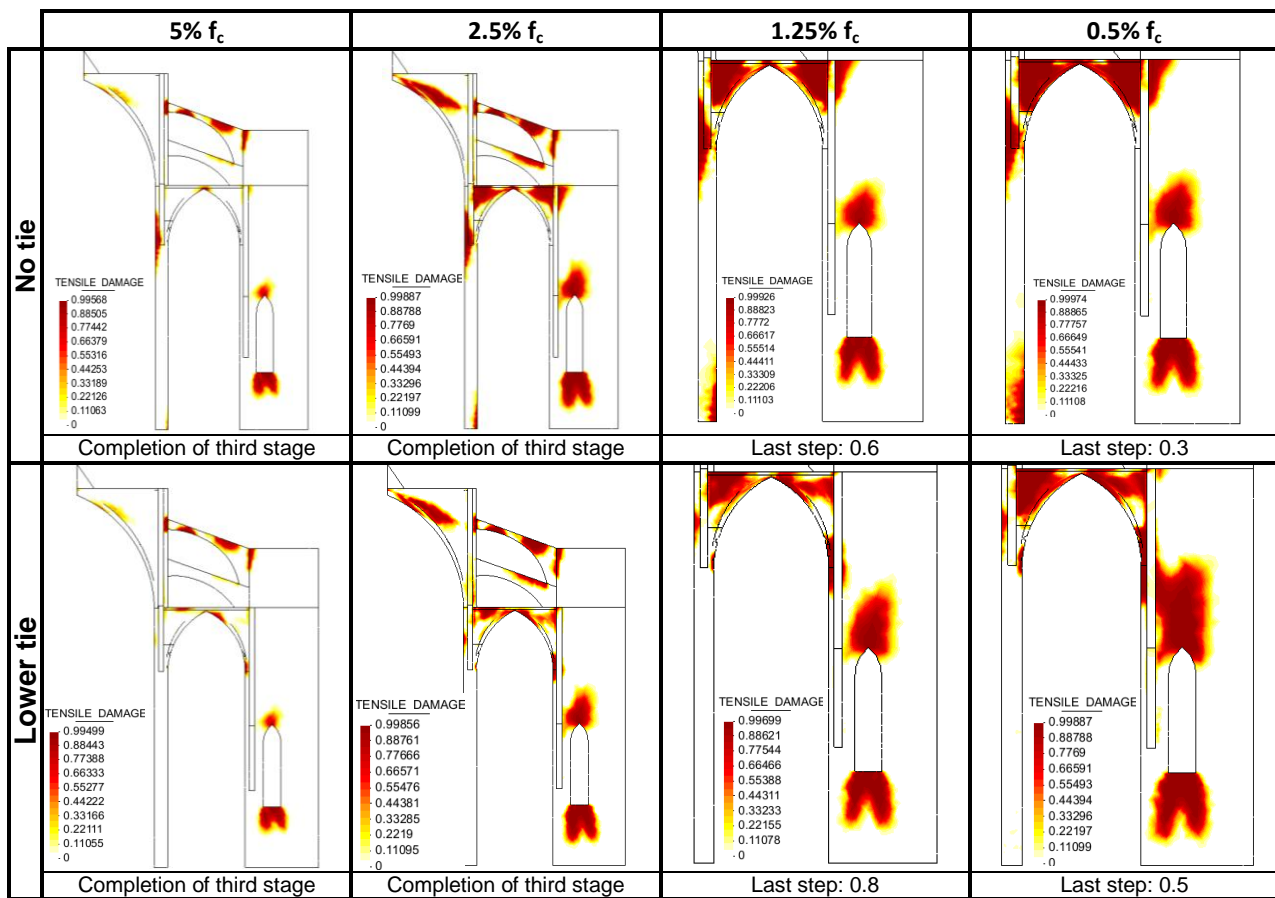


**Table 23** – Comparison of the tensile damage contour for either the last converging step or the end of the third stage for 2 configurations.

## 6. CONCLUSIONS

### 6.1. Summary

This thesis has been focused on the simulation of the effect of auxiliary ties used during the construction process of Mallorca Cathedral. First a thorough historical research on the use of iron during the gothic era as a structural component has been carried out. This research has allowed to show the widespread use of iron as a construction material in Europe in gothic architecture. After a succinct description of the main iron elements present in gothic architecture, a special interest has been considered on iron ties. It has been observed the existence of two types of such ties: temporary ties that were auxiliary devices used during the construction process and long-lasting ties designed as a permanent structural member of the construction. Numerous European examples of these two categories have been given in order to show visual evidences of the widespread use of ties as well as their characteristics (locations, appearance, size, etc). In addition it has been noticed that ties were sometimes installed in the construction after its completion during strengthening works. A section on the assumed properties of medieval wrought iron from the literature has also been developed together with the main differences between direct and indirect processes, the two methods of producing iron during medieval times.

Afterwards, a state-of-the-art of the studies dealing with Mallorca Cathedral has been carried out. A focus has been done on the history of the cathedral, its dimensions and interesting features, the existing damages together with the construction process of the fourth bay of the cathedral and its previous structural analyses. The research presented by Roca et al. (2013, 2012) has revealed the importance of taking into account the construction process in the models as well as the influence of the long-term creep behavior on the structural behavior of the construction. Some FEM models of the fourth bay have been implemented and uploaded. Nevertheless has not been carried a study on the possible use of temporary iron ties during the construction process. Indeed it has been considered that the structure during the construction phases was able to withstand the thrust of the vaults of the lateral naves by its own, thank to its tensile strength, leading to the stability of the construction but at the cost of significant deformations.

An advanced on-site investigation of the interior of the cathedral has revealed the presence of two remaining iron ties for two of the bays as well as iron remains at strategic locations for the majority of the bays. These visual observations have been correlated with the photogrammetry study previously done, showing remarkable similarities. From the on-site investigation and the previous photogrammetric study two sets of ties have been assumed: a lower one, and an upper one leading to three possible temporary ties configurations.

The three different ties configurations have been added to the FEM model previously developed by Roca et al. (2013, 2012) in order to carry out an analysis of the construction process of the fourth bay

of the cathedral taking into account the use of temporary iron ties. Four stages have been considered: the construction of the lower part of the bay, the completion of the bay, the cut of the ties and the evolution of the deformations with time, considering the long-term creep behavior of the masonry. In order to obtain more realistic results, the coordinates of the upper part of the construction have been corrected considering the horizontal and vertical deformations taking place after the completion of the first stage. The results obtained for the three configurations have shown a significant reduction of the lateral deformation of the inside pier, highlighting the structural role of the ties during the construction process. In addition two parametrical studies have been carried out: one based on the influence of the tie cross section and another one based on the influence of the masonry tensile strength.

## **6.2. Main contributions**

The present work has brought the following contributions:

- A thorough research on the use of iron during the gothic era leading to a better understanding of its utmost importance in gothic architecture, the data collected in this work coming from several up-to-date papers.
- A detailed mapping of the presence of ties remains in Mallorca Cathedral based on a previous photogrammetric study as well as an on-site investigation. From this mapping it has been possible to estimate the positions of the ties as well as their dimensions.
- New insight concerning the influence of auxiliary ties during the construction process of gothic architecture with the example of Mallorca Cathedral. The different models developed in this study have shown the significant reduction of the horizontal deformations of the piers together with the modification of the tensile damage pattern when such temporary devices were added in the construction process.
- Understanding of the influence of the cross-section of the ties together with the influence of the tensile strength of the masonry when a configuration with ties is considered.
- A preliminary study, to be completed in future research, about the effect of ties on time-dependent deformation of one representative bay.

## **6.3. Suggestions for future work**

The present work has shown the non-negligible influence of the effect of auxiliary ties used in the construction of Mallorca Cathedral. In order to gain a better understanding of the structural behavior of the construction, further on-site investigations should be carry out with more suitable devices. It would be useful indeed to reach the ties remains to specify their nature and find their accurate dimensions and positions. It would be also interesting to monitor the two remaining ties. Concerning the FEM analyses, a thorough long-term behavior of the structure should be carry out, considering the different temporary configurations as well as different parameters to define the creep behavior of masonry.

Another interesting study would be to model this long-term behavior considering long-lasting ties and to compare the results with the ones obtained previously.

This page is left blank on purpose.

## 7. REFERENCES

### Papers, books and publications

Acland J.H., Medieval structure: the gothic vault, Toronto University, 1972.

Bernardi P, Dillmann P., La place du métal dans la construction, in Vingtain (D.), Monument de l'Histoire – Construire reconstruire le Palais des Papes, XIVème-XIXème siècles, Avignon, RMG Editions – Palais des Papes : Avignon, 2002.

Bernardi P., Dillmann P., Stone skeleton or iron skeleton : The provision and use of metal in the construction of the Papal Palace at Avignon in the 14th century, in Bork (R.), De re Metallica, The uses of metal in the Middle Ages, Ashgate, 2005.

Brown R., Sacred Architecture: Its Rise, Progress and Present State, &c., London, Fisher, Son & Co., 1845.

Brunet E., La restauration de la cathédrale de Soissons, Bulletin monumental, 1928 ; 57.

Cervera M., Viscoelasticity and rate-dependent continuum damage models, Monography: 79. Barcelona: CIMNE, Technical University of Catalonia, 2003.

Cervera M., Hinton E., Hassan O., Non-linear analysis of reinforced concrete plate and shell structures using 20-noded isoparametric brick elements. Comput Struct 1987: 25(6): 845-69.

Cervera M, Oliver J., Faria R., Seismic evaluation of concrete dams via continuum damage models, Earthquake Eng Struct D 1995: 24 (9): 1225-45.

Cervera M., Agelet de Saracibar C., Chiumenti M., COMET: Coupled mechanical and thermal analysis – data input manual version 5.0, Technical report IT-308, CIMNE: Barcelona, 2002.

Cervera M., Pelà L., Clemente R., Roca P., A crack-tracking technique for localized damage in quasi-brittle materials, Eng Fract Mech 2010: 77(13): 2431-50.

Choisy A, Histoire de l'architecture, Gauthier-Villars, Imprimeur-Libraire, 1899 ; Volume 2 : 316, 337.

Clemente R., Analisis estructural de edificios historicos mediante modelos localizados de fisuracion, UPC thesis, 2006.

Clemente R., Roca P., Cervera M., Damage Model with Crack Localization – Application to Historical Buildings, Structural Analysis of Historical Constructions, New Delhi 2006, P.B. Lourenço, P. Roca, C. Modena, S. Agrawal (Eds).

Coutinho D., Seismic analysis and strengthening of Mallorca Cathedral, SAHC thesis, 2010.

Dillmann P., Fluzin P., Chevallier P., Determination of iron making processes using synchrotron microprobe, in Jerem E., Biro K.T., Archaeometry 98, Proceedings of the 31th Symposium, Archaeopress – Archaeolingua, BAR, 2002: 327-334.

Dillmann P., Bernardi, P., Fluzin P., Use of iron for the building of medieval monuments. The Palais des Papes in Avignon and other French buildings, Archaeometallurgy in Europe, 2003; 1.

Dillmann P., Etudes des alliages ferreux anciens : élaboration, utilisation, dégradation. Apport des techniques microfaisceau, 2006.

Dillmann P., De Soissons à Beauvais: le fer des cathédrales de Picardie, in L'emploi du et du plomb dans l'architecture gothique, Actes du colloque de Noyon, 2006.

Faria R, Oliver J., Cervera M., A strain-based plastic viscous-damage model for massive concrete structures, Int J Solids Struct 1998;35:1533-58.

Fitchen J., The Construction of Gothic Cathedrals – A Study of Medieval Vault Erection, The University of Chicago Press, 1981.

Gau M, De l'emploi du fer comme moyen de consolidation dans les monuments historiques, Revue générale de l'architecture et des travaux publics 1841; Volume II : 21.

GiD: the personal pre and post-processor”, CIMNE, Barcelona: 2002. Available: <http://gid.cimne.upc.es>.

González R., Caballé F., Domengue J., Vendrell M., Giráldez P., Roca P., González J.L., Construction process, damage and structural analysis. Two case studies, Taylor and Francis Group, 2008.

Guadet J., Les éléments de la composition dans les édifices d'usage public, Elements et théories de l'architecture 1909.

Juhin A., Structure métallographique et comportement mécanique des tirants de fer du donjon du château de Vincennes, Final Dissertation of science of materials and nano objects, Universities of Paris 6 Pierre et Marie Curie and Paris-Sud 11, 2005.

L'Héritier, Juhin A., Dillmann P., Aranda R., Benoit P., Utilisation des alliages ferreux dans la construction monumentale du Moyen Age. Etat des lieux de l'avancée des études métallographiques et archéométriques, ArchéoSciences 2005 ; 25 : 117-132.

L'Héritier M., L'utilisation du fer dans l'architecture gothique: le cas de Troyes et de Rouen, Thesis, Université Paris I Panthéon-Sorbonne, U.F.R. d'Archéologie, 2007.

L'Héritier M., Dillmann P., Benoit P., L'emploi du fer dans la construction monumentale à la fin du Moyen Age : production et utilisation, 2007.

Laurent J.M., Construction et restauration des bâtiments en pierre – Histoire, Technique, Pratique, Editions Vial, 2007.

Laurent J.P., Histoire des techniques – Construction gothique, 2008.

Lethaby W., Westminster Abbey and the King's Craftmen, London, Duckworth, 1906.

Leutwiler O.A., Elements of Machines design, M.E.E. - McGRAW – Hill, 1917.

Martinez G., Vulnerabilidad sismica para edificios históricos de obra de fábrica de mediana y gran luz, Ph.D. thesis, Barcelona: Technical University of Catalonia, 2007.

Material of old metal bridges - literature overview, Sustainable Bridges 2007: 17(218).

Mechanical Engineering LAXMMI Publications (P) L/TD, 2009.



Moufle D., Etude préalable à la restauration de la tour couronnée, Médiathèque du Patrimoine, 2000.

Pelà L., Continuum Damage Model for Nonlinear Analysis of Masonry Structures, Ph.D. thesis, Technical University of Catalonia (UPC), Spain, University of Ferrara, Italy, 2009.

Pelà L., Cervera M., Roca P., An orthotropic damage model for the analysis of masonry structures, *Construction and Building Materials* 2013; 41:957-967.

Roca P., Studies on the structure of Gothic Cathedrals, *Historical Constructions*, P.B. Lourenço, P. Roca (Eds), Guimarães, 2001.

Roca P., Cervera M., Pelà L., Clemente R., Chiumenti M., Viscoelasticity and Damage Model for Creep Behavior of Historical Masonry Structures, *The Open Civil Engineering Journal* 2012;6 (Suppl 1-M7): 188-199.

Roca P., Cervera M., Pelà L., Clemente R., Chiumenti M., Continuum FE models for the analysis of Mallorca Cathedral, *Engineering Structures* 2013; 46: 653-670.

Roca P., Cervera M., Gariup G. and Pelà L., Structural Analysis of Masonry Historical Constructions. Classical and Advanced Approaches, *Archives of Computational Methods in Engineering* 2010; 17:299–325.

Rouillard, J., L'homme et la rivière: histoire du bassin de la Vanne au Moyen Age (XII<sup>e</sup>-XVI<sup>e</sup> siècle), Thesis in History, University Paris 1 Panthéon-Sorbonne under the direction of M. Bourrin, 2003.

Sean L., Sanjay R., Lutenege A.J., Variability of the Mechanical Properties of Wrought Iron from Historic American Truss Bridges, *American Society of Civil Engineers*, 2011.

Taupin J.-L., *Le fer des cathédrales*, Monumental, 1996.

Taupin J.-L., *Le fer des cathédrales, la naissance d'une réflexion et son évolution : l'exemple de Beauvais*, L'emploi du fer et du plomb dans l'architecture gothique, Actes du colloque de Noyon, 2006.

Timbert A., Dillmann P., *Le squelette de fer des cathédrales gothiques*, cité-sciences.fr, Videodiffusion, 2010.

Vasic M., Coronelli D., Poggi C., A Multidisciplinary approach for the assessment of great historical structures: ties of "Duomo di Milano", *International Conference Built Heritage* 2013, Milan, Italy, 18-20 November 2013.

Viollet-Le-Duc E., *Dictionnaire Raisoné de l'Architecture française du XI<sup>e</sup> au XVI<sup>e</sup> siècle*, Paris B. Rance Editeur, 1854-1868. Articles : Armature ; Chaînage, Tirant.

Whitney M.O., Aston J., *Johnson's Materials of Construction Rewritten*, 1926.

## **Norms and codes**

RiL805: Guideline 805 of German railways, Germany, 2002.

RT/CE/C/025, United Kingdom, 2004

SBB Weisung I-AM 08/02 25/05/2002, Switzerland, 2002.

## Websites

<http://www.engineeringtoolbox.com>

<http://www.ferronneriedelabrie.com>

## ANNEX A: VISCOELASTICITY AND DAMAGE MODEL

The model developed here has been firstly developed by Cervera, 2003 and adapted for the case of masonry structures by Roca et al., 2013, 2012. The purpose of this model is to simulate the time-dependent strain accumulation in the material as a result to long-term exposure to creep. The main concept is the adoption of a time-dependent stiffness. In the following, a mathematical description of the model, mainly based on the work of Roca et al., 2013 is presented.

### Viscoelasticity model

Considering a uniaxial case, a Maxwell chain is defined in order to schematize the adopted rheological model. This chain is composed by two parts placed in parallel: the first part is defined by a spring with an elastic stiffness of  $E_\infty$  and the second part is defined by another spring with an elastic stiffness of  $E_v$  together with a dashpot with a viscosity parameter  $\eta$ . One can notice that the springs response is linear elastic whereas the viscous stress in the dashpot is proportional to the viscous strain state, according to the following law:

$$\sigma_v = \eta \dot{\epsilon}_v$$

Considering the dashpot infinitely stiff at the beginning, the initial instantaneous stiffness of the model  $E_0$  can be defined as follows:

$$E_0 = E_\infty + E_v$$

Now considering the system at  $t = +\infty$ , the dashpot is completely slackened at the end of the deformation process. The resulting stiffness is given by:

$$E = E_\infty$$

At this point it is possible to define two parameters:

- The participation ratio, which represents the amount of stiffness that can be affected by viscosity:

$$\xi = \frac{E_v}{E_0}$$

- The retardation time:

$$\vartheta = \frac{\eta}{E_v}$$

It is possible to calculate the total stress sustained by the Maxwell chain:

$$\sigma = \sigma_e + \sigma_v = E_\infty \varepsilon + \xi E_0 (\varepsilon - \varepsilon_v)$$

Where:

$\varepsilon$  : total deformation of the system;

$\varepsilon_v$  : viscous strain of the Maxwell chain.

The strain rate of the system is given by:

$$\dot{\varepsilon} = \frac{\dot{\sigma}_v}{E_v} + \frac{\sigma_v}{\eta}$$

Considering now a multidimensional case, one can obtain the following equation (the terms in bold correspond to matrices and **C** corresponds to the isotropic linear-elastic constitutive tensor):

$$\xi \mathbf{C} : \dot{\varepsilon} = \dot{\sigma}_v + \frac{\sigma_v}{\vartheta}$$

In which the following relationship can be included:

$$\sigma_v = \xi \mathbf{C} : (\varepsilon - \varepsilon_v)$$

To give:

$$\dot{\varepsilon}_v = \frac{1}{\vartheta} (\varepsilon - \varepsilon_v)$$

Finally, by integrating the previous equation, one can obtain the solution of the differential equation for a generic time step  $t_{n+1}$  (Cervera, 2003):

$$\varepsilon_v(t_{n+1}) = \varepsilon_v(t_n) + \frac{\Delta t}{\vartheta} [\varepsilon(t_{n+1}) - \varepsilon_v(t_n)]$$

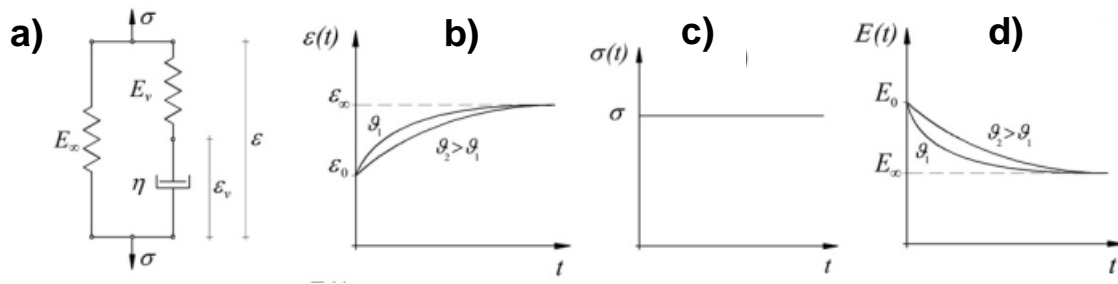


**Figure 109** – Viscoelasticity model: (a) Maxwell chain schematization, (b) strain, (c) stress and (d) stiffness time dependent laws. (Roca et al., 2013)

### Tension –Compression Damage Model

This model (Cervera, 1995; Faria, 1998) is based on the concept of effective stress tensor  $\bar{\sigma}$  which is directly linked to the total deformation of the system via Hook's Law:

$$\bar{\sigma} = \mathcal{C} : \varepsilon$$

Because of the different mechanical behavior in tension and in compression of the masonry, the effective stress is divided into tensile and compressive components:

- tensile component:

$$\bar{\sigma}^+ = \sum_{i=1}^3 \langle \bar{\sigma}_i \rangle \mathbf{p}_i \otimes \mathbf{p}_i$$

Where  $\bar{\sigma}_i$  represents the principal stress value from tensor  $\bar{\sigma}$  at the  $i^{\text{th}}$  time step,  $\mathbf{p}_i$  the unit vector associated with its respective principal direction and the symbols  $\langle . \rangle$  are the Macauley brackets:

$$\langle x \rangle = x, \text{ if } x \geq 0, \langle x \rangle = 0, \text{ if } x \leq 0$$

- compressive component:

$$\bar{\sigma}^- = \bar{\sigma} - \bar{\sigma}^+$$

Defining now the internal damage variables  $d^+$  and  $d^-$ , respectively the tensile one and the compressive one:

$$\bar{\sigma} = (1 - d^+) \bar{\sigma}^+ + (1 - d^-) \bar{\sigma}^-$$

Note that the internal damage variables are equal to 0 when the material is undamaged and equal to 1 when it is fully damaged. The damage function is different for each of the two cases in order to separate the tensile damage of the material (i.e. cracking) with its compressive damage (i.e. crushing). They are defined as follows:

$$\varphi^{\pm}(\tau^{\pm}, r^{\pm}) = \tau^{\pm} - r^{\pm} \leq 0$$

Where  $\tau^{\pm}$  correspond to scalar positive quantities, termed as equivalent stresses and defined in order to compare different stress states in 2D or 3D:

$$\tau^{\pm} = [\bar{\sigma}^{\pm} : \Lambda^{\pm} : \bar{\sigma}^{\pm}]^{1/2}$$

Where  $\Lambda^{\pm}$  correspond to the shape of each damage criterion. It is assumed that:

$$\Lambda^{+} = \mathbf{p}_1 \otimes \mathbf{p}_1 \otimes \mathbf{p}_1 \otimes \mathbf{p}_1 \text{ corresponding to the Rankine criterion in tension;}$$

$$\Lambda^{-} = \mathbf{C}/E \text{ corresponding to the shape of the compression damage.}$$

On the other hand the current damage threshold is represented by the internal stress-like variables  $r^{\pm}$ . The size of the monotonically expanding damage surface is controlled by their values. The initial values of the damage thresholds are:

$$r_0^{\pm} = f^{\pm}$$

Where  $f^{+}$  and  $f^{-}$  are respectively the uniaxial strength in tension and the uniaxial strength in compression.

The evolution law of  $r^{\pm}$  is given as follows:

$$r^{\pm} = \max [r_0^{\pm}, \max (\tau^{\pm})]$$

A final step is to define the damage variables  $d^{+}$  and  $d^{-}$ . They are defined in the form of a monotonically increasing function such that  $0 \leq d^{\pm}(r^{\pm}) \leq 1$ . The following exponential expressions have been assumed:

$$d^{\pm}(r^{\pm}) = 1 - \frac{r_0^{\pm}}{r^{\pm}} \exp \left\{ 2H_{dis}^{\pm} \left( \frac{r_0^{\pm} - r^{\pm}}{r_0^{\pm}} \right) \right\}$$

Where the positive constants  $H_{dis}^{\pm}$  are the discrete softening parameters that are related to the material normalized tensile and compressive fracture energies (Cervera, 2010, 1987).

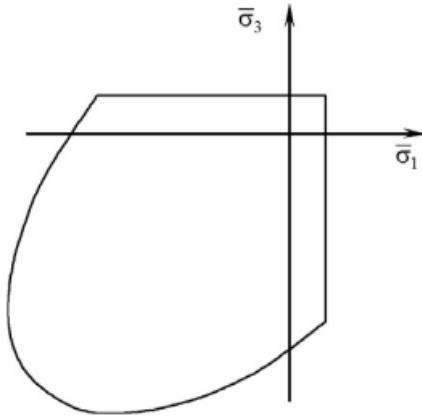
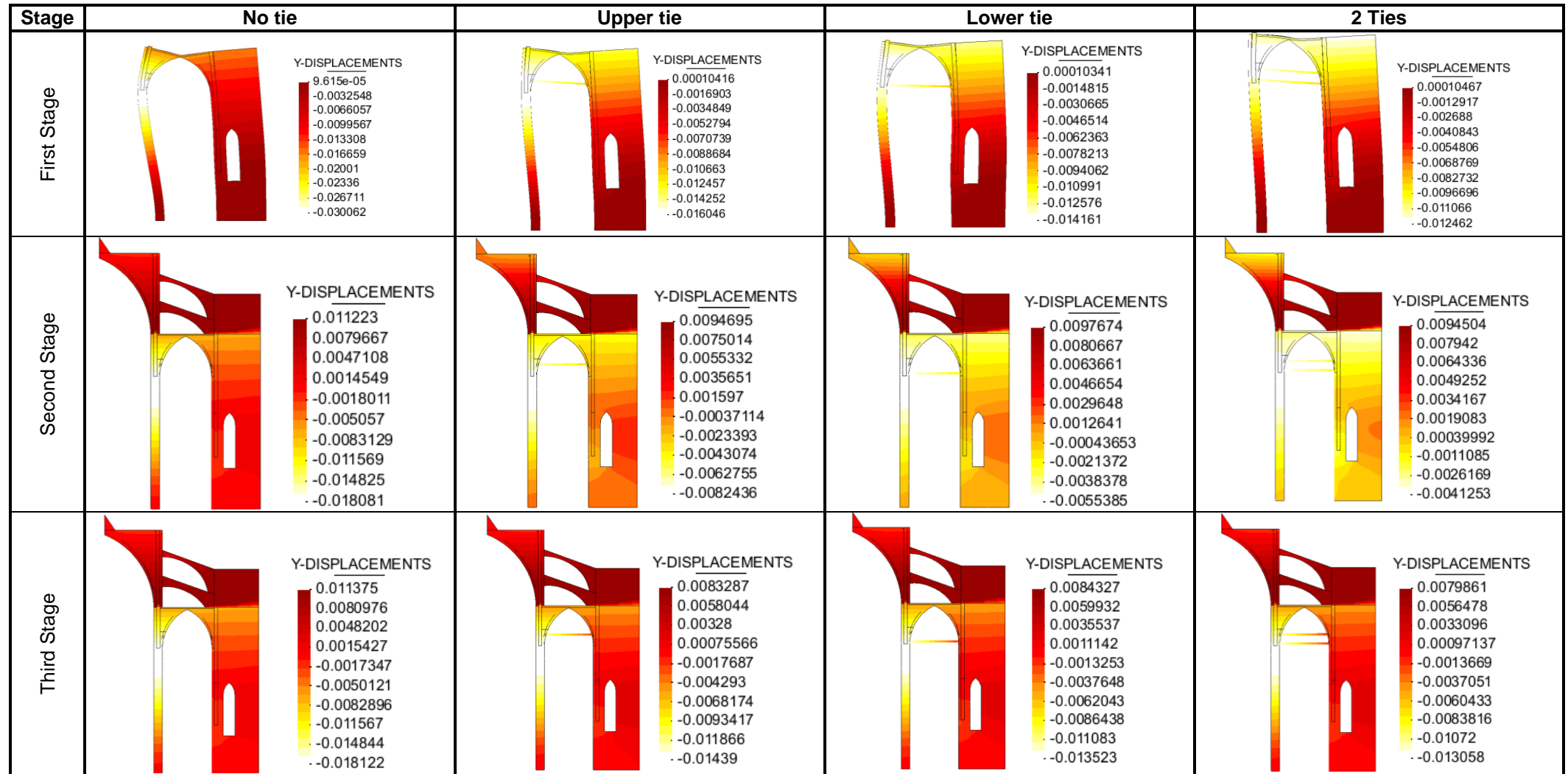


**Figure 110** – Composite damage surface adopted for the masonry (Roca et al., 2013).

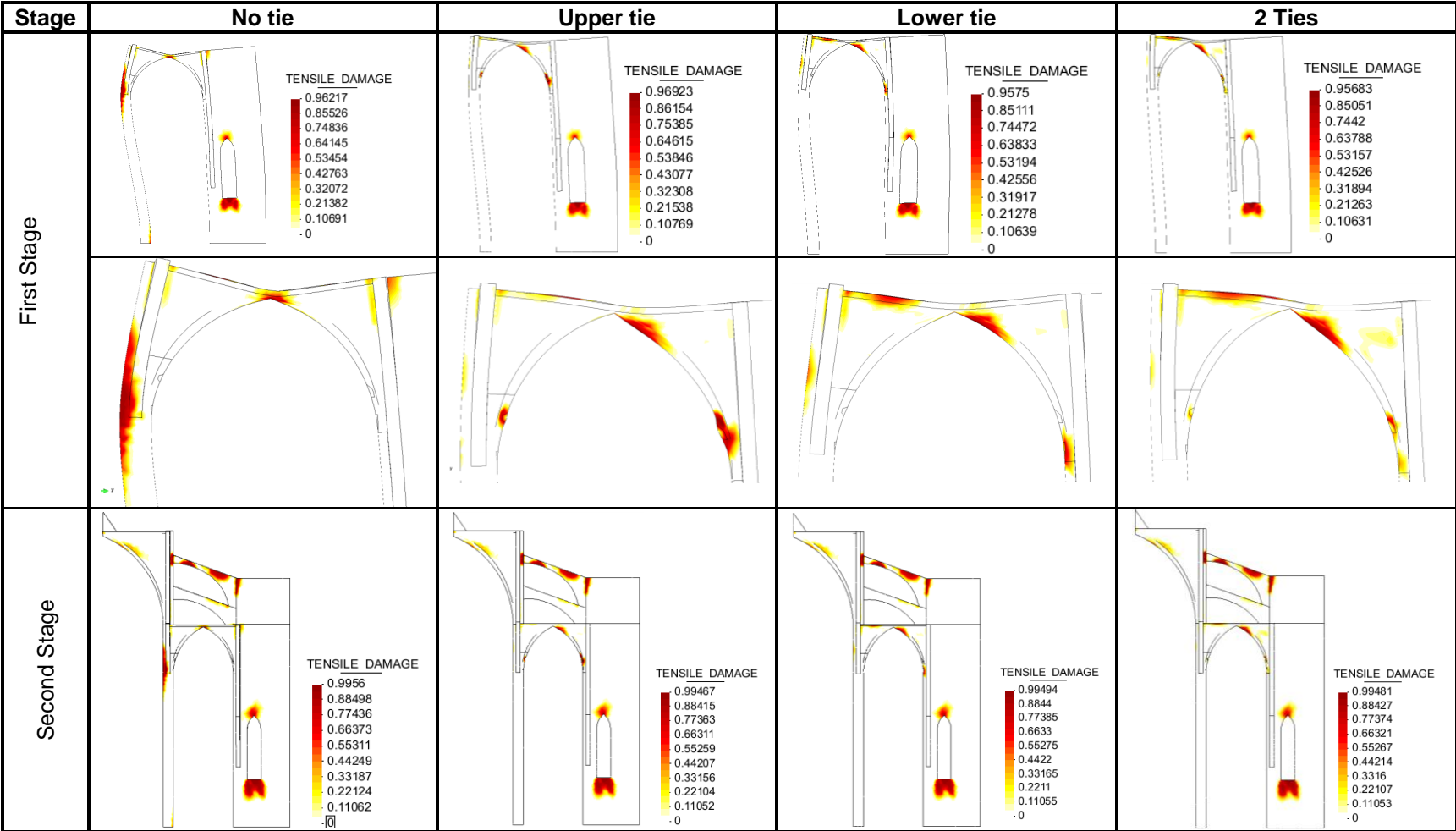
This page is left blank on purpose.

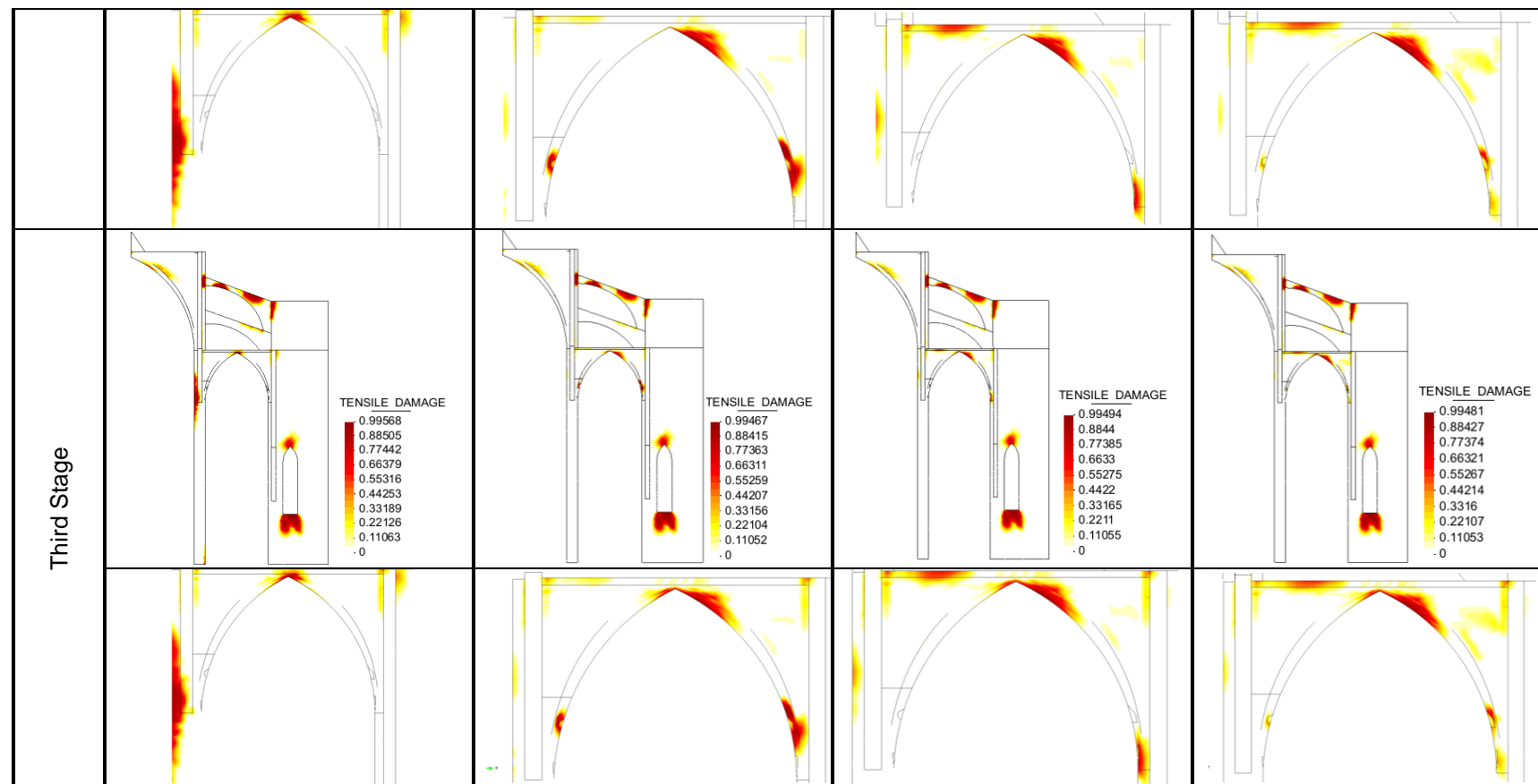


**ANNEX B: HORIZONTAL DISPLACEMENTS AT STAGES 1, 2 AND 3 FOR THE FOUR DIFFERENT TIES CONFIGURATIONS UNDER THE ASSUMPTION OF SMALL STRAINS/LARGE DISPLACEMENTS (RESULTS ARE GIVEN IN METERS). TIES AREA: 25 CM<sup>2</sup>.**



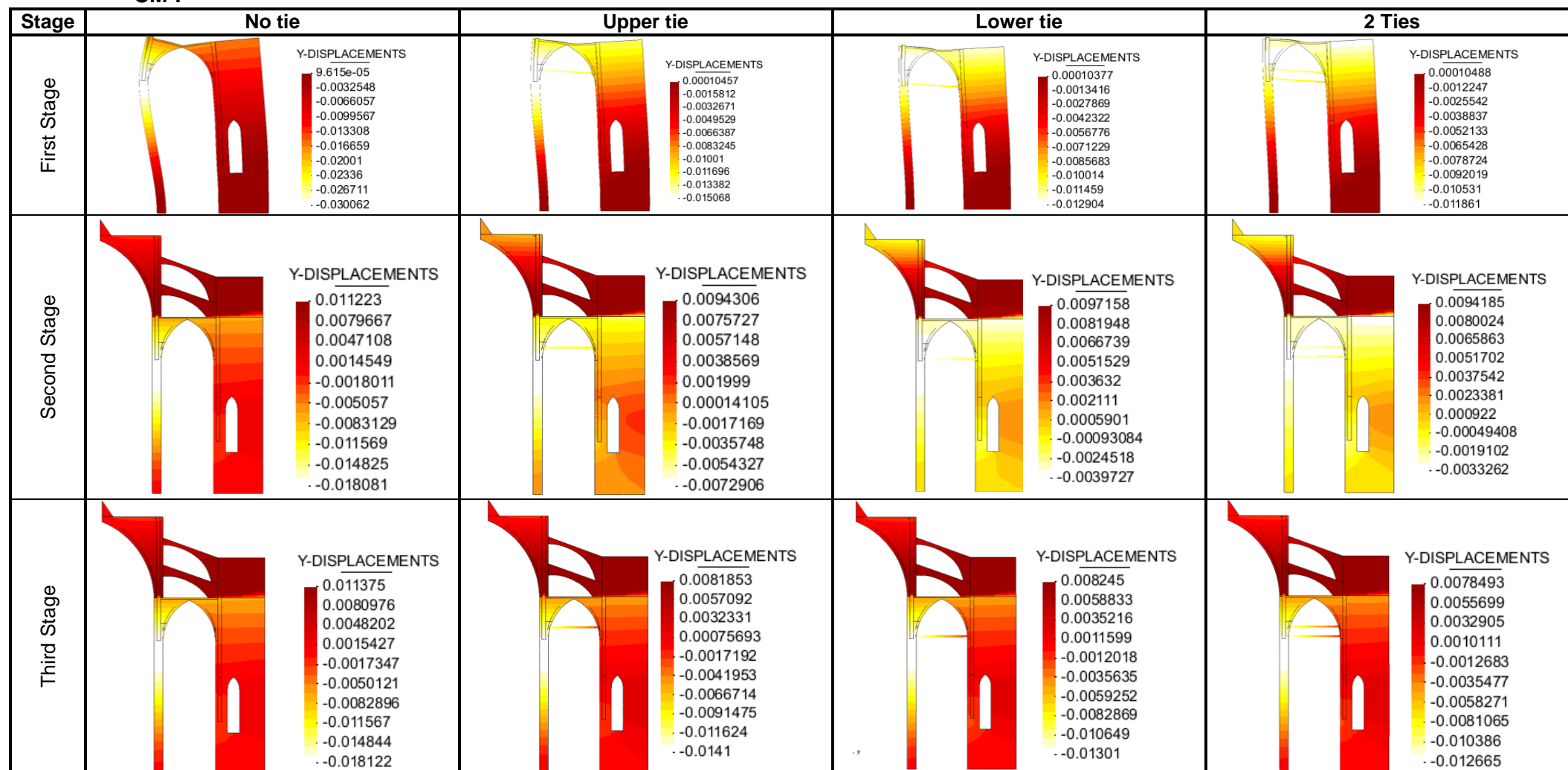
**ANNEX C: TENSILE DAMAGE AT STAGES 1, 2 AND 3 FOR THE FOUR DIFFERENT TIES CONFIGURATIONS UNDER THE ASSUMPTION OF SMALL STRAINS/LARGE DISPLACEMENTS. TIES AREA: 25 CM<sup>2</sup>.**





This page is left blank on purpose.

**ANNEX D: HORIZONTAL DISPLACEMENTS AT STAGES 1, 2 AND 3 FOR THE FOUR DIFFERENT TIES CONFIGURATIONS UNDER THE ASSUMPTION OF SMALL STRAINS/LARGE DISPLACEMENTS (RESULTS ARE GIVEN IN METERS). TIES AREA: 50 CM<sup>2</sup>.**



**ANNEX E: TENSILE DAMAGE AT STAGES 1, 2 AND 3 FOR THE FOUR DIFFERENT TIES CONFIGURATIONS UNDER THE ASSUMPTION OF SMALL STRAINS/LARGE DISPLACEMENTS. TIES AREA: 50 CM<sup>2</sup>.**

